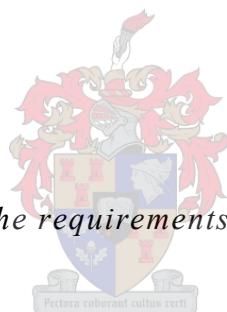


High resolution ^{195}Pt and ^{119}Sn NMR characterization of platinum(II)-tin(II) complexes

Thesis submitted to the

STELLENBOSCH UNIVERSITY



In fulfilment of the requirements for the degree of

MASTER OF SCIENCE

By

SHANI BARKHUYSEN

Supervisor: Professor Klaus R. Koch

December 2011

Declaration

By submitting this thesis electronically, I declare that the entirety of the work contained herein is my own, original work, that I am the owner of the copyright therefore (unless to the extent explicitly otherwise stated) and that I have not previously in its entirety or in part submitted it for obtaining any qualification.

December 2011

Aknowledgements

I would sincerely like to thank

- My supervisor, Professor Klaus R. Koch, for all his support, motivation, enthusiasm and guidance through my studies.
- Dr. Wilhelmus J. Gerber for his time, advise and editing of my thesis.
- Anglo Platinum and University of Stellenbosch for funding.
- NMR lab staff, Elsa Malherbe and Dr. Jaco Brand.
- The technical staff of the Analytical Chemistry department, Shafiek Mohammed, Deidre Davids and Roger Lawrence
- The PGM group for their friendship and support.
- Family and friends for their love and support throughout my studies.
- God for the life he gave me.

List of Abbreviations

AQ-336	Aliquat-336 (methyltrioctylammonium chloride)
Chloroform- <i>d</i>	deuterated chloroform
D ₂ O	deuterium oxide
v/v	volume/volume
UV/Vis	Ultra violet visible
K	Kelvin
ppm	parts per million (NMR)
Hz	Hertz, s ⁻¹
δ(¹⁹⁵ Pt)	chemical shift of ¹⁹⁵ Pt NMR signal
δ(¹¹⁹ Sn)	chemical shift of ¹¹⁹ Sn NMR signal
γ	gyromagnetic ratio
¹ J(^{119/117/115} Sn- ¹⁹⁵ Pt)	condensed form for ¹ J(¹¹⁹ Sn- ¹⁹⁵ Pt), ¹ J(¹¹⁷ Sn- ¹⁹⁵ Pt) and ¹ J(¹¹⁵ Sn- ¹⁹⁵ Pt) satellites
NSA	Natural Statistical Abundance

Conference Proceedings

This work was presented at the following conferences:

RSC SACI Inorg, September 2009, Bloemfontein, Poster presented

Title: High resolution ^{195}Pt and ^{119}Sn NMR characterization of the series of complex $[\text{Pt}(\text{SnX}_3)_n\text{X}_{4-n}]^{2-}$ ($\text{X} = \text{Cl}^-/\text{Br}^-$) and $[\text{Pt}(\text{SnX}_3)_5]^{3-}$ anions

Analitika, December 2010, Stellenbosch, Poster presented

Title: High resolution ^{195}Pt and ^{119}Sn NMR characterization of mixed halide platinum(II)-tin(II) complexes

RSC SACI, January 2011, Johannesburg, Poster presented

Title: High resolution ^{195}Pt and ^{119}Sn NMR characterization of mixed halide platinum(II)-tin(II) complexes

Abstract

A detailed high resolution ^{195}Pt and ^{119}Sn NMR study of the series of heteroleptic $[\text{Pt}(\text{Sn}_5\text{Cl}_n\text{Br}_{15-n})]^{3-}$ ($n = 0 - 15$) complexes has been conducted. During this study, all 16 possible species in this series have successfully been synthesized and characterized by means of high resolution ^{195}Pt NMR spectroscopy proving what a powerful tool ^{195}Pt NMR is to study the speciation of these species in solution.

The ^{195}Pt NMR spectra of the homoleptic $[\text{Pt}(\text{SnX}_3)_5]^{3-}$ ($X = \text{Cl}^-/\text{Br}^-$) species in Aliquat-336 (20 % v/v) in CDCl_3 were studied first. The ^{195}Pt NMR spectra of the homoleptic $[\text{Pt}(\text{SnX}_3)_5]^{3-}$ ($X = \text{Cl}^-/\text{Br}^-$) complex anions are assigned to 18 isotopologues of the complex anions, 10 of which have never been reported before. The unambiguous assignment of the respective $^1\text{J}(^{119/117/115}\text{Sn}-^{195}\text{Pt})$ satellites are based on the excellent agreements obtained when the calculated NSA's of each of the 112 possible isotopologues are compared to the experimental ^{195}Pt NMR signal areas. Moreover, these assignments are confirmed by the great agreement between the respective $^1\text{J}(^{119/117}\text{Sn}-^{195}\text{Pt})/^1\text{J}(^{117/115}\text{Sn}-^{195}\text{Pt})$ ratios and the $\gamma(^{119/117}\text{Sn})/\gamma(^{117/115}\text{Sn})$ ratios.

The ^{195}Pt NMR spectra of the heteroleptic $[\text{Pt}(\text{Sn}_5\text{Cl}_n\text{Br}_{15-n})]^{3-}$ ($n = 0 - 15$) showed unprecedented resolution which allowed for the unambiguous assignment of all sixteen main ^{195}Pt NMR signals to the sixteen possible species. Moreover, each set of $^1\text{J}(^{119/117/115}\text{Sn}-^{195}\text{Pt})$ satellites are unambiguously assigned to a particular isotopologue/isotopomer of a $[\text{Pt}(\text{Sn}_5\text{Cl}_n\text{Br}_{15-n})]^{3-}$ ($n = 0 - 15$) species. In this manner more than 600 isotopologue and isotopomer species are identified. Moreover, the $^1\text{J}(^{195}\text{Pt}-^{119/117/115}\text{Sn})$ coupling constants of each species are dependent on the configuration of the tin-halide ligands and decrease in the order $\text{SnCl}_3^- > \text{SnCl}_2\text{Br}^- > \text{SnClBr}_2^- > \text{SnBr}_3^-$. Thus separate sets of signals are observed for the respective isotopologues and isotopomers of each species which implies that *intra-* or *inter-* molecular *halide exchange* does not occur on the ^{195}Pt NMR acquisition time scale.

Furthermore, with the information obtained from the ^{195}Pt NMR spectra recorded for the solutions, the ^{119}Sn NMR spectra could be fully elucidated, despite of the bad signal-to-noise ratio. The ^{119}Sn NMR spectra showed sets of resonances that were tentatively assigned to species with SnCl_3^- , SnCl_2Br^- , SnClBr_2^- and SnBr_3^- as ligands on average. However, each set of resonances consisted of 5 – 6 individual lines, which, with the help of ^{195}Pt NMR could now be assigned to the $[\text{Pt}(^{119}\text{SnCl}_3)(\text{Sn}_4\text{Cl}_n\text{Br}_{12-n})]^{3-}$, $[\text{Pt}(^{119}\text{SnCl}_2\text{Br})(\text{Sn}_4\text{Cl}_n\text{Br}_{12-n})]^{3-}$,

$[\text{Pt}({}^{119}\text{SnClBr}_2)(\text{Sn}_4\text{Cl}_n\text{Br}_{12-n})]^{3-}$ and $[\text{Pt}({}^{119}\text{SnBr}_3)(\text{Sn}_4\text{Cl}_n\text{Br}_{12-n})]^{3-}$ ($n = 0 - 12$) species, where each individual line is assigned to a species with a different value of 'n'. This implies that separate resonances are observed for respective isotopomers of a species, thus again implying that *intra*- or *inter*- molecular halide exchange does not occur on the NMR acquisition time scale. On the other hand, single resonances are observed, which means that *intra*- molecular site-exchange, such as Berry-pseudo rotation, occurs rapidly on the ${}^{119}\text{Sn}$ NMR acquisition time-scale, and that no distinction can be made between equatorial and axial tin ligands.

High-resolution ${}^{195}\text{Pt}$ NMR spectroscopy has enabled the unambiguous assignment of all 16 heteroleptic $[\text{Pt}(\text{Sn}_5\text{Cl}_n\text{Br}_{15-n})]^{3-}$ ($n = 0 - 15$) complex anions with unprecedented resolution. Furthermore, ${}^{195}\text{Pt}$ NMR shows significantly higher resolution compared to ${}^{119}\text{Sn}$ NMR for these systems, allowing for the complete assignment of all ${}^{119}\text{Sn}/{}^{117}\text{Sn}/{}^{115}\text{Sn}$ chlorido-bromido isotopologues and isotopomers of these species.

Opsomming

‘n Gedetailleerde studie van die reeks heteroleptiese $[\text{Pt}(\text{Sn}_5\text{Cl}_n\text{Br}_{15-n})]^{3-}$ ($n = 0 - 15$) kompleks anione is uitgevoer deur middel van hoë resolusie ^{195}Pt en ^{119}Sn KMR. Tydens hierdie studie is al die sestien moontlike spesies in hierdie reeks geïdentifiseer en gekarakteriseer met hoë resolusie ^{195}Pt KMR, wat bewys lewer van wat ‘n magtige tegniek ^{195}Pt KMR is vir die studie van die soortvorming van hierdie spesies in oplossing.

Eerstens is die ^{195}Pt KMR spektra van die homoleptiese $[\text{Pt}(\text{SnX}_3)_5]^{3-}$ ($X = \text{Cl}/\text{Br}^-$) spesies in “Aliqaut-336” (20 % v/v) in CDCl_3 ondersoek. Die ondersoek het gelei tot die identifisering van 18 “isotopologues”, waarvan 10 nog nooit van te vore gepubliseer is nie. Die toedelings van die $^1\text{J}(^{119/117/115}\text{Sn}-^{195}\text{Pt})$ satelliete is gebaseer op die goeie verwantskap wat verkry is tussen die berekende natuurlike statistiese volopheid (NSV) van elk van die 112 moontlike “isotopologues” met die eksperimenteel verkryde areas van die ^{195}Pt KMR seine. Hierdie toedelings is bevestig deur die besondere verwantskap wat verkry is wanneer die onderskeidelike $^1\text{J}(^{119/117}\text{Sn}-^{195}\text{Pt})/^1\text{J}(^{117/115}\text{Sn}-^{195}\text{Pt})$ verhoudings met die $\gamma(^{119/117}\text{Sn})/\gamma(^{117/115}\text{Sn})$ verhoudings vergelyk word.

Die ongeëwenaarde resolusie wat verkry is in die ^{195}Pt KMR spektra van die heteroleptiese $[\text{Pt}(\text{Sn}_5\text{Cl}_n\text{Br}_{15-n})]^{3-}$ ($n = 0 - 15$) spesies in “Aliqaut-336” (20 % v/v) in CDCl_3 het die eenduidige toedeling van elkeen van die sestien ^{195}Pt KMR seine tot ‘n spesifieke spesies moonlik gemaak. Daarenbove is elke stel $^1\text{J}(^{119/117/115}\text{Sn}-^{195}\text{Pt})$ satelliete van ‘n bepaalde spesies toegeskryf aan ‘n bepaalde “isotopologue” of “isotopomer” van ‘n $[\text{Pt}(\text{Sn}_5\text{Cl}_n\text{Br}_{15-n})]^{3-}$ ($n = 0 - 15$) spesies. Meer as 600 “isotopologue” and isotopomeer spesies is op hierdie manier geïdentifiseer. Verder is ook gevind dat die grootte van die $^1\text{J}(^{119/117/115}\text{Sn}-^{195}\text{Pt})$ koppelings-konstantes aangewese is op die samestelling van die $(\text{SnCl}_n\text{Br}_{3-n})^-$ ($n = 0 - 3$) ligande en afneem in die orde $\text{SnCl}_3^- > \text{SnCl}_2\text{Br}^- > \text{SnClBr}_2^- > \text{SnBr}_3^-$. Die aparte ^{195}Pt KMR seine wat dus verkry is vir “isotopologues” en isotopomere van ‘n bepaalde spesies impliseer dat *intra-* en *inter-* molekulere halied uitruiling nie op die ^{195}Pt KMR tyd-skaal plaasvind nie.

Met behulp van die informasie verkry met ^{195}Pt KMR is elke individuele ^{119}Sn KMR sein binne die vier stelle seine van die $[\text{Pt}(\text{Sn}_5\text{Cl}_n\text{Br}_{15-n})]^{3-}$ ($n = 10 - 15$) spesies identifiseerbaar, ten spyte van die lae ‘S/N’ verhouding. Ongelukkig is die resolusie van die ^{119}Sn KMR spektra van die $[\text{Pt}(\text{Sn}_5\text{Cl}_n\text{Br}_{15-n})]^{3-}$ ($n = 0 - 9$) spesies nie goed genoeg om toedelings van elke individuele sein te maak nie. Nie te min, dit is bevestig dat die vier stelle ^{119}Sn KMR

seine toegeskryf kan word aan die $[\text{Pt}^{(119}\text{SnCl}_3)(\text{Sn}_4\text{Cl}_n\text{Br}_{12-n})]^{3-}$, $[\text{Pt}^{(119}\text{SnCl}_2\text{Br})(\text{Sn}_4\text{Cl}_n\text{Br}_{12-n})]^{3-}$, $[\text{Pt}^{(119}\text{SnClBr}_2)(\text{Sn}_4\text{Cl}_n\text{Br}_{12-n})]^{3-}$ and $[\text{Pt}^{(119}\text{SnBr}_3)(\text{Sn}_4\text{Cl}_n\text{Br}_{12-n})]^{3-}$ ($n = 0 - 12$) spesies, waar elke individuele sein binne 'n stel toegeskryf kan word aan 'n spesies met ander waarde "n". Die aparte ^{119}Sn KMR seine verkry vir twee isomere van 'n spesies impliseer dat *intra*- en *inter*-molekulêre halied uitruiling ook nie plaasvind op die ^{119}Sn KMR tydskaal nie. Tog word enkele ^{119}Sn KMR seine steeds verkry wat daarop dui dat *intra*-molekulêre "site"-uitruiling steeds vinnig plaasvind op die ^{119}Sn KMR tydskaal en dat daar nie tussen ^{119}Sn ligande in die ekwatoriale en aksiale posisies kan onderskei word nie.

Hoë-resolusie ^{195}Pt KMR spektroskopie het dit dus moontlik gemaak om al sestien heteroleptiese $[\text{Pt}(\text{Sn}_5\text{Cl}_n\text{Br}_{15-n})]^{3-}$ ($n = 10 - 15$) spesies eenduidig te identifiseer en te karakteriseer in oplossing. ^{195}Pt KMR toon baie beter resolusie en is ook baie meer sensitief as ^{119}Sn KMR wat dit 'n uitmuntende tegniek maak vir die studie van die soortvorming van hierdie spesies.

Table of Content

Declaration.....	i
Acknowledgements.....	ii
List of Abbreviations	iii
Conference Proceedings.....	iv
Abstract.....	v
Opsomming.....	vii
Table of Content	ix
List of Figures.....	xii
List of Tables	xv
List of Schemes.....	xvii

CHAPTER 1

1.1. Reactions of Platinum with Stannous Chloride in Hydrochloric Acid Medium.....	1
1.1.1. Nature of coloured Pt-Sn species.....	2
1.2. The nature of SnX_3^- ($\text{X} = \text{Cl}^-/\text{Br}^-$) as a ligand	5
1.3. Application of ^{119}Sn and ^{195}Pt NMR Spectroscopy as a tool to study the Nature of Pt-Sn complexes.....	7
1.4. Catalytic Properties of Trichlorostannato-Platinum Complexes.....	10
1.5. Aims and Objectives of this study.....	12

CHAPTER 2

2.1. Synthesis of the $[\text{Pt}(\text{Sn}_5\text{Cl}_n\text{Br}_{15-n})]^{3-}$ ($n = 0 - 15$) complex anions.....	13
2.1.1. Synthesis and extraction of $[\text{Pt}(\text{SnCl}_3)_5]^{3-}$ complex anions	13
2.1.2. Synthesis and extraction of the $[\text{Pt}(\text{SnBr}_3)_5]^{3-}$ complex anions	15
2.1.3. Synthesis of the heteroleptic $[\text{Pt}(\text{Sn}_5\text{Cl}_n\text{Br}_{15-n})]^{3-}$ ($n = 1 - 14$) complex anions .	16
2.2. Preliminary UV/Vis investigations	16

2.3. Experimental	19
2.3.1. Reagents	19
2.3.2. Instrumentation	20

CHAPTER 3

3.1. Introduction	21
3.2. Results and Discussion	25
3.2.1. ^{119}Sn NMR of the homoleptic $[\text{Pt}(\text{SnCl}_3)_5]^{3-}$ complex anion	25
3.2.2. ^{119}Sn NMR of the homoleptic $[\text{Pt}(\text{SnBr}_3)_5]^{3-}$ complex anion	30
3.2.3. ^{195}Pt NMR of the homoleptic $[\text{Pt}(\text{SnCl}_3)_5]^{3-}$ complex anions	31
3.2.4. ^{195}Pt NMR of the homoleptic $[\text{Pt}(\text{SnBr}_3)_5]^{3-}$ complex anions	37
3.3. Conclusion	42

CHAPTER 4

4.1. Introduction	43
4.2. Results and Discussion	46
4.2.1. ^{195}Pt NMR of the series of $[\text{Pt}(\text{Sn}_5\text{Cl}_n\text{Br}_{15-n})]^{3-}$ ($n = 0 - 15$) complex anions ...	46
4.2.2. Revisiting the ^{119}Sn NMR Spectra acquired for the heteroleptic $[\text{Pt}(\text{Sn}_5\text{Cl}_n\text{Br}_{15-n})]^{3-}$ ($n = 0 - 15$) species	62
4.3. Conclusions	74

CHAPTER 5

Conclusions	75
-------------------	----

REFERENCES	77
-------------------------	----

<i>Appendix A</i>	81
-------------------------	----

<i>Appendix B</i>	82
<i>Appendix C</i>	102

List of Figures

- Figure 2.1:** Dependence of Pt-Sn complexes on HCl concentration (M) where $[HCl] = 0.5\text{ M}$ in (a) and 3 M in (b). Both spectra are recorded as a function of time, with spectrum 1 being recorded directly after the reaction had started, and spectrum 2 indicates that equilibrium has been reached. For both solutions equilibrium was reached after ± 50 minutes.
- Figure 2.2:** Dependence of Pt-Sn complexes on the initial Pt:Sn ratio used. The $[Pt]$ is kept constant at $1 \times 10^{-4}\text{ M}$, while the $[Sn]$ is increased. In (a) the spectra recorded for solution with Pt:Sn ratios of 1:1, 1:2, 1:3, 1:4, 1:5 and 1:7 are shown. In (b) the spectra recorded for the solutions with Pt:Sn solutions of 1:5 and 1:7 are compared to the spectrum assigned to the $[Pt(SnCl_3)_5]^{3-}$ species.
- Figure 2.3:** Change in the absorbance spectrum of the $[Pt(SnX_3)_5]^{3-}$ ($X = Cl^-/Br^-$) as the ratio of Br:Cl in solution changes.
- Figure 3.1:** ^{119}Sn NMR spectrum recorded for (a) the $[Pt[SnCl_3)_5]^{3-}$ complex anion in acetone- d_6 by Nelson et al ²⁶ at 186.36 MHz and (b) the $[Pt[SnBr_3)_5]^{3-}$ complex anion extracted into 20% (v/v) Aliquat-336 - $CDCl_3$ by Koch ⁸⁹ at 74.56 MHz .
- Figure 3.2:** The ^{119}Sn NMR spectrum obtained for $[Pt(SnCl_3)_5]^{3-}$ in $CDCl_3$ (20% AQ-336) at 293 K. The respective satellites are observed due to (a) $^1J(^{119}Sn-^{195}Pt)$ coupling in isotopologue **2**, (b) $^1J(^{119}Sn-^{195}Pt)$ and $^2J(^{119}Sn-^{117}Sn)$ coupling within isotopologue **3**, (c) $^2J(^{119}Sn-^{117}Sn)$ coupling in both isotopologues **4** and **5**, and (d) $^2J(^{119}Sn-^{117}Sn)$ couplings in isotopologue **6**.
- Figure 3.3:** ^{119}Sn NMR spectrum obtained for $[Pt(SnBr_3)_5]^{3-}$ in $CDCl_3$ (20% AQ-336(Br)) at 293 K. Chemical shifts in ppm relative to Me_4Sn (neat).
- Figure 3.4:** ^{195}Pt NMR spectrum obtained for $[Pt(SnCl_3)_5]^{3-}$ in $CDCl_3$ (20% AQ-336) at 293 K. Chemical shifts in ppm relative to K_2PtCN_4 (in D_2O) at $\delta^{195}Pt = -4\ 700.0$ ppm. Where (a) and (b) represent the respective $^1J(^{195}Pt-^{119}Sn)$ and $^1J(^{195}Pt-^{117}Sn)$ satellites observed for isotopologues **1.1** and **8** in Scheme 3.7. The encircled signals have not been reported in literature.

- Figure 3.5:** ^{195}Pt NMR spectrum obtained for $[\text{Pt}(\text{SnCl}_3)_5]^{3-}$ in CDCl_3 (30% AQ-336(Br) at 293 K. Chemical shifts in ppm relative to K_2PtCN_4 (in D_2O). The ^1J satellites indicated by the symbols (a) to (f) are assigned to the $^1\text{J}({}^{119/117/115}\text{Sn}-^{195}\text{Pt})$ couplings of the respective isotopologues shown in Scheme 3.8. The $^1\text{J}({}^{119/117}\text{Sn}-^{195}\text{Pt})$ satellites shown in C, (d), (e) and (f), resulted from successive splitting of the $^1\text{J}({}^{119/117}\text{Sn}-^{195}\text{Pt})$ satellite signals in B by either $^1\text{J}({}^{119}\text{Sn}-^{195}\text{Pt})$ or $^1\text{J}({}^{117}\text{Sn}-^{195}\text{Pt})$ coupling.
- Figure 3.6:** ^{195}Pt NMR spectrum obtained for $[\text{Pt}(\text{SnBr}_3)_5]^{3-}$ in CDCl_3 (20% AQ-336(Br) at 293 K. The ^1J satellites indicated by (a) to (f) is assigned to $^1\text{J}({}^{119/117/115}\text{Sn}-^{195}\text{Pt})$ couplings of the isotopologues shown in Scheme 3.9. Similarly to the analogous chlorido species, the $^1\text{J}({}^{119/117}\text{Sn}-^{195}\text{Pt})$ satellites obtained for isotopologues **II.2**, **X** and **III** result from successive splitting.
- Figure 4.1:** ^{119}Sn NMR spectrum obtained by Koch ⁸⁹ for a solution containing equal volumes of $[\text{Pt}(\text{SnCl}_3)_5]^{3-}$ and $[\text{Pt}(\text{SnBr}_3)_5]^{3-}$ in Aliquat 336 at 25 °C.
- Figure 4.2:** ^{195}Pt NMR spectra (128.93 MHz) obtained at 20 °C for (A) $[\text{Pt}(\text{SnCl}_3)_5]^{3-}$ and (E) $[\text{Pt}(\text{SnBr}_3)_5]^{3-}$ in CDCl_3 (20% AQ-336). The spectra shown in (B), (C) and (D) are of the mixtures of $[\text{Pt}(\text{SnCl}_3)_5]^{3-}$ and $[\text{Pt}(\text{SnBr}_3)_5]^{3-}$ with volume ratios of 2:1, 1:1 and 1:2 respectively. Expansions of these ^{195}Pt NMR spectra are given in Appendix C.
- Figure 4.3:** Plot of the ^{195}Pt NMR chemical shifts of the 16 $[\text{Pt}(\text{Sn}_5\text{Cl}_n\text{Br}_{15-n})]^{3-}$ ($n = 0 - 15$) species as a function of the number of Br^- ligands present in the complex anion. An excellent second order correlation is obtained.
- Figure 4.4:** ^{195}Pt NMR spectrum obtained for solution with $[\text{Pt}(\text{SnCl}_3)_5]^{3-}$ to $[\text{Pt}(\text{SnBr}_3)_5]^{3-}$ ratio of 2:1. Only a partial part of the spectrum is shown as to focus specifically on the ^{195}Pt NMR signal obtained for $[\text{Pt}(\text{Sn}_5\text{Cl}_{14}\text{Br})]^{3-}$ ($\delta(^{195}\text{Pt}) = -5862$ ppm) and its respective ^1J satellites. The main resonance signals, as well as the ^1J satellites observed due to coupling in isotopologues/isotopomers with one magnetically active tin nucleus, are encircled. The expansion focuses specifically on these ^1J satellites.

- Figure 4.5:** ^{195}Pt NMR spectrum obtained for solution with $[\text{Pt}(\text{SnCl}_3)_5]^{3-}$ to $[\text{Pt}(\text{SnBr}_3)_5]^{3-}$ ratio of 2:1. Only a partial part of the spectrum is shown as to focus specifically on the ^{195}Pt NMR signal obtained for $[\text{Pt}(\text{Sn}_5\text{Cl}_{14}\text{Br})]^{3-}$ ($\delta(^{195}\text{Pt}) = -5\,862$ ppm) and its respective ^1J satellites.
- Figure 4.6:** Trends obtained when plotting the coupling constants of the respective satellites against the chemical shift of the $[\text{Pt}(\text{SnCl}_n\text{Br}_{15-n})]^{3-}$ ($n = 0 - 15$) complex anions.
- Figure 4.7:** ^{119}Sn NMR spectra (223.7 MHz) obtained at 20 °C for (A) $[\text{Pt}(\text{SnCl}_3)_5]^{3-}$ and (D) $[\text{Pt}(\text{SnBr}_3)_5]^{3-}$ in CDCl_3 (20% AQ-336). The spectra shown in (B) and (C) are those of the mixtures of $[\text{Pt}(\text{SnCl}_3)_5]^{3-}$ and $[\text{Pt}(\text{SnBr}_3)_5]^{3-}$ with volume ratios of 2:1 and 1:1 respectively.
- Figure 4.8:** ^{119}Sn NMR spectrum recorded for the solution with a $[\text{Pt}(\text{SnCl}_3)_5]^{3-}$ to $[\text{Pt}(\text{SnBr}_3)_5]^{3-}$ volume ratio of 2 to 1. The arrows represent the ^1J and ^2J couplings obtained for the $^{119}\text{SnCl}_3^-$ and $^{119}\text{SnCl}_2\text{Br}^-$ ligands, respectively.
- Figure 4.9:** An expansion of the ^{119}Sn NMR spectrum recorded for the solution with a $[\text{Pt}(\text{SnCl}_3)_5]^{3-}$ to $[\text{Pt}(\text{SnBr}_3)_5]^{3-}$ volume ratio of 2 to 1 to focus on the ^{119}Sn NMR signals centred at -123 ppm. The symbols (a) to (e) indicate the $^1\text{J}(^{195}\text{Pt}-^{119}\text{Sn})$ satellites due to the respective isotopologues. The isotopologues/isotopomers responsible for the individual ^{119}Sn NMR signals in the main set of signals are indicated by the arrows.
- Figure 4.10:** An expansion of the ^{119}Sn NMR spectrum recorded for the solution with a $[\text{Pt}(\text{SnCl}_3)_5]^{3-}$ to $[\text{Pt}(\text{SnBr}_3)_5]^{3-}$ volume ratio of 2 to 1 to focus on the ^{119}Sn NMR signals centred at -170 ppm. The symbols (f) to (j) indicate the $^1\text{J}(^{195}\text{Pt}-^{119}\text{Sn})$ satellites due to the respective isotopologues. The isotopologues/ isotopomers responsible for the individual ^{119}Sn NMR signals in the main set of signals are indicated by the arrows.
- Figure 4.11:** ^{119}Sn NMR spectrum of the solution with a $[\text{Pt}(\text{SnCl}_3)_5]^{3-}$ to $[\text{Pt}(\text{SnBr}_3)_5]^{3-}$ ratio of 2 to 1. Only a partial part of the spectrum is shown as to focus on the upfield shift obtained when Br^- adds to the NMR active ^{119}Sn ligand, as suppose to adding to an NMR inactive tin ligand.

List of Tables

- Table 1.1:** Magnetic Properties of Pt and Sn Isotopes with $I = \frac{1}{2}$
- Table 3.1:** Natural Abundances of the stable tin and platinum isotopes and the magnetic properties of those with $I = \frac{1}{2}$ which are highlighted.
- Table 3.2:** The NSA's calculated for the respective isotopologues of the $[\text{Pt}(\text{SnCl}_3)_5]^{3-}$ complex anion compared to the ^{119}Sn NMR signal areas experimentally obtained for the $^1\text{J}(^{195}\text{Pt}-^{119}\text{Sn})$ and $^2\text{J}(^{117}\text{Sn}-^{119}\text{Sn})$ satellites due to the respective isotopologues.
- Table 3.3:** Experimentally obtained ^{119}Sn NMR data compared to values reported in literature.
- Table 3.4:** Comparison of the ^{195}Pt NMR signal areas experimentally obtained with ^{195}Pt NMR to calculated NSA's of the possible isotopologues of the $[\text{Pt}(\text{SnCl}_3)_5]^{3-}$ complex anion.
- Table 3.5:** Comparison of the ratio of ^1J coupling constants to the ratio of gyromagnetic ratios of magnetically-active Sn isotopes present in respective isotopologues.
- Table 3.6:** Comparison of the ^{195}Pt NMR signal areas experimentally obtained with ^{195}Pt NMR to calculated NSA's of the possible isotopologues of the $[\text{Pt}(\text{SnBr}_3)_5]^{3-}$ complex anion.
- Table 3.7:** Comparison of the ratio of ^1J coupling constants of respective ^1J satellites to the ratio of gyromagnetic ratios of magnetically-active Sn isotopes present in respective isotopologues.
- Table 3.8:** ^{195}Pt NMR data obtained for the $[\text{Pt}(\text{SnCl}_3)_5]^{3-}$ and the $[\text{Pt}(\text{SnBr}_3)_5]^{3-}$ complex anions.
- Table 3.9:** Comparative Pt-Sn and Sn-X bond lengths for $[\text{Pt}(\text{SnX}_3)_5]^{3-}$ ($X = \text{Cl}$ or Br) determined by DFT calculations.
- Table 4.1:** ^{195}Pt NMR Chemical shifts and tentative assignments of the $[\text{Pt}(\text{SnCl}_n\text{Br}_{15-n})]^{3-}$ ($n = 0 - 15$) species.

- Table 4.2:** Comparison of the ratio of ^1J coupling constants of respective ^1J satellites to the ratio of gyromagnetic ratios of magnetically-active Sn isotopes present in respective isotopologues.
- Table 4.3:** Comparison of the ^{195}Pt NMR signal areas experimentally obtained for $[\text{Pt}(\text{SnCl}_3)_5]^{3-}$ and $[\text{Pt}(\text{SnCl}_3)_4(\text{SnCl}_2\text{Br})]^{3-}$ with ^{195}Pt NMR to the calculated NSA's of the possible isotopologues/isotopomers of the species.
- Table 4.4:** Coupling constants measured for the $^1\text{J}(^{119/117}\text{Sn}-^{195}\text{Pt})$ satellites of isotopologues/isotopomers 7 to 13 of the $[\text{Pt}(\text{Sn}_5\text{Cl}_{14}\text{Br})]^{3-}$ complex anion
- Table 4.5:** ^{195}Pt NMR $\delta(^{195}\text{Pt})$ and $^1\text{J}(^x\text{Sn}-^{195}\text{Pt})$ parameters and assignments of the $[\text{Pt}(\text{SnCl}_n\text{Br}_{15-n})]^{3-}$ ($n = 0 - 15$) species.
- Table 4.6:** Ratios calculated for respective $^1\text{J}(^{119}\text{Sn}-^{195}\text{Pt})/^1\text{J}(^{117}\text{Sn}-^{195}\text{Pt})$ to be compared to the $\gamma(^{119}\text{Sn})/\gamma(^{117}\text{Sn})$ ratio, 1.046.
- Table 4.7:** $^1\text{J}(^{195}\text{Pt}-^{119}\text{Sn})$ coupling constants measured for ^1J satellites of the set of ^{119}Sn NMR signals centred at -123 ppm obtained with ^{195}Pt NMR compared to those obtained with ^{119}Sn NMR.
- Table 4.8:** Assignment of each individual ^{119}Sn NMR signal in the set of signals centred at - 123.0 ppm to a isotopologue/isotopomer of the respective heteroleptic $[\text{Pt}(\text{Sn}_5\text{Cl}_n\text{Br}_{15-n})]^{3-}$ ($n = 11 - 15$) species.
- Table 4.9:** $^1\text{J}(^{195}\text{Pt}-^{119}\text{Sn})$ coupling constants measured for ^1J satellites of the set of ^{119}Sn NMR signals centred at -170 ppm obtained with ^{195}Pt NMR compared to those obtained with ^{119}Sn NMR.
- Table 4.10:** Assignment of each individual ^{119}Sn NMR signal in the set of signals centred at - 170.0 ppm to a isotopologue/isotopomer of the respective heteroleptic $[\text{Pt}(\text{Sn}_5\text{Cl}_n\text{Br}_{15-n})]^{3-}$ ($n = 11 - 14$) species.

List of Schemes

Scheme 1.1: Anionic complexes of Ru(II), Rh(I), Ir(III) and Pt(II) characterized by Young and co-workers.

Scheme 2.1: Reaction scheme for the synthesis of the homoleptic $[\text{Pt}(\text{SnCl}_3)_5]^{3-}$ complex anion.

Scheme 2.2: Structure of the ion-exchanger, trioctylammonium chloride, used to extract $[\text{Pt}(\text{SnCl}_3)_5]^{3-}$ into chloroform-*d*.

Scheme 3.1: Single Crystal structure obtained by Alcock and Nelson for the red $[\text{Pt}(\text{SnCl}_3)_5]^{3-}$ complex anion.

Scheme 3.2: A schematic representation of different isotopologues that are possible for the $[\text{Pt}(\text{SnX}_3)_5]^{3-}$ ($\text{X} = \text{Cl}^-/\text{Br}^-$) complex anions. Replacement of any of the five tin atoms and/or the platinum atom with another isotope of Sn and/or Pt, respectively, results in a different isotopologue. All Cl^-/Br^- are left out for clarity.

Scheme 3.3: A schematic representation of different isotopomers of the $[\text{Pt}(\text{SnX}_3)_5]^{3-}$ ($\text{X} = \text{Cl}^-/\text{Br}^-$) complex anions. (a) and (b) are isotopomers of each other as they have the same number of each isotopic atom, but in (a) ^ySn is in the equatorial position and in (b) ^ySn is in the axial position.

Scheme 3.4: Isotopologues of the $[\text{Pt}(\text{SnCl}_3)_5]^{3-}$ complex anion with the general formula $[\text{}^i\text{Pt}(\text{}^{119}\text{SnCl}_3)_n(\text{}^i\text{SnCl}_3)_{5-n}]^{3-}$ ($n = 1 = 5$) that are collectively referred to as isotopologue **G1** ($\text{Pt} \neq \text{}^{195}\text{Pt}$).

Scheme 3.5: Various isotopologues observed in the ^{119}Sn NMR spectrum recorded for the $[\text{Pt}(\text{SnCl}_3)_5]^{3-}$ complex anion. Due to rapid Berry-pseudo rotation on the NMR acquisition time scale, it is not possible to distinguish between isotopomers and isotopologues. All chlorides were left out for clarity. Isotopologues **3**, **5** and **6** have not previously been observed with ^{119}Sn NMR.

- Scheme 3.6:** Isotopologues of the $[\text{Pt}(\text{SnCl}_3)_5]^{3-}$ complex anion with the general formula $[\text{}^{195}\text{Pt}(\text{}^{119}\text{SnCl}_3)_n(\text{}^{119}\text{SnCl}_3)_{5-n}]^{3-}$ ($n = 1 = 5$) that are collectively referred to as isotopologue **G2** ($\text{Pt} = \text{}^{195}\text{Pt}$).
- Scheme 3.7:** Various isotopologues of $[\text{Pt}(\text{SnBr}_3)_5]^{3-}$ observed with ^{119}Sn NMR. Due to rapid Berry-pseudo rotation on the NMR acquisition time scale, it is not possible to distinguish between isotopomers and isotopologues. All Br were left out for clarity.
- Scheme 3.8:** Isotopologues of $[\text{Pt}(\text{SnCl}_3)_5]^{3-}$ observed with ^{195}Pt NMR. Due to the rapid Berry-pseudo rotations, it is not possible to distinguish isotopomers from isotopologues. All Cl^- were left out for clarity. Isotopologues **2.2**, **3**, **9** and **10** have not been reported in literature.
- Scheme 3.9:** Isotopologues of $[\text{Pt}(\text{SnBr}_3)_5]^{3-}$ observed with ^{195}Pt NMR. Isotopologues **IX**, **II.2**, **X** and **III** have not been reported in literature.
- Scheme 4.1:** Structure of the heteroleptic $[\text{Pt}(\text{Sn}_5\text{Cl}_{14}\text{Br})]^{3-}$ species, showing the two types of coordinating tin ligands, SnCl_3^- and SnCl_2Br^- .
- Scheme 4.2:** Structures of the various isotopologues and isotopomers possible for the $[\text{Pt}(\text{Sn}_5\text{Cl}_{14}\text{Br})]^{3-}$ complex anion. Only isotopologues with one spin-active Sn nucleus is shown. Structures a to c, and d to f are isotopologues of each other, whereas a and d, b and e, c and f are isotopomer pairs.
- Scheme 4.3:** The isotopologues of the 14 heteroleptic species responsible for the ^{195}Pt NMR signals numbered 2 – 15 in Figure 4.2. All the isotopologues contain ^{195}Pt and no magnetically-active Sn nuclei. Several isotopomers are also possible for these species and are illustrated in Appendix B. These 14 particular isotopologues/isotopomers are encircled in Appendix B.
- Scheme 4.4:** The 14 isotopologues and isotopomers possible for the $[\text{Pt}(\text{Sn}_5\text{Cl}_{14}\text{Br})]^{3-}$ complex anion. The double headed arrows show isotopomers associated with a particular isotopologue. For example **28** is an isotopomer of **25** in the sense that in **25** three Cl^- are bonded to ^{119}Sn compared to the two Cl^- and one Br^- bonded to ^{119}Sn in **28**.

Scheme 4.5: The 7 mixed halide complex anions, known from the ^{195}Pt NMR spectrum, to be present in the solution with a $[\text{Pt}(\text{SnCl}_3)_5]^{3-}$ to $[\text{Pt}(\text{SnBr}_3)_5]^{3-}$ ratio of 2 to 1. It should be noted that only one representative isomer of each species is shown here, though many more are possible.

Scheme 4.6: Isotopomers of the 6 $[\text{Pt}(\text{Sn}_5\text{Cl}_n\text{Br}_{15-n})]^{3-}$ ($n = 10 - 15$) heteroleptic complex anions with the general formula $[\text{Pt}(^{119}\text{SnCl}_3)(\text{Sn}_4\text{Cl}_n\text{Br}_{12-n})]^{3-}$ ($n = 7 - 12$). In parenthesis are given the corresponding isotopologues that contain the magnetically-active ^{195}Pt nucleus and are illustrated in Schemes 3.6, 4.4 and the Schemes shown in Appendix B.

Scheme 4.7: Isotopomers of the 5 $[\text{Pt}(\text{Sn}_5\text{Cl}_n\text{Br}_{15-n})]^{3-}$ ($n = 11 - 15$) heteroleptic complex anions with the general formula $[\text{Pt}(^{119}\text{SnCl}_2\text{Br})(\text{Sn}_4\text{Cl}_n\text{Br}_{12-n})]^{3-}$ ($n = 8 - 12$). In parenthesis are given the corresponding isotopologues that contain the magnetically-active ^{195}Pt nucleus and are illustrated in Scheme 4.4 and the Schemes shown in Appendix B.

Chapter 4

Characterization of the heteroleptic $[Pt(Sn_5Cl_nBr_{15-n})]^{3-}$ ($n = 0 - 15$) complex anions by means of high resolution ^{195}Pt and ^{119}Sn NMR

Chapter I

General Introduction, Background and Objectives of Study

The reaction of stannous chloride with the ions or complexes of the platinum group metals (Pt, Rh, Ir, Pd, Ru and Os) in solution was a key chemical reaction in the discovery of these noble elements, in that trace levels of these metal ions could be determined by their characteristic colours.¹ The interest of these complexes increased with the discovery of their high catalytic activity toward hydrogenation and isomerization reactions.

1.1. Reactions of Platinum with Stannous Chloride in Hydrochloric Acid Medium

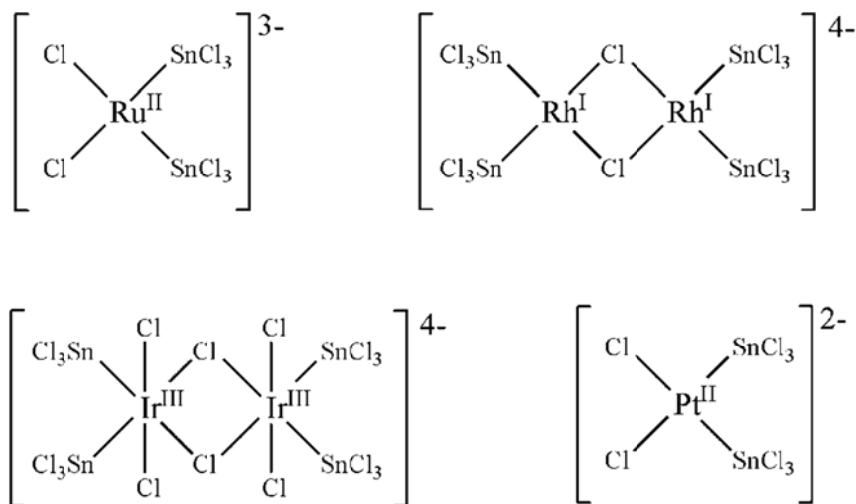
The reaction of platinum group metals (PGM) with stannous chloride in hydrochloric acid has thus a long and interesting history.¹⁻³ These reactions are characteristic for the intense colours they produce ranging from blue to green, yellow and blood-red in 1 - 6 M HCl solution. This phenomenon was first observed more than two centuries ago, in 1804, by W. H. Wollaston¹ who reported a colour change from pale yellow to intense blood-red when an acid solution of platinum(II/IV) was treated with excess stannous chloride. This reaction greatly resembled that of “Purple of Cassius”, wherein the reaction of Sn(II) chloride with Au(III) produces a purple colour ascribed to finely dispersed metallic gold that is absorbed onto an insoluble form of hydrous stannic oxide. “Purple of Cassius” is recognised as one of the earliest qualitative colorimetric methods for the determination of trace levels of Au.^{4,5} Due to the similarities between these two reactions, the reaction between Pt(IV) and stannous chloride was readily adopted as a qualitative spot test for trace levels of platinum.^{6,7,8} However, the nature of the species responsible for these coloured solutions was not clear until the late 1950's.⁶⁻¹¹

1.1.1. Nature of coloured Pt-Sn species

In 1907, Wöhler reported the formation of an intense blood-red colour when Pt(IV) reacted with stannous chloride in a diluted hydrochloric medium.^{9,10} As this reaction is analogous to the reaction of “purple of Cassius”, it was assumed that the intense blood-red colour was obtained due to the reduction of Pt(IV) to colloidal platinum. Other authors attributed the colour formation to chloroplatinous acid,^{11,12} while others still claimed it to form due to a simple reduction of Pt(IV) to Pt(II) by tin(II)chloride.^{13,14} In 1934 H. Wölbing demonstrated the extractability of the red Pt-Sn compounds into ethyl acetate, and thus disproved the proposed formation of colloidal platinum as in the case of “purple of Cassius”.⁶ Furthermore, Wölbing demonstrated a quantitative colorimetric method for the determination of trace levels of Platinum.⁶

In an attempt to elucidate the correct nature of the species responsible for the intense colour formed between Sn(II) chloride and platinum^{7,8,15}, palladium⁸, rhodium⁸ in HCl, Ayres and Meyer undertook a series of detailed spectrophotometric investigations. During these studies it was shown that the coloured material readily passes through a semi-permeable membrane, and that it is rapidly and completely extracted into organic solvents, ruling out the formation of colloidal platinum.^{7,8} Ayres and Meyer postulated that the predominant species formed in 3 M HCl is a cation, $[\text{Pt}^0\text{Sn}_4\text{Cl}_4]^{4+}$, in which the platinum was thought to be reduced to the zerovalent state.^{7,8,15} This postulate was based on the observation that tin(IV) was found in solutions of $\text{PtCl}_4^{2-}/\text{PtCl}_6^{2-}$ treated with stannous chloride.¹⁵ Elizarova and Matvienko¹⁶ studied the same system by means of potentiometric and polarographic methods and came to similar conclusions as Ayres and Meyer.

The existence of a cationic $[\text{Pt}^0\text{Sn}_4\text{Cl}_4]^{4+}$ species was however readily disproved by Shukla^{17,18} who showed by means of electrophoresis that anionic species are present in dilute hydrochloric solutions in both the rhodium and the platinum-tin systems. Young and co-workers^{19,20} came to similar conclusions in their study of platinum group metals with tin(II) chloride. From this study it was found that rhodium, platinum, ruthenium and iridium all formed coloured solutions in the presence of Sn(II) chloride. Furthermore it was shown that on addition of large cations such as tetramethyl ammoniumchloride all the solutions readily formed precipitates, suggesting that the anionic complexes of Pt(II), Rh(I), Ir(III) and Ru(I) shown in Scheme 1.1 are formed.

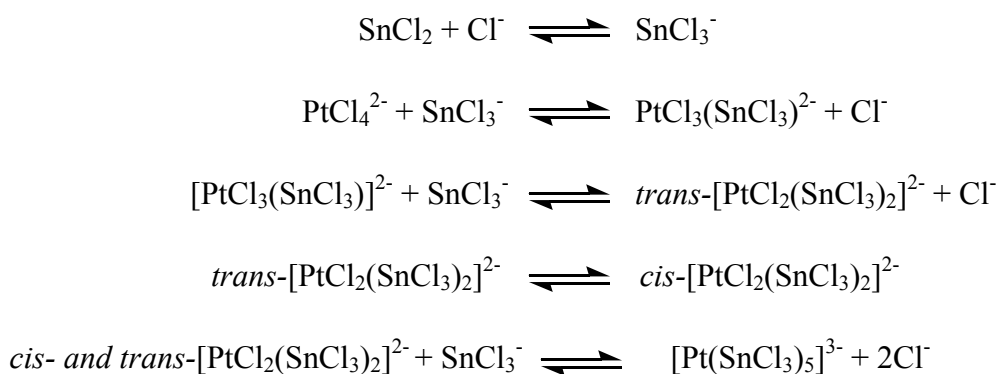


Scheme 1.1: Anionic complexes of Ru(II), Rh(I), Ir(III) and Pt(II) characterized by Young and co-workers.^{19,20}

With this Young and co-workers^{19,20} confirmed the presence of anionic species in the aqueous acid solutions. Moreover, Young *et al*¹⁹ formulated these complexes to be complexes of tin(II) and not tin(IV), as in the case of π -C₅H₅W(CO)₃SnCl₃.^{21, 22} Increased interest in the elucidation of the nature of the Pt-Sn species was spurred on by the discovery of the high catalytic activity of these complexes towards homogeneous hydrogenation and isomerization reactions.²³

The correct nature of the highly coloured species formed by reaction of Pt(II) and Rh(II) with tin(II) chloride was first revealed by two independent groups.^{20,23} As part of their study on homogeneous hydrogenation of ethylene and acetylene with Pt-SnCl complexes, Cramer *et al*²³ isolated and crystallized compounds such as red [(C₆H₅)₃PCH₃]₃[Pt(SnCl₃)₅] and yellow [(C₆H₅)₃PCH₃]₃[PtCl₂(SnCl₃)₂], as well as the pale yellow, uncharged [Pt(P(C₆H₅)₃)₂(SnCl₃)Cl] compound. Cramer *et al* was the first group that successfully isolated these red and yellow compounds.^{23,24} The red [(C₆H₅)₃PCH₃]₃[Pt(SnCl₃)₅] species is the first example of a *five coordinate* Pt(II) species with monodentate ligands. At more or less the same time Young *et al*^{19,20} isolated two isomers of the square-planar complexes of platinum, *cis*- and *trans*-[PtCl₂(SnCl₃)₂]²⁻, from solutions containing Sn:Pt ratios of 2:1. From the electronic spectra obtained the yellow crystal was assigned to the *cis*-isomer. Moreover, Young *et al* concluded that the red isomer, *trans*-[PtCl₂(SnCl₃)₂]²⁻, are kinetically favored, while the yellow form is thermodynamically more stable.¹⁹ This was attributed to the stronger

d_{π} - d_{π} bonding between tin and platinum in the yellow isomer compared to relatively weaker π -back bonding within the red isomer, due to competition between the two SnCl_3^- groups for the same d-orbitals of the Pt(II) ion. Young *et al*¹⁹ suggested that several equilibria exist simultaneously in solution:



Both the groups of Young *et al*¹⁹ and Stolberg *et al*²⁵ suggested that the initial formation of the *trans*-isomer was favored due to the stronger *trans*-effect of SnCl_3^- compared to Cl^- . More than a decade later, Parish and Rowbotham²⁶ showed by means of ^{119}Sn NMR and Mossbauer spectroscopy that only two Pt-Sn species exist in solution, the one being *cis*- $[\text{PtCl}_2(\text{SnCl}_3)_2]^{2-}$ and the other being either the *trans*-isomer or the *five-coordinate* $[\text{Pt}(\text{SnCl}_3)_5]^{3-}$ species. It was found that in the presence of excess tin(II) chloride, the yellow solution turns red, indicating that the species formed in solution are dependent on the concentration of tin(II) added to the solution. As an isomerization equilibrium do not depend on the concentration of tin(II), Parish and Rowbotham²⁶ suggested that the substance responsible for the intense red colour in solution is the $[\text{Pt}(\text{SnCl}_3)_5]^{3-}$ species. Since then, several authors have confirmed by means of ^{119}Sn and ^{195}Pt NMR that the $[\text{Pt}(\text{SnCl}_3)_5]^{3-}$ species are responsible for the blood-red colour.^{2,27,28,29} In addition to the $[\text{PtCl}_3(\text{SnCl}_3)]^{2-}$, *cis*- $[\text{PtCl}_2(\text{SnCl}_3)_2]^{2-}$ and $[\text{Pt}(\text{SnCl}_3)_5]^{3-}$ complex anions, Pregosin and Rügger²⁸ showed that the $[\text{PtCl}(\text{SnCl}_3)]^{2-}$ and $[\text{Pt}(\text{SnCl}_3)_4]^{2-}$ complex anions also exist in solution. Thus, several Pt-Sn complex anions are in equilibrium in solutions of tin(II)chloride and platinum(II/IV)chloride, depending on the concentration of tin(II) added. Moreover, unlike for gold(III/I) ions which are completely reduced to metallic gold nano-particles ('purple of Cassius') by stannous chloride, Pt(IV/II) forms complexes with tin(II) chloride in which the SnCl_3^- acts as a ligand to Pt(II).

1.2. The nature of SnX_3^- ($\text{X} = \text{Cl}^-/\text{Br}^-$) as a ligand

In the reactions of Pt(II/IV) with tin(II)chloride, the tin(II)chloride acts as both reducing agent and as ligand in the form of the SnCl_3^- moiety.^{2,3,30-37} Relative little work has been done pertaining to the redox reactions with the platinum group metals in general.³ Moodley and Nicol³⁰ showed that Pt(IV) in HCl is rapidly reduced by tin(II) chloride according to the overall rate law:³⁰

$$-d[\text{Pt(IV)}]/dt = k_{\text{obs}}[\text{Pt(IV)}][\text{Sn(II)}] \quad \dots(1.1)$$

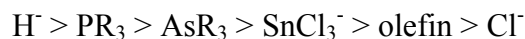
Where $k_{\text{obs}} = 473 \pm 22 \text{ dm}^3 \text{ mol}^{-1} \text{ s}^{-1}$ at 297 K. It was shown that the rate of reduction of Pt(IV) by Sn(II)chloride is much faster than the rate of formation of a complex with Pt:Sn 1:1. Several studies have been done on the SnCl_3^- moiety as a ligand.^{2,31,32,33} The SnCl_3^- ligands are usually coordinated to the metal ion through the tin atom.^{23,24,31-33} However, the electronic nature of the trichlorostannato anion and its unusual ability to stabilize the *five-coordinate* platinum is surrounded by some controversy. Parshall³⁴ studied the σ -donor and π -acceptor ability of the SnCl_3^- ligand by analyzing the ^{19}F NMR shielding parameters of fluorophenyl platinum complexes, where the SnCl_3^- ligand is *trans* to the phenyl group. With this method Parshall characterized SnCl_3^- as weak σ -donors and strong π -acceptors. Graham *et al*^{35,36} came to similar conclusions as Parshall by analyzing the carbonyl force constants of $(\text{SnCl}_3)\text{Mn}(\text{CO})_5$ (obtained by the Cotton and Kraihanzel method³⁷). However, there are differences of opinion regarding the relative σ -donor and π -acceptor abilities of SnCl_3^- compared to SnBr_3^- .^{29,32,38} From the identical Fe-Sn bond lengths obtained in the $(\eta^5\text{-C}_5\text{H}_5)\text{Fe}(\text{CO})_2(\text{SnX}_3)$ ($\text{X} = \text{Cl}^-/\text{Br}^-$) compounds, Stokely *et al* suggested that there is not a difference in the relative σ -donor and π -acceptor abilities of SnCl_3^- and SnBr_3^- .³⁸ In contrast, Antonov *et al*³² found, by analysis of the relative change in Mössbauer (^{119}Sn) isomer shifts ($\Delta\delta$) and quadrupole splittings (ΔQ) of the free ion in $\text{Et}_4\text{N}[\text{SnX}_3]$ ($\text{X} = \text{Cl}^-/\text{Br}^-$) as compared to the coordinated ligand in the *trans*- $[\text{XPt}(\text{SnX}_3)(\text{PPh}_3)_2]$ and *trans*- $[\text{HPt}(\text{SnX}_3)(\text{PPh}_3)_2]$ ($\text{X} = \text{Cl}^-/\text{Br}^-$) complexes, that the SnBr_3^- ligand is a stronger σ -donor, as well as a slightly stronger π -acceptor than SnCl_3^- . Yet another opinion, by Nelson *et al*, is that SnCl_3^- is a better σ -donor and/or π -acceptor toward Pt(II) than is SnBr_3^- .²⁹ Nelson *et al* based their argument on the X-ray data obtained for the *cis*- $[\text{PtX}_2(\text{SnX}_3)]^{2-}$ ($\text{X} = \text{Cl}^-/\text{Br}^-$) complex anions, as well as on ^{119}Sn and ^{195}Pt NMR data obtained for *cis*- $[\text{PtX}_2(\text{SnX}_3)]^{2-}$ and $[\text{Pt}(\text{SnX}_3)_5]^{3-}$ ($\text{X} = \text{Cl}^-/\text{Br}^-$)

complex anions. The X-ray data showed that Pt-Sn bond lengths are elongated for the SnBr_3^- complexes, and the ^{119}Sn NMR data showed that the platinum-tin coupling constants are larger for the SnCl_3^- complexes than for the SnBr_3^- complexes.

Even though the relative π -acceptor abilities of the SnCl_3^- and SnBr_3^- ligands differ, both are shown to be strong π -acceptors. As it has been shown that other strong π -acceptors, such as CO and CN^- , are strong *trans* directors^{39,40,41} it is suggested that it is the combination of SnCl_3^- ions being weak σ -donors and strong π -acceptors that causes the *trans* directing behavior thereof.²⁵ Furthermore, the d_{π} - d_{π} overlap between transition metals and tin(II) is responsible for the *trans* activating nature of the SnCl_3^- anion.^{19,42} Care should be taken to avoid ambiguity when referring to the *trans* influence and *trans* effect. The former is an thermodynamic concept, describing the extent to which that ligand weakens the bond *trans* to it in the equilibrium state of the substrate, whereas the latter is a kinetic effect that relates to the influence of a coordinated group upon the rate of substitution of ligands *trans* to it.⁴¹ Lindsey *et al.*²⁵ studied the *trans* effect of the SnCl_3^- ligand by criteria described by Chatt and co-workers.^{43,44} These investigators set up a *trans* series by ranking ligands (X) in terms of their ability to shift the Pt-H infrared stretching frequency and ^1H NMR frequency in *trans*- $[(\text{C}_2\text{H}_5)_3\text{P}]_2\text{PtHX}$ compounds. Lindsey *et al.*²⁵ showed that the SnCl_3^- ligand lies between NCS^- and CN^- , the two most powerful ligands in the Chatt series:



Conversely to its high *trans* effect, SnCl_3^- appears to have a moderate *trans* influence, as evidenced by the *trans* influence series derived by Rügger *et al.*⁴⁵ based on $^1\text{J}(^{119}\text{Sn}-^{195}\text{Pt})$ coupling constants of $(\text{PPN})[\text{Pt}(\text{SnCl}_3)_3\text{L}_2]$ containing similar L ligands:



A separate study done by Albinati *et al.*⁴⁶ on the effect of SnCl_3^- on the $^2\text{J}(\text{Pt}-\text{CH}_3)$ of the *trans*- $[\text{Pt}(\text{SnCl}_3)(\text{CH}_3)(\text{PEt}_3)_2]$ complex, supported the findings of Rügger *et al.*⁴⁵ in that they also suggested the *trans* influence of SnCl_3^- to be similar to that of an olefin. This low *trans* influence of the SnCl_3^- ligand agrees with the weak σ -donor properties suggested earlier. Furthermore, the mutual influence of the ligands in *trans*- $[\text{HPtX}(\text{PPh}_3)_2]$ and *trans*- $[\text{XPt}(\text{SnX}_3)(\text{PPh}_3)_2]$ ($\text{X} = \text{Cl}^-, \text{Br}^-, \text{SnCl}_3^-, \text{or SnBr}_3^-$) has been studied Antonov *et al.*³² From the $\nu(\text{Pt}-\text{H})$ wavenumbers and the $\delta(\text{Pt}-\text{H})$ chemical shifts, ligands X can be arranged in order of *trans* influence:



The strong *trans*-activation of $\text{SnCl}_3^-/\text{SnBr}_3^-$ undoubtedly plays an important role in the catalytic activity and facile ligand-exchange reactions observed for platinum metal-tin halide complexes. The strong π -acceptor ability of the SnX_3^- ($X = \text{Cl}^-/\text{Br}^-$) removes electron density from the Pt(II) centre and so protects Pt(II) against reduction to the metal form as is the case with “Purple of Cassius”.^{23,25} In the presence of excess SnX_3^- ($X = \text{Cl}^-/\text{Br}^-$) the *five-coordinate* $[\text{Pt}(\text{SnX}_3)_5]^{3-}$ complex anion is predominant in solution.

1.3. Application of ^{119}Sn and ^{195}Pt NMR Spectroscopy as a tool to study the Nature of Pt-Sn complexes

^{119}Sn and ^{195}Pt NMR spectroscopy has proven to be an indispensable tool for determining the stoichiometry and geometry of transition-metal tin complexes.² Tin has ten natural occurring isotopes, of which three have spin, $I = 1/2$, ^{119}Sn , ^{117}Sn and ^{115}Sn . Platinum only has one nucleus suitable for NMR observation, ^{195}Pt . The magnetic properties of the NMR-active Pt and Sn nuclei are given in Table 1.1.⁴⁷

Table 1.1: Magnetic Properties of Pt and Sn Isotopes with $I = 1/2$.

NMR-active isotope	Natural Abundance / %	Spin	Gyromagnetic Ratio ^a $\gamma/2\pi$ MHz T ⁻¹	Receptivity ($^{13}\text{C} = 1$)
^{195}Pt	33.7	$1/2$	9.1534	19.1
^{119}Sn	8.58	$1/2$	-15.869	25.6
^{117}Sn	7.61	$1/2$	-15.168	19.9
^{115}Sn	0.35	$1/2$	-13.922	0.715

^a $\gamma/2\pi$ ^1H is 42.467

Although both ^{119}Sn and ^{117}Sn can be detected using NMR to characterize tin complexes, ^{119}Sn has a slightly higher receptivity (natural abundance x sensitivity), Table 1.1, and is therefore usually preferred. Due to the low natural abundance of ^{115}Sn , it has been ignored in

literature. The natural abundance of the ^{195}Pt isotope (33.7%), together with an NMR receptivity of 19.1 relative to ^{13}C implies that ^{195}Pt NMR spectra are easily obtainable.⁴⁷ Furthermore ^{195}Pt shieldings are especially sensitive to the oxidation state and among other things the molecular structure of the complex in solution. This together with the extremely large ^{195}Pt chemical shift range ($^{195}\text{Pt} > 13000$ ppm) makes ^{195}Pt NMR an ideal method for speciation studies.⁴⁸ In view of this, ^{119}Sn and ^{195}Pt NMR are mostly utilized to elucidate the structures of these Pt-Sn complexes in solution. The three types of measurable quantities in NMR that are of importance for structure elucidation are chemical shifts, coupling constants and relaxation times.⁴⁹

The chemical shift measured for a particular compound is an indication of the degree of shielding experienced by the nucleus in question, which in turns gives information about the electron cloud surrounding that nucleus.⁴⁷ The relationship between ν_A , the Larmour Frequency, B_0 , the applied magnetic field, σ_A , the magnetic shielding constant of nucleus A and the gyromagnetic ratio, γ , is:

$$\nu_A = \frac{\gamma}{2\pi} B_0 (1 - \sigma_A) \quad \dots(1.2)$$

However, this analysis is complicated by the fact that there are several factors that may contribute to the shielding, σ_A , of a nucleus in a molecular environment.

$$\sigma_A = \sigma_d + \sigma_p + \sigma_n \quad \dots(1.3)$$

Where σ_d and σ_p represent the diamagnetic and paramagnetic contributions to the shielding arising from the local electron cloud, and σ_n represents all the contributions from remote sources. In the case of tin-transition metal complexes, the complex bonding interactions between tin-based ligands and transition metals result in an unusually large chemical shift range (> 2000 ppm) in the ^{119}Sn NMR spectrum.^{2,47} This is interpreted as being due to σ_p being the controlling factor in ^{119}Sn chemical shifts and σ_p being greatly affected by a ligand such as SnCl_3^- bonding with a transition metal. The reason for this is that SnCl_3^- acts as a weak σ - donor, but a strong π -acceptor. These π -interactions provide a low-energy electronic state, thereby reducing the magnitude of the average excitation energy, ΔE , which in turn affects the shielding arising from the local electron cloud, σ_p . However, many more factors

come into play, such as the solvent, concentration and temperature effects that might affect the chemical shift. Therefore, interpretation of the chemical shift obtained for ^{119}Sn is limited to a qualitative level. Nonetheless, the stoichiometry of the complex and the chemical environment of the respective nuclei can still be determined from the chemical shifts observed for the NMR-active nuclei, as well as from the relative signal intensities measured.²

The ^{195}Pt chemical shift values of compounds ($\delta(^{195}\text{Pt})$) is exceptionally sensitive to changes within the coordination sphere of the compound.^{45,48} This is evidenced by the large upfield shifts of the ^{195}Pt resonances obtained for catalytically active Pt-Sn complexes such *trans*-[PtH(SnCl₃)(PEt₃)], *trans*-[Pt(SnCl₃)₂(PEt₃)₂] and [PtCl(SnCl₃)(PEt₃)₂] on replacing Cl with SnCl₃.^{45,49} Therefore ^{195}Pt chemical shifts provide important information regarding the stoichiometry of compounds and the chemical environment of the ^{195}Pt nuclei. However, when it comes to the assignment of structures to tin-transition metal complexes, coupling constants are usually more important than the chemical shifts measured.^{51,52,53} Unusually large spin-spin couplings are obtained for these Pt(II)-Sn(II) complexes,^{2,27,49,50} including the largest one bond spin-spin coupling ever measured, $^1J(^{119}\text{Sn}-^{195}\text{Pt}) = 28\,954\text{ Hz}$, which was measured for the *trans*-[PtCl(SnCl₃)(PEt₃)₂] complex by Ostoja Starzewski and Pregosin.^{49,50} These extremely large one bond couplings between Pt and Sn can be understood in terms of the Fermi contact expression used by Pople and Santry:⁵⁴

$$^1J(A, B) \propto \gamma_A \gamma_B |\Psi_{ns_A}(0)|^2 |\Psi_{ns_B}(0)|^2 \pi_{A,B} \quad \dots(1.4)$$

$$\pi_{A,B} = \sum_i^{occ} \sum_j^{unocc} (\epsilon_j - \epsilon_i)^{-1} c_{i,A} c_{j,A} c_{i,B} c_{j,B} \quad \dots(1.5)$$

The symbols γ represent the gyromagnetic ratios of nuclei, the terms $|\Psi_{ns}(0)|^2$ are the valence s-electron densities at the nuclei, A and B, and $\pi_{A, B}$ is the mutual polarizability. The $\pi_{A, B}$ expression contains the s coefficients of the atomic orbitals used in the linear combinations that make up the occupied and unoccupied molecular orbitals, as well as a difference term $(\epsilon_j - \epsilon_i)$ where ϵ_i is the energy of an occupied and ϵ_j an unoccupied molecular orbital. The amount of s-character in the metal-metal bond is presumably increased by the presence of the three electron-withdrawing chlorido substituents on the tin. Thus, in view of this expression, the high mutual polarizability of the s-orbitals on Pt and Sn, a high s-character in the bond, and the relatively large gyromagnetic ratios of Sn and Pt all account for

the unusually large spin-spin couplings of these complexes. The ^{119}Sn and ^{195}Pt NMR data obtained by several groups⁴⁵⁻⁶² for Pt-Sn species has led to the following empiricisms:^{57,59}

1. Increasing the number of coordinated SnCl_3^- ligands shifts $\delta(^{195}\text{Pt})$ to successively higher field
2. Increasing the number of coordinated SnCl_3^- ligands shifts $\delta(^{119}\text{Sn})$ to successively lower field
3. SnCl_3^- has an cis effect on $^1\text{J}(^{195}\text{Pt}-^{119}\text{Sn})$
4. $^2\text{J}(^{119}\text{Sn}-^{117}\text{Sn})_{\text{trans}} > ^2\text{J}(^{119}\text{Sn}-^{117}\text{Sn})_{\text{cis}}$
5. $^2\text{J}(^{119}\text{Sn}-^{117}\text{Sn})$: larger in five-coordinate complexes than in four coordinate *cis* complexes

Moreover, $^1\text{J}(^{195}\text{Pt}-^{119}\text{Sn})$ is in the order of kHz (sometimes > 30 kHz) and depends on the trans ligand. $^2\text{J}(^{119}\text{Sn}-^{117}\text{Sn})$ is also in the order of kHz with $^2\text{J}(^{119}\text{Sn}-^{117}\text{Sn})_{\text{trans}}$ routinely exceeding 20 000 Hz,^{45,50} whereas $^2\text{J}(^{119}\text{Sn}-^{117}\text{Sn})_{\text{cis}}$ show much more ‘modest’ values of less than 10 000 Hz. Even more, Seddon *et al*⁶³ reported the remarkably large $^3\text{J}(^{117}\text{Sn}-^{119}\text{Sn})$ coupling constant of 24 300 Hz obtained for $[\text{Pt}_2(\text{SnCl}_3)_2(\mu\text{-dppm})_2]$ by means of ^{119}Sn and ^{117}Sn NMR.

1.4. Catalytic Properties of Trichlorostannato-Platinum Complexes

The early interest in solutions of chloroplatinic acid and stannous chloride as catalyst was sparked by the discovery that these systems catalyzed the homogeneous hydrogenation of ethylene and acetylene at room temperature and atmospheric pressure of hydrogen.²³ Cramer *et al* showed that the reaction of ethylene at atmospheric pressure with a solution of K_2PtCl_4 in the presence of stannous chloride in HCl gave quantitative conversion to Zeise’s salt, $\text{KPtCl}_3\text{C}_2\text{H}_4\cdot\text{H}_2\text{O}$ within 1.5 h. In the absence of stannous chloride, no Zeise’s salt was formed. On the other hand, it is known that simple chloro-complexes of platinum catalyzes the formation of $[\text{Pt}(\text{olefin})\text{Cl}_3]^-$ complexes. However, under catalytic conditions, these reactions go hand-in-hand with the formation of colloidal metal deposits, which decreases the rate of the reaction. The catalytic effectiveness of complexes of the type ML_2X_2 ($\text{L} = \text{PR}_3/\text{AsR}_3$, $\text{M} = \text{Pd}/\text{Pt}$ and $\text{X} = \text{halide}/\text{pseudohalide}$) is enhanced by the presence of chlorides of group IVB (Si, Ge, Sn) which are believed to form metal-metal bonded compounds.⁶⁴ For example, the addition of ethylene to $[\text{PtCl}_2(\text{SnCl}_3)_2]^{2-}$ is almost thirty times easier than to PtCl_4^{2-} . This phenomenon is ascribed to the higher *trans* effect of SnCl_3^-

compared to Cl^- and thus the more pronounced π -acceptor character of SnCl_3^- bonded to Pt(II) as discussed earlier.^{25,29,34-36}

The rate of homogeneous hydrogenation is found to be maximum with a Pt:Sn ratio of more than 1:5, conditions that has proven favourable for the $[\text{Pt}(\text{SnCl}_3)_5]^{3-}$ species to be predominant.⁶⁴ However, as the formation of a Pt-olefin complex is a necessary step in hydrogenation reactions, and considering that $\text{cis-}[\text{PtCl}_2(\text{SnCl}_3)_2]^{2-}$ is the only active species for absorption of ethylene, the *cis* – *trans* isomerization is the rate determining step in the reaction. These reactions are to a great extent influenced by solvent effects.^{65,66} Moreover, Cramer *et al* showed that the $[\text{Pt}(\text{SnCl}_3)_5]^{3-}$ complex cleaves dihydrogen to form $[\text{PtH}(\text{SnCl}_3)_4]^{3-}$, a species that, under preparative conditions, promote homogeneous hydrogenation of olefins.²⁴ Again, these results are thought to be due to the high *trans* effect of the $(\text{SnCl}_3)^-$ ligand, which in turn is attributed to its high π -acceptor ability. Furthermore, Clark and Halpern⁶⁷ showed that tin(II) catalyzes the insertion of ethylene into the platinum-hydride bond of HPtL_2Cl . Shirshikova *et al*⁶⁸ showed that for the complexes of the type $[\text{MX}(\text{SnX}_3)_5]^{n-}$ ($\text{X} = \text{Cl}^-/\text{Br}^-$, and $\text{M} = \text{Pt}/\text{Ru}/\text{Os}/\text{Rh}/\text{Ir}$) the Pt compounds are extremely reactive for the isomerization of allyl benzene, whereas rhodium and iridium show lower activity and ruthenium and osmium are inert. Moreover, the catalytic activity of these complex anions is increased when Cl^- is replaced by Br^- in the SnX_3^- ligand. This phenomenon is due to the rise in lability of the coordinated link between the ligand and the metal centre which increases the concentration of the intermediate metal hydride and therefore increases the catalytic activity of the complex anion.⁶⁸

Thus, even though the role of tin(II) chloride in these catalytic systems is not completely understood, it is generally agreed that the SnCl_3^- ligand stabilizes reduction of Pt(II) by H_2 to the metallic state with the formation of complex hydride species. What is more is that the strongly “ π -acid” nature thereof labializes the often kinetically inert complexes of PGM to ligand substitution.^{3,24} This, together with the wide variety of readily available organotin compounds, increases the scope of many catalytic systems.

1.5. Aims and Objectives of this study

The species responsible for the formation of the blood red colour when SnCl_3^- is added to a dilute hydrochloric acid solution of PtCl_4^{2-} was first characterized by single crystal X-ray diffraction as the trigonal bipyramidal $[\text{Pt}(\text{SnCl}_3)_5]^{3-}$ complex anion.^{19,23} It was later confirmed by ^{119}Sn NMR and ^{195}Pt NMR spectroscopy that these species retain its trigonal bipyramidal structure in solution.²⁹ To date a crystal structure of the species formed when SnBr_3^- is added to a dilute hydrobromic acid solution of PtBr_4^{2-} could not be obtained. However, ^{119}Sn NMR and ^{195}Pt NMR studies have confirmed that the predominant species formed in these solutions are the homoleptic bromido complex anion, $[\text{Pt}(\text{SnBr}_3)_5]^{3-}$.^{2,29,69} Thus, ^{119}Sn and ^{195}Pt NMR are proven to be powerful tools for the characterization of Pt-Sn species in solution. In view of this, it is envisaged that high resolution ^{195}Pt and ^{119}Sn NMR can be used to study the speciation of the heteroleptic $[\text{Pt}(\text{Sn}_5\text{Cl}_n\text{Br}_{15-n})]^{3-}$ ($n = 0 - 15$) complex anions that may exist in mixed halide Pt-Sn solutions.

In this context, this study involves a detailed high resolution ^{195}Pt and ^{119}Sn NMR investigation of the possible isotopologues and isotopomers of the homoleptic $[\text{Pt}(\text{SnBr}_3)_5]^{3-}$ ($X = \text{Cl}^-/\text{Br}^-$) complex anions, as well as those of the heteroleptic $[\text{Pt}(\text{Sn}_5\text{Cl}_n\text{Br}_{15-n})]^{3-}$ ($n = 0 - 15$) species possible in solution.

Therefore, the specific objectives of this study are:

- i) to re-investigate the homoleptic $[\text{Pt}(\text{SnX}_3)_5]^{3-}$ ($X = \text{Cl}^-/\text{Br}^-$) complex anions by means of ^{119}Sn and ^{195}Pt NMR spectroscopy, with specific focus on the identification of all the isotopologues obtained for these species,
- ii) to do a detailed analysis of all the heteroleptic $[\text{Pt}(\text{Sn}_5\text{Cl}_n\text{Br}_{15-n})]^{3-}$ ($n = 0 - 15$) complex anions obtained in solution and its respective isotopologues and isotopomers by means of high-resolution ^{195}Pt and ^{119}Sn NMR spectroscopy.

Chapter II

Experimental, Methods of analysis and Preliminary investigations

In this chapter the synthesis of the homoleptic $[\text{Pt}(\text{SnX}_3)_5]^{3-}$ ($X = \text{Cl}^-/\text{Br}^-$) and the heteroleptic $[\text{Pt}(\text{Sn}_5\text{Cl}_n\text{Br}_{15-n})]^{3-}$ ($n = 0 - 15$) complex anions, as well as the methods used to characterize them are described. These complexes were synthesized in acidic aqueous solutions from which the anionic complexes were extracted into chloroform-*d* by means of an ion-pair solvent extraction reaction using methyltrioctylammonium chloride (Aliquat-336) as ion-pairing reagent. Moreover, in order to establish the optimal experimental conditions under which the 5-coordinate, trigonal bipyramidal species predominates, preliminary UV-Vis spectroscopy experiments were carried out, the results of which are discussed here.

2.1. Synthesis of the $[\text{Pt}(\text{Sn}_5\text{Cl}_n\text{Br}_{15-n})]^{3-}$ ($n = 0 - 15$) complex anions

All solutions were prepared using boiled-out ultrapure Milli-Q water ($\text{MQ} > 18\text{M}\Omega$) which was cooled and stored under nitrogen. Concentrated hydrochloric acid (analytical grade) and hydrobromic acid were also saturated with nitrogen by bubbling the gas through the acid for at least 15 minutes prior to use.

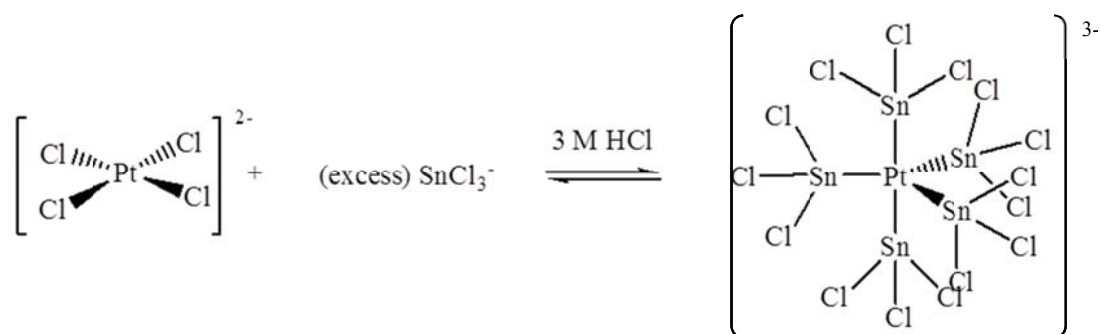
2.1.1. Synthesis and extraction of $[\text{Pt}(\text{SnCl}_3)_5]^{3-}$ complex anions

The homoleptic chlorido species prepared for the UV-vis and the NMR experiments were prepared in the same manner, with only varying the initial concentrations of the respective reagents used.

To prepare the solutions for UV-Vis analysis, the platinum(II) concentration was always kept constant at 1×10^{-4} mM, while the HCl concentration was changed from 0.5 to 3 M (Figure 2.1) and the Pt(II):Sn(II) ratio was varied from 1:1 to 1:15 (Figure 2.2). Moreover, separate Pt and Sn solutions were prepared separately and then added together. The orange K_2PtCl_4 salt was first weighed and dissolved in diluted hydrochloric acid (0.5 M or 3 M). Secondly the

amount of $\text{SnCl}_2 \cdot 2\text{H}_2\text{O}$ required to obtain the desired Pt:Sn ratio was weighed and first dissolved in concentrated HCl before being diluted to the required HCl concentration with ultrapure Milli-Q water ($\text{MQ} > 18 \text{ M}\Omega$). The $\text{SnCl}_2 \cdot 2\text{H}_2\text{O}$ is first dissolved in concentrated HCl to prevent oxidation from Sn(II) to Sn(IV) by atmospheric oxygen. The platinum and tin solutions were then added together. For the solutions where the Pt(II) concentration and the Pt:Sn ratio was kept constant and the HCl concentration was changed from 0.5 M to 3 M the UV-vis spectra of were recorded immediately after the two solutions were added together. The solutions where the Pt:Sn ratios were varied were allowed to stand for a hour before the UV-vis spectra were recorded.

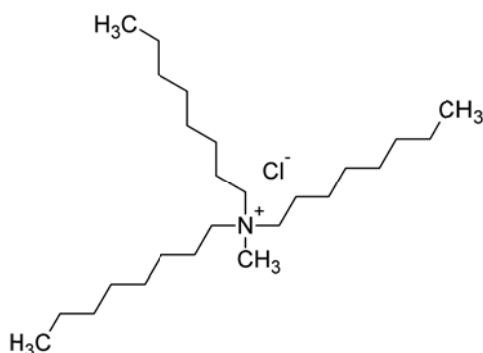
For ^{119}Sn and ^{195}Pt NMR analysis solutions of 0.2 M Pt(II) in 3 M HCl and with a Pt:Sn ratio of 1:7 were prepared. A 20 mL stock solution of 0.4 M PtCl_4^{2-} was prepared by dissolving K_2PtCl_4 in 3 M HCl. The tin solutions were always freshly prepared to minimize the effect of tin oxidation by atmospheric oxygen. The $\text{SnCl}_2 \cdot 2\text{H}_2\text{O}$ was dissolved in concentrated HCl and diluted with ultrapure Milli-Q water ($\text{MQ} > 18\text{M}\Omega$) to 3 M HCl. 0.5 mL of the Pt(II) stock solution was added to the 0.5 mL Sn(II) solution giving a solution of 0.2 M Pt(II) in 3 M HCl and with a Pt:Sn ratio of 1:7. The blood red solution was left for approximately an hour for the reaction to reach equilibrium, Scheme 2.1, before extracted into an organic phase.



Scheme 2.1: Reaction scheme for the synthesis of the homoleptic $[\text{Pt}(\text{SnCl}_3)_5]^{3-}$ complex anion.

The $[\text{Pt}(\text{SnCl}_3)_5]^{3-}$ was extracted into chloroform-*d* using trioctylammonium chloride (Aliquat-336), illustrated in Scheme 2.2, as ion-exchanger. Three molar equivalents of Aliquat-336 is needed to extract 1 mole of $[\text{Pt}(\text{SnCl}_3)_5]^{3-}$. Therefore a solution of 20 % (v/v) Aliquat-336 in chloroform-*d* was prepared by weighing off the required mass of Aliquat-336

and adding it to chloroform-*d*. After the hour had passed, the organic phase was added to the blood red aqueous Pt-Sn solution (0.5 mL) and the mixture was stirred slowly for 15 minutes.



Scheme 2.2: Structure of the ion-exchanger, triethylammonium chloride, used to extract $[\text{Pt}(\text{SnCl}_3)_5]^{3-}$ into chloroform-*d*.

Equation 2.1 Reaction scheme for the extraction of $[\text{Pt}(\text{SnCl}_3)_5]^{3-}$ into chloroform-*d* using Aliquat-336 as ion-exchanger.

The solutions was left to stand overnight to allow essentially all the coloured complexes to be extracted into the organic phase by the reaction showed in Equation 2.1. The blood red organic phase was transferred into a NMR tube for ^{119}Sn and ^{195}Pt NMR analysis.

2.1.2. Synthesis and extraction of the $[\text{Pt}(\text{SnBr}_3)_5]^{3-}$ complex anions

The homoleptic bromido species was synthesized only for ^{119}Sn and ^{195}Pt NMR analysis. The method as described above was used to synthesize the $[\text{Pt}(\text{SnBr}_3)_5]^{3-}$ species with the only change being the starting materials which is now K_2PtBr_4 , SnBr_2 and HBr . However, the K_2PtBr_4 salt proved to be troublesome, and K_2PtCl_4 was rather used and was dissolved in 3 M HBr . After mixing the two solutions and allowing it to reach equilibrium, it was observed that the bromido species are noticeably deeper in colour than the analogous chlorido species.

Before extracting the synthesized complex into the organic phase, the ion-exchanger, Aliquat-336 was converted to the bromido form. This was achieved by washing 20 % (v/v) Aliquat-336 in chloroform-*d* five times with 3 M HBr , followed by removal of the chloroform-*d* in attempt to exclude chlorides from the system. The organic phase was added

to the blood-red aqueous phase, stirred for 15 minutes and left overnight until essentially all the coloured species was extracted into the organic phase.

2.1.3. Synthesis of the heteroleptic $[\text{Pt}(\text{Sn}_5\text{Cl}_n\text{Br}_{15-n})]^{3-}$ ($n = 1 - 14$) complex anions

The heteroleptic species were prepared using two methods. For the first method, the homoleptic chlorido species were synthesized as described above. The total Cl^- concentration of the solution was calculated and appropriate amount of KBr was weighed off and added to the solution in order to obtain the required $\text{Cl}:\text{Br}$ ratios; 9:1, 6:1, 3:1 and 1:1. However, this was problematic as not all the KBr dissolved in the solution and which prohibited the accurate determination of the $\text{Cl}:\text{Br}$ ratio in solution. To overcome this problem, a second method of synthesis was used wherein the homoleptic chlorido and bromido species were both synthesized and extracted into chloroform-*d* as described above, both solutions having the same Pt , Sn and acid concentrations. These solutions were then added together to obtain final $(\text{R}_3\text{NMe})_3[\text{Pt}(\text{SnCl}_3)_5]:(\text{R}_3\text{NMe})_3[\text{Pt}(\text{SnBr}_3)_5]$ volume ratios of 2:1, 1:1 and 1:2 respectively. These solutions were left overnight before using them for NMR experiments.

UV-vis spectra were recorded of the solution prepared using the first method. For these solutions the same method that was used to synthesize the $[\text{Pt}(\text{SnCl}_3)_5]^{3-}$ species, as described in Section 2.1.1, was used to synthesize these solutions where the solutions are in 3 M HCl and have $\text{Pt}:\text{Sn}$ ratios of 1:7.

2.2. Preliminary UV/Vis investigations

The reaction of $\text{Pt}(\text{II/IV})$ with SnCl_2 in acidic aqueous media can yield several 4-coordinated $[\text{PtCl}_n(\text{SnCl}_3)_{4-n}]^{2-}$ ($n = 1 - 4$) complex anions, as well as the trigonal bipyramidal $[\text{Pt}(\text{SnCl}_3)_5]^{3-}$ complex anions, depending on the specific experimental conditions used.^{2,8,19,23,26,27,58,59,70,71} As the aim of this study is to investigate the trigonal bipyramidal species, preliminary UV-Vis experiments were conducted in order to establish the experimental conditions under which the $[\text{Pt}(\text{SnCl}_3)_5]^{3-}$ species prevails.

The main parameters that influence the preferred formation of $[\text{Pt}(\text{SnCl}_3)_5]^{3-}$ at constant temperature (298 K) and pressure (1 atm) are the HCl concentration and the $\text{Pt}(\text{II}):\text{Sn}$ ratio.

Keeping the Sn:Pt ratio constant at 20:1 and changing the HCl concentration from 0.5 M to 3 M yield the UV-Vis spectra shown in Figures 2.1 (a) and (b), respectively. For both solutions, the first UV-Vis spectrum was recorded directly after the tin solution was added to the platinum solution. In both cases, the absorbance at all wavelengths initially increased relatively rapidly, and after ± 50 minutes for both solutions, the UV-Vis spectra remained unchanged, indicative of equilibrium being reached. Figure 2.1(a) shows the UV-Vis spectrum recorded for the yellow-to-orange platinum-tin solution obtained in 0.5 M HCl. The spectrum shows four absorption maxima, $\lambda_{\max} = 275, 375, 430$ and 510 nm. Changing the HCl concentration to 3 M yields the UV-Vis spectrum shown in Figure 2.1(b), with $\lambda_{\max} = 310$ and 400 nm. The UV-Vis spectrum shown in Figure 2.1(a) is characteristic of the 4-coordinate $[\text{PtCl}_2(\text{SnCl}_3)_2]^{2-}$ species,^{29,70,71} whereas the spectrum shown in Figure 2.1(b) is characteristic of the 5-coordinate $[\text{Pt}(\text{SnCl}_3)_5]^{3-}$ species.^{29,71}

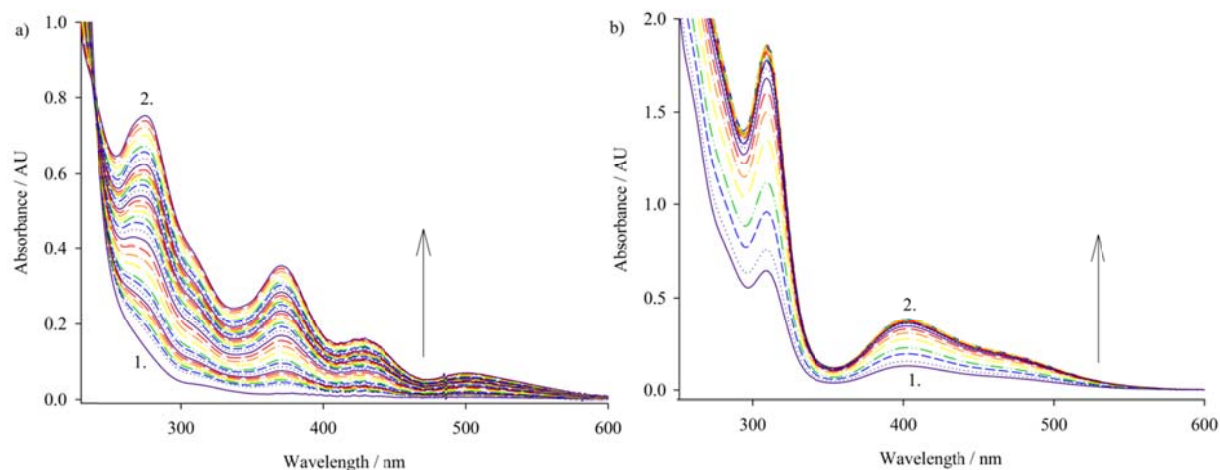


Figure 2.1: Dependence of Pt-Sn complexes on HCl concentration (M) where $[\text{HCl}] = 0.5$ M in (a) and 3 M in (b). Both spectra are recorded as a function of time, with spectrum 1 being recorded directly after the reaction had started, and spectrum 2 indicates that equilibrium has been reached. For both solutions equilibrium was reached after ± 50 minutes.

Moreover, the formation of $[\text{Pt}(\text{SnCl}_3)_5]^{3-}$ is also influenced by the initial Pt(II):Sn ratio. The UV-Vis spectra recorded for the series solutions containing Pt:Sn ratios of 1:1, 1:2, 1:3, 1:4, 1:5 and 1:7 were prepared in 3 M HCl are shown in Figure 2.2 (a). It is clear that the UV-Vis spectrum changes as the ratio platinum to tin increases. The spectra recorded for the solutions with Pt:Sn ratios of 1:1 to 1:3 all show $\lambda_{\max} = 275$ and 310 nm. Definite spectral changes are observed for the solution with a Pt:Sn ratio of 1:4 ratio. Once a ratio of 1:5 is reached, the spectrum resembles that obtained for the $[\text{Pt}(\text{SnCl}_3)_5]^{3-}$ species, with $\lambda_{\max} = 400$ nm.

Unfortunately, due to the higher initial $[\text{PtCl}_4]^{2-}$ concentration, the absorption at 310 nm was saturated. From the comparison of the UV-vis spectrum of the $[\text{Pt}(\text{SnCl}_3)_5]^{3-}$ to those of solutions that contain Pt:Sn ratios of 1:5 and 1:7, Figure 2.2 (b), it is clear that only at a Pt:Sn ratio of 1:7 the desired $[\text{Pt}(\text{SnCl}_3)_5]^{3-}$ complex anion is obtained.

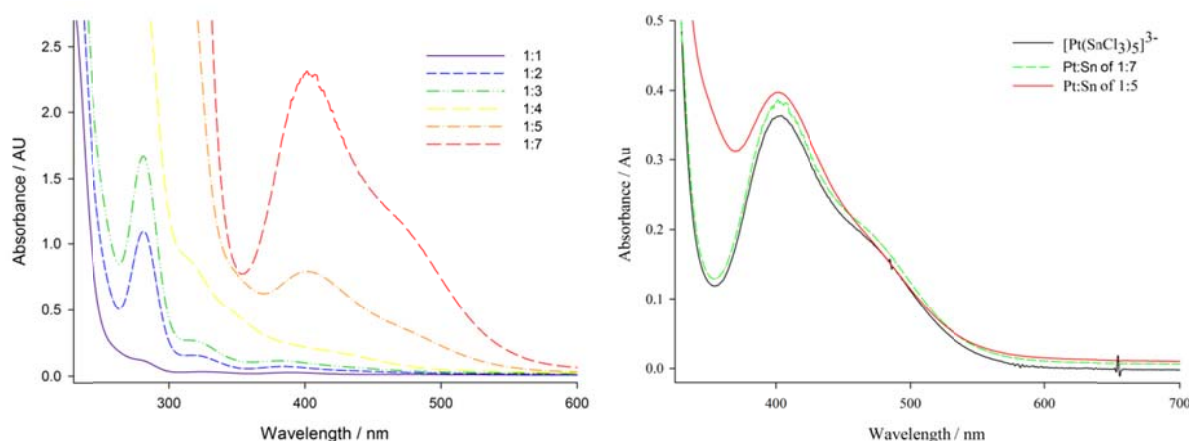


Figure 2.2: Dependence of Pt-Sn complexes on the initial Pt:Sn ratio used. The $[\text{Pt}]$ is kept constant at 1×10^{-4} M, while the $[\text{Sn}]$ is increased. In (a) the spectra recorded for solution with Pt:Sn ratios of 1:1, 1:2, 1:3, 1:4, 1:5 and 1:7 are shown. In (b) the spectra recorded for the solutions with Pt:Sn solutions of 1:5 and 1:7 are compared to the spectrum assigned to the $[\text{Pt}(\text{SnCl}_3)_5]^{3-}$ species.

From these results it is clear that for further investigation of the $[\text{Pt}(\text{SnCl}_3)_5]^{3-}$ complex anions 3 M HCl solutions containing a Pt:Sn ratio of 1:7 is required. In view of this, all the solutions prepared for NMR analysis are in 3 M acidic solutions that contain Pt:Sn ratios of 1:7.

The UV-vis spectra recorded of these solutions to which KBr were added are shown in Figure 2.3. As the Br:Cl ratio increases a bathochromic shift is observed which is indicative of chlorides being substituted by bromides.

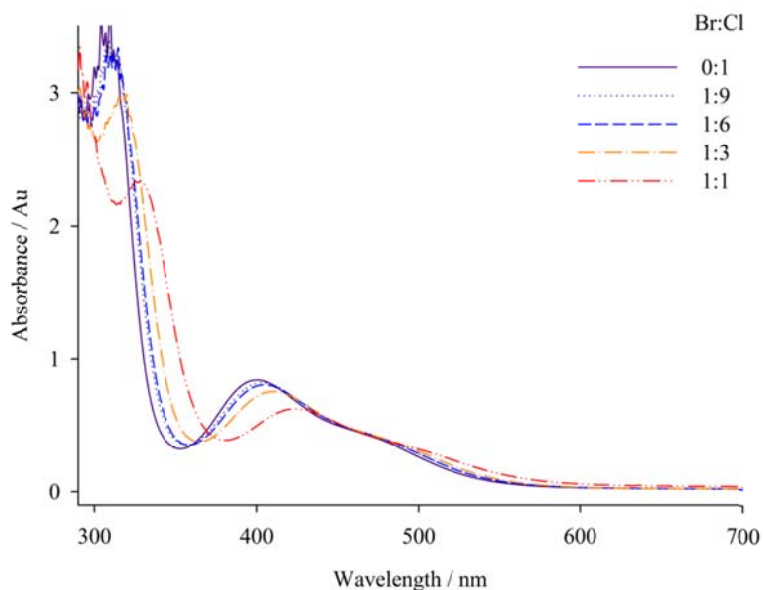


Figure 2.3: Change in the absorbance spectrum of the $[\text{Pt}(\text{SnX}_3)_5]^{3-}$ ($\text{X} = \text{Cl}^-/\text{Br}^-$) as the ratio of Br:Cl in solution changes.

2.3. Experimental

2.3.1. Reagents

Potassium tetrachloroplatinate(II) (99.9+ %, K_2PtCl_4 , Sigma-Aldrich) and tin(II)chloride ($\text{SnCl}_2 \cdot 2\text{H}_2\text{O}$, Johnson Matthey Chemicals limited) were of reagent grade quality and was stored in a dessicator prior to use. Potassium bromide (KBr, 99.5%, Aldrich) was also of reagent grade quality and used as is. All aqueous solutions were prepared using ultrapure Milli-Q water ($\text{MQ} > 18\text{M}\Omega$) that was degassed with nitrogen for at least an hour prior to use in order to remove O_2 . The hydrochloric acid (HCl, 32%, Riedel-de Haën) and hydrobromic acid (HBr, 48%, Associated Chemical enterprises) were also degassed with nitrogen prior to use. Chloroform-*d* (CDCl_3 , 99.8%, Merck) was used as solvent to obtain a lock signal for NMR measurements. Methyltrioctylammonium chloride (Aliquat-336, $\text{CH}_3\text{N}[(\text{CH}_2)_7\text{CH}_3]_3\text{Cl}$, Aldrich) was used as ion-pairing reagent to extract complexes into chloroform-*d*.

2.3.2. Instrumentation

2.3.2.1. UV/Vis spectroscopy

All UV-Vis spectra were recorded on an Agilent 8453 Ultraviolet-visible spectrometer at 20 °C using a 0.5 cm quartz cell. Solutions in the sample and blank cells were similar in every respect except that the latter contained no platinum-stannous chloride solutions. The spectra were run between 190 and 1500 nm at a scan speed of 200 nm/min.

2.3.2.2. ^{119}Sn NMR and ^{195}Pt NMR spectroscopy

All ^{119}Sn NMR spectra were recorded at 223.7 MHz using a Varian INOVA 600 MHz spectrometer at 20 °C and a 5 mm broad-band probe. All chemical shifts are quoted relative to an external reference of neat $\text{Sn}(\text{CH}_3)_4$ sealed in a 1 mm capillary surrounded by $^2\text{H}_2\text{O}$. Spectra were recorded under conditions of optimal resolution using an excitation pulse of 2.0 μs , with an acquisition time 1.016 s, and no relaxation delay was applied. The T_1 values for the ^{119}Sn NMR nuclei in these systems were measured to be 0.1 – 0.5 s, so that essentially quantitative resonance intensities are obtained.

^{195}Pt NMR spectra were recorded at 128.7 MHz using a Varian INOVA 600 MHz spectrometer at 20 °C and a 5 mm broad-band probe. A 1 mm coaxial insert tube containing a 0.1 M $[\text{PtCN}_4]^{2-}$ solution ($\delta^{195}\text{Pt} = -4700$ ppm relative to PtCl_6^{2-} ($\delta^{195}\text{Pt} = 0.0$ ppm), 500 mg cm^{-3} K_2PtCN_4 in 30% v/v $\text{D}_2\text{O}/1$ M HCl) was used as a reference. The spectra were recorded under the same conditions as ^{119}Sn NMR. The T_1 relaxation times of ^{195}Pt NMR nuclei in these systems were measured to be less than 2 s.

In both cases broad band ^1H -decoupling was applied in all measurements. A line broadening factor of 20 Hz was applied in processing, resulting in an effective line-width at half height. Spectral widths of up to 2000 ppm were used.

Chapter III

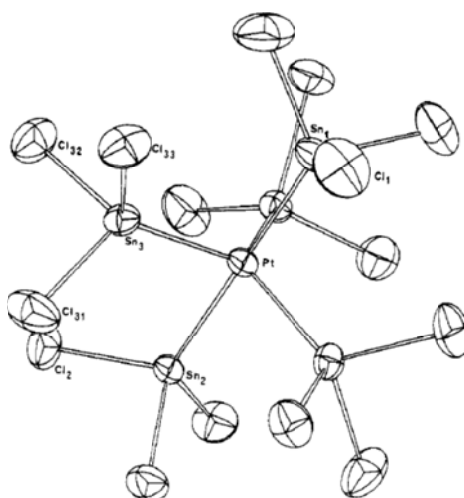
Characterization of the homoleptic $[Pt(SnX_3)_5]^{3-}$ (where $X = Cl^-$ or Br^-) complex anions by means of ^{119}Sn and high resolution ^{195}Pt NMR spectroscopy

3.1. Introduction

The correct nature of the intense red species formed by the reaction of platinum(II) with excess tin(II) chloride was first elucidated by Young *et al*¹⁹ and Cramer *et al*.^{23,24} In order to precipitate the $(NMe_4)_3[Pt(SnCl_3)_5]$ solid, Young *et al*¹⁹ added tetramethylammonium chloride to hydrochloric acid solutions with Pt:Sn ratios ranging from 1:2 up to 1:10. Cramer *et al*^{23,24} prepared the same complex anion using $[(C_6H_5)_3PCH_3]^+$ as the counter cation. From the X-ray diffraction data obtained²³ it was concluded that the $[Pt(SnCl_3)_5]^{3-}$ complex anion has an unusual trigonal bipyramidal configuration. According to the structural data^{23,24} all five platinum-tin bonds have the same length which is ‘unusual’ for d^8 trigonal bipyramidal complexes since the axial bonds are expected to be somewhat shorter than the equatorial bonds.^{72,73} This was subsequently confirmed by Alcock and Nelson⁶⁰ two decades later by single crystal X-ray diffraction, Scheme 3.1, where a difference of 0.0192 (12) Å between the axial and equatorial Pt-Sn bond lengths was observed in the solid state. Interestingly, this is a small difference in bond length by comparison to structurally analogous compounds such as $[Pt(GeCl_3)_5]^{3-}$ ($\Delta d = 0.034$ Å), $[CuCl_5]^{3-}$ ($\Delta d = 0.095$ Å), $[CuBr_5]^{3-}$ ($\Delta d = 0.069$ Å), and $[Fe(CO)_5]^{3-}$ ($\Delta d = 0.027$ Å).³⁸

From a ^{119}Sn NMR spectroscopy perspective the difference in the Pt-Sn axial and equatorial bond lengths suggests that the electronic environment would differ for the ^{119}Sn nuclei in the axial with respect to the equatorial coordination position. This in turn might be expected to result in a difference in the extent of shielding experienced by the ^{119}Sn nuclei yielding ^{119}Sn NMR chemical shifts that differ. However, in two separate studies^{26,69} the ^{119}Sn NMR spectra recorded for the $[Pt(SnCl_3)_5]^{3-}$ and $[Pt(SnBr_3)_5]^{3-}$ species only show a single main ^{119}Sn NMR signal at -130.7 ppm and -234.3 ppm respectively, Figure 3.1. This suggests that the SnX_3^- ($X = Cl^-/Br^-$) ligands undergo rapid intra-molecular site-exchange on the NMR acquisition

time scale yielding an average axial-equatorial chemical shift for the ^{119}Sn nuclei. This site-exchange process most probably occurs via a Berry-pseudo rotation mechanism.⁶⁰



Scheme 3.1: Single Crystal structure obtained by Alcock and Nelson for the red $[Pt(SnCl_3)_5]^{3-}$ complex anion.⁶⁰

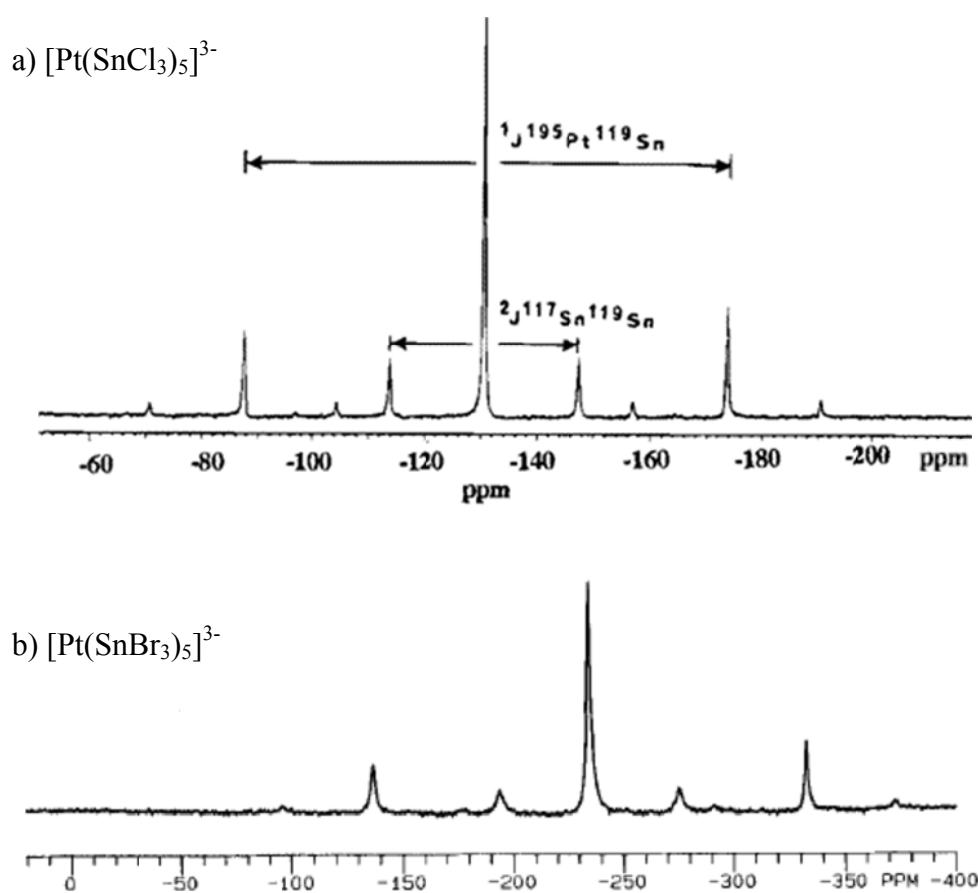
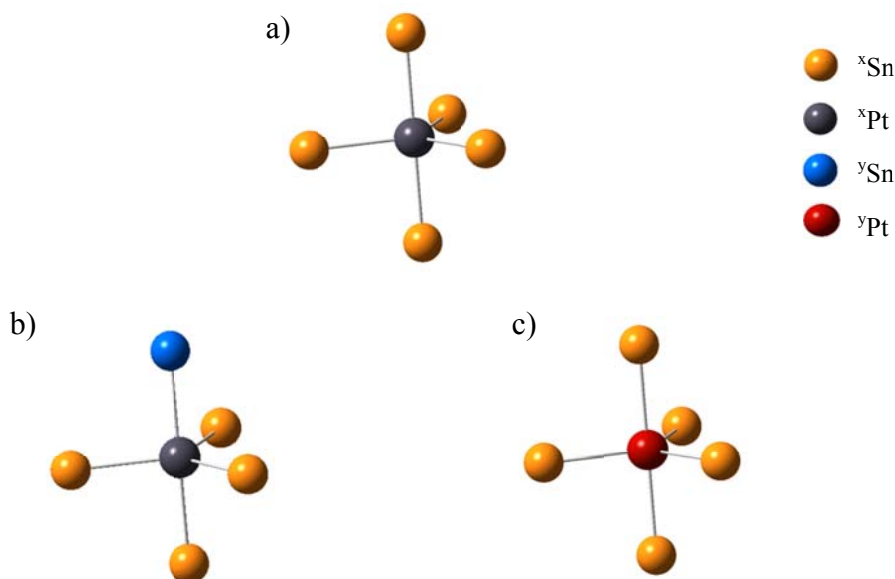
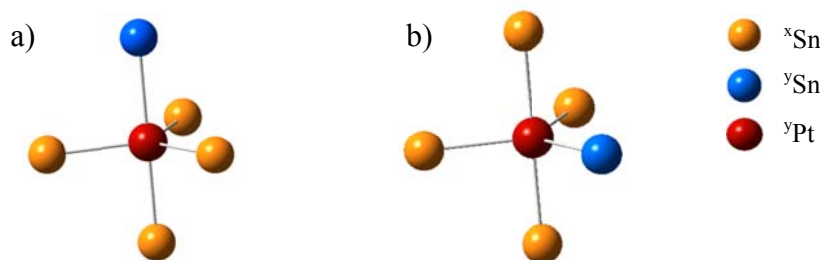


Figure 3.1: ^{119}Sn NMR spectrum recorded for (a) the $[Pt(SnCl_3)_5]^{3-}$ complex anion in acetone-*d* by Nelson *et al.*²⁹ at 186.36 MHz and (b) the $[Pt(SnBr_3)_5]^{3-}$ complex anion extracted into 20% (v/v) Aliquat-336- $CDCl_3$ by Koch⁶⁹ at 74.56 MHz.

Recently, it was shown in a ^{195}Pt NMR study that a detailed analysis of the isotopologue and isotopomer distribution of aqua-chlorido Pt(IV) species led to the unambiguous identification and assignment of the isotopic stereoisomers of $[PtCl_5(H_2O)]^-$ and *cis/trans*- $[PtCl_4(H_2O)_2]$.⁷⁴ To the best of our knowledge a detailed investigation of the many possible isotopologues and isotopomers of the Pt-Sn-halide system (see Appendix B), with respect to the $[Pt(SnX_3)_5]^{3-}$ ($X = Cl/Br^-$) complex anions, has not been done. The term *isotopologues* refers to chemical species that differ only in isotopic composition of their molecules or ions,⁷⁵ as illustrated in Scheme 3.2 for several isotopologues of the $[Pt(SnCl_3)_5]^{3-}$ complex anion. As there are 10 isotopes of tin and 6 isotopes of platinum, Table 3.1, numerous isotopologues of the $[Pt(SnCl_3)_5]^{3-}$ complex anion are possible. In addition, an isotopologue can also be present as several distinguishable isotopomers. *Isotopomers* are isomers with the same number of each isotope, but differing in the position in the molecule or ion.⁷⁵ Two isotopomers are illustrated in Scheme 3.3, where in (a) ySn is in the axial position and in (b) it is in the equatorial position.



Scheme 3.2: A schematic representation of different isotopologues that are possible for the $[Pt(SnX_3)_5]^{3-}$ ($X = Cl/Br^-$) complex anions. Replacement of any of the five tin atoms and/or the platinum atom with another isotope of Sn and/or Pt, respectively, results in a different isotopologue. All Cl^-/Br^- are left out for clarity.



Scheme 3.3: A schematic representation of different isotopomers of the $[Pt(SnX_3)_5]^{3-}$ ($X = Cl/Br^-$) complex anions. (a) and (b) are isotopomers of each other as they have the same number of each isotopic atom, but in (a) ySn is in the equatorial position and in (b) ySn is in the axial position.

Table 3.1: Natural Abundances of the stable tin and platinum isotopes and the magnetic properties of those with $I = \frac{1}{2}$ which are highlighted.

NMR-active isotope	Natural Abundance / %	Spin	Gyromagnetic Ratio	Receptivity ($^{13}C = 1$)
Pt				
^{190}Pt	0.014	0		
^{192}Pt	0.78	0		
^{194}Pt	32.97	0		
^{195}Pt	33.7	$\frac{1}{2}$	9.1534	19.1
^{196}Pt	25.24	0		
^{198}Pt	7.16	0		
Sn				
^{112}Sn	0.97	0		
^{114}Sn	0.66	0		
^{115}Sn	0.35	$\frac{1}{2}$	-13.922	0.715
^{116}Sn	14.54	0		
^{117}Sn	7.61	$\frac{1}{2}$	-15.168	19.9
^{118}Sn	24.22	0		
^{119}Sn	8.58	$\frac{1}{2}$	-15.869	25.6
^{120}Sn	32.58	0		
^{122}Sn	4.63	0		
^{124}Sn	5.79	0		

In this study a detailed investigation of the possible isotopologues/isotopomers of the homoleptic [Pt(SnX₃)₅]³⁻ (X = Cl⁻/Br⁻) complex anions are performed by means of high resolution ¹¹⁹Sn and ¹⁹⁵Pt NMR spectroscopy. In view of this, the investigation is partially limited to 224 isotopologues of the [Pt(SnX₃)₅]³⁻ (X = Cl⁻/Br⁻) complex anions as only one Pt isotope and three Sn isotopes are magnetically-active, Table 3.1. Furthermore, the rapid intra-molecular site-exchange of the equatorial and axial SnX₃⁻ (X = Cl⁻/Br⁻) ligands on the ¹¹⁹Sn NMR time-scale will probably prevent the observation of ¹¹⁹Sn NMR signals due to isotopomers.

3.2. Results and Discussion

3.2.1. ¹¹⁹Sn NMR of the homoleptic [Pt(SnCl₃)₅]³⁻ complex anion

The high-resolution ¹¹⁹Sn NMR spectrum obtained for [Pt(SnCl₃)₅]³⁻ extracted into chloroform-*d* (20% (v/v) Aliquat-336) is shown in Figure 3.2. The main features of this spectrum is a single main ¹¹⁹Sn NMR signal (line width at half height ($\Delta\nu_{1/2}$) = 104.311 Hz) at -124.3 ppm, flanked by its respective ¹J(¹⁹⁵Pt-¹¹⁹Sn) and ²J(¹¹⁷Sn-¹¹⁹Sn) “satellites”, due to coupling.

In order to facilitate the discussion of these results the manner in which the natural statistical abundance (NSA) of the possible 112 isotopologues of the [Pt(SnCl₃)₅]³⁻ complex anion is calculated (see Appendix A)* is covered first.† The NSA of an isotopologue may be calculated using Equation 3.1,² where n_x is the number of isotope x present in the specific isotopologue (e.g. $x = ^{119}\text{Sn}$) and ρ_x is the natural abundance of isotope x (e.g. $\rho_x = 0.0858$).

$$\rho(n_1 n_2 \dots n_x) = \frac{(\sum_{i=1}^x n_i)!}{n_1! n_2! \dots n_x!} \rho_1^{n_1} \cdot \rho_2^{n_2} \cdot \rho_x^{n_x} \quad \dots (3.1)$$

* The NSA's calculated for the 112 possible isotopologues of the [Pt(SnCl₃)₅]³⁻ complex anion using Equation 3.1 are listed in Table A1 in Appendix A.

† The relative experimental signal areas obtained with ¹¹⁹Sn and ¹⁹⁵Pt NMR for different isotopologues should to a good approximation be equal to the NSA of the respective isotopologues as the change in standard reaction Gibbs energy for the interconversion between isotopologues of the [Pt(SnX₃)₅]³⁻ (X = Cl⁻/Br⁻) complex anions is relatively small.

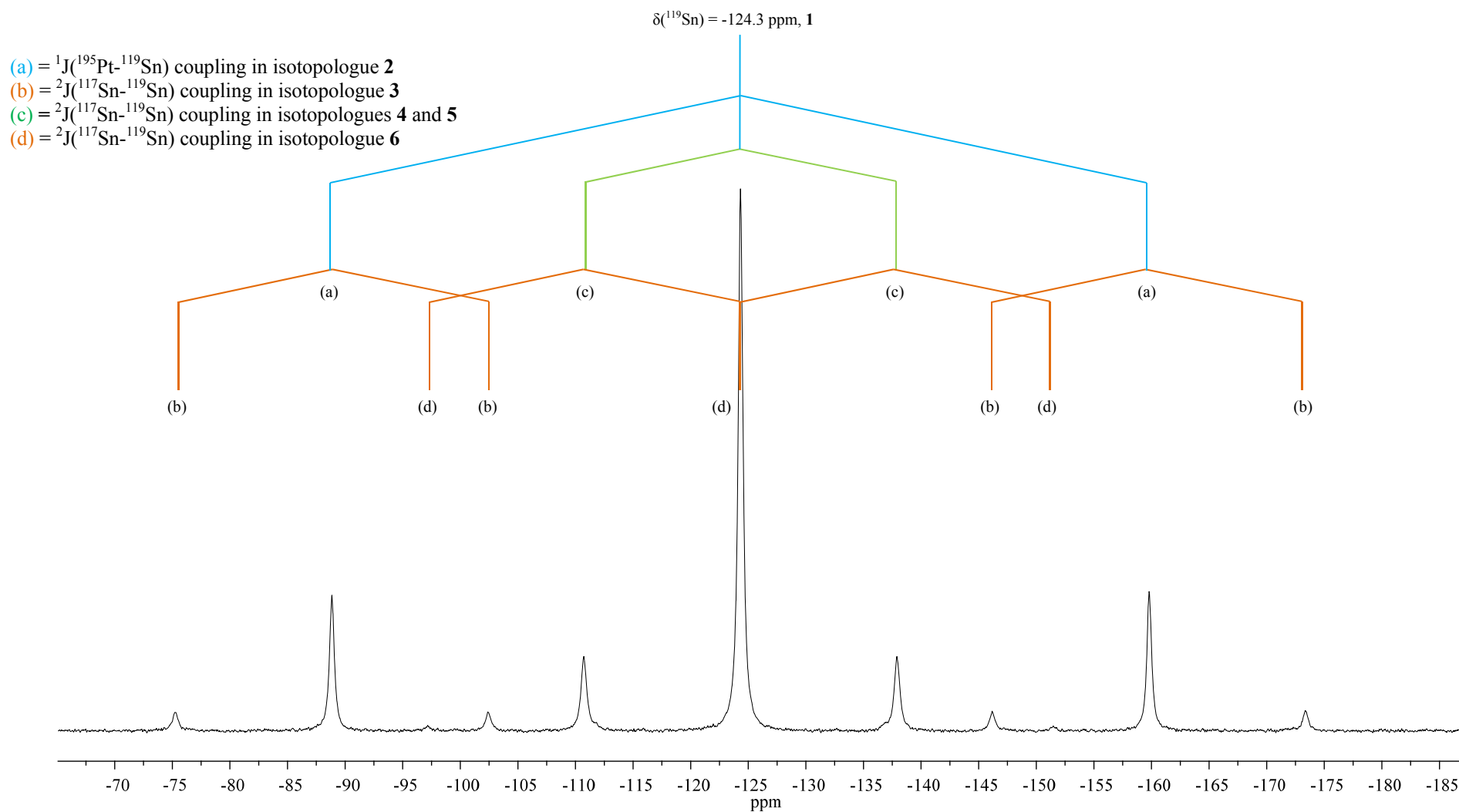
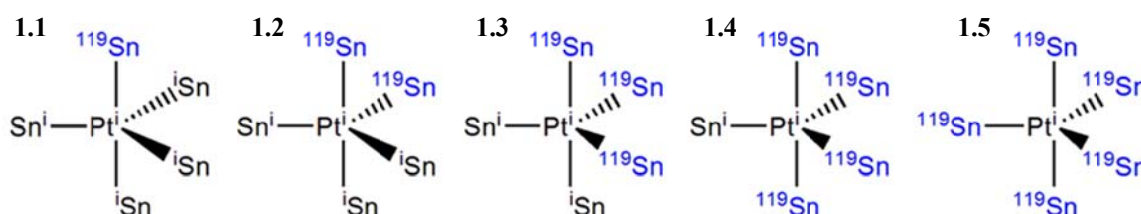
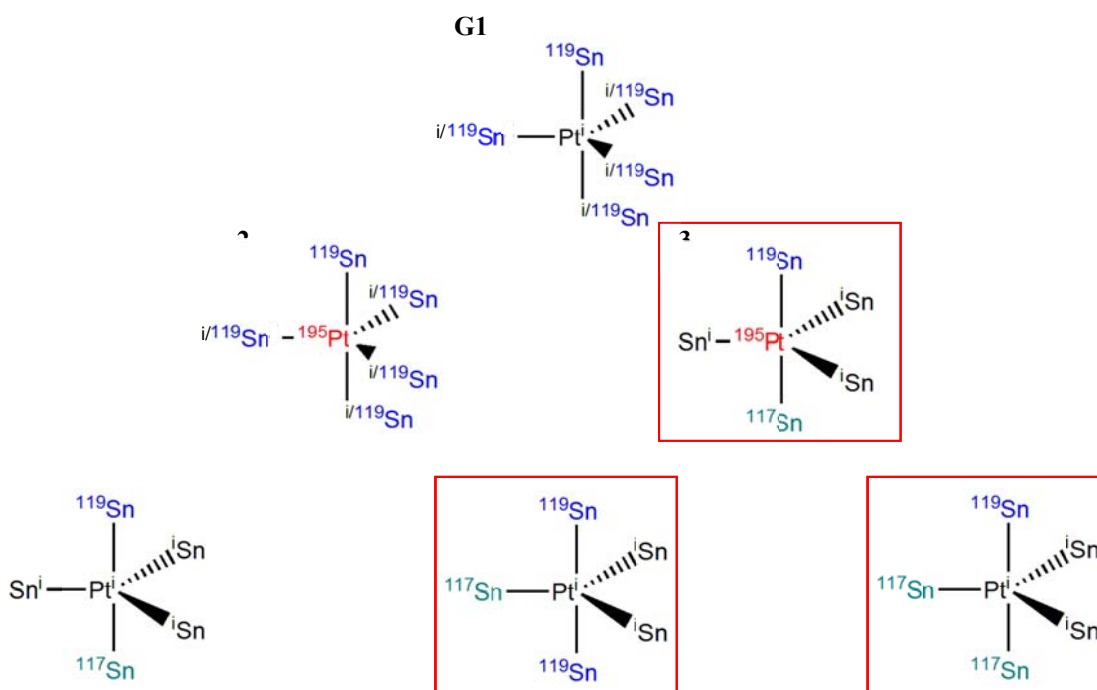


Figure 3.2: The ^{119}Sn NMR spectrum obtained for $[Pt(SnCl_3)_5]^{3-}$ in $CDCl_3$ (20% AQ-336) at 293 K. The respective satellites are observed due to (a) $^1J(^{119}Sn-^{195}Pt)$ coupling in isotopologue **2**, (b) $^1J(^{119}Sn-^{195}Pt)$ and $^2J(^{119}Sn-^{117}Sn)$ coupling within isotopologue **3**, (c) $^2J(^{119}Sn-^{117}Sn)$ coupling in both isotopologues **4** and **5**, and (d) $^2J(^{119}Sn-^{117}Sn)$ coupling in isotopologue **6**.

The relative area of the ^{119}Sn NMR signal at $\delta(^{119}\text{Sn}) = -124.3$ ppm consists of the sum of the NSA's of all the $[Pt(SnCl_3)_5]^{3-}$ isotopologues containing the ^{119}Sn isotope and no other magnetically-active Pt or Sn isotope, Scheme 3.4. These isotopologues, with increasing number of ^{119}Sn atoms bound to Pt, are collectively referred to as isotopologue **G1** (group 1), as illustrated in Scheme 3.5. The sum of the NSA's calculated for isotopologue **G1**, using Equation 3.1, is 0.173, Table 3.2. Note that the NSA's of isotopologues **1.1** and **1.2** account for 98.4 % of this value. For ease of comparison of the relative ^{119}Sn NMR signal areas shown in Figure 3.2, this value is normalized to 1 (relative intensity of ^{119}Sn NMR signal at $\delta(^{119}\text{Sn}) = -124.3$ ppm set to 1).

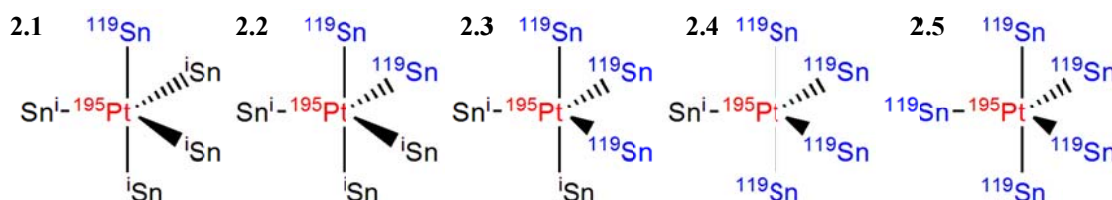


Scheme 3.4: Isotopologues of the $[Pt(SnCl_3)_5]^{3-}$ complex anion with the general formula $[Pt(^{119}\text{SnCl}_3)_n(^i\text{SnCl}_3)_{5-n}]^{3-}$ ($n = 1 = 5$) that are collectively referred to as isotopologue **G1**. ($\text{Pt} \neq ^{195}\text{Pt}$)



Scheme 3.5: Various isotopologues observed in the ^{119}Sn NMR spectrum recorded for the $[Pt(SnCl_3)_5]^{3-}$ complex anion. Due to rapid Berry-pseudo rotation on the NMR acquisition time scale, it is not possible to distinguish between isotopomers and isotopologues. All chlorides were left out for clarity. The bordered isotopologues **3**, **5** and **6** have not previously been observed with ^{119}Sn NMR.^{29,69}

When both ¹⁹⁵Pt and ¹¹⁹Sn are present in the [Pt(SnCl₃)₅]³⁻ complex (the isotopologues shown in Scheme 3.6), a doublet due to ¹J(¹⁹⁵Pt-¹¹⁹Sn) coupling is expected. These isotopologues are collectively referred to as isotopologue **G2** (group 2), Scheme 3.5. As before, the sum of the NSA's of isotopologue **G2** amount to a normalized value of 0.497, Table 3.2. Each ¹J(¹⁹⁵Pt-¹¹⁹Sn) satellite of isotopologue **G2** should thus have a relative area of 0.249, Table 3.2. From the excellent agreement between the experimentally determined relative areas of the satellites indicated by the symbol (a) in Figure 3.2 and the NSA calculated for isotopologue **G2** (Table 3.2) these satellites, with a ¹J(¹⁹⁵Pt-¹¹⁹Sn) coupling constant of 15 868 Hz, are unambiguously assigned to isotopologue **G2** (shown in Scheme 3.5).



Scheme 3.6: Isotopologues of the [Pt(SnCl₃)₅]³⁻ complex anion with the general formula [¹⁹⁵Pt(¹¹⁹SnCl₃)_n(ⁱSnCl₃)_{5-n}]³⁻ (n = 1 = 5) that are collectively referred to as isotopologue **G2**. (Pt = ¹⁹⁵Pt).

The relative ¹¹⁹Sn NMR signal areas of the doublet of doublets indicated by symbol (b) in Figure 3.2 agree well with the NSA calculated for isotopologue **3** shown in Scheme 3.5, Table 3.2 and are therefore assigned to both ¹J(¹⁹⁵Pt-¹¹⁹Sn) (15 868 Hz) and ²J(¹¹⁷Sn-¹¹⁹Sn) (6 060 Hz) coupling in isotopologue **3**. Similarly, the relative ¹¹⁹Sn NMR signal areas of the ²J(¹¹⁷Sn-¹¹⁹Sn) satellites indicated by (c) in Figure 3.2 compare well to the sum of the NSA's calculated for the isotopologues **4** and **5** shown in Scheme 3.5 and are assigned accordingly, Table 3.2. Unfortunately, the relative ¹¹⁹Sn NMR signal areas of the satellites indicated by the symbol (d) in Figure 3.2 could not be reliably determined due to its low intensity. Nonetheless, these satellites are assigned to isotopologue **6** based on an expected triplet due to two ²J(¹¹⁷Sn-¹¹⁹Sn) couplings in isotopologue **6**, Figure 3.2. Moreover, the chemical shift of the ¹¹⁹Sn NMR signal, as well as the coupling constants measured for the respective ¹J(¹⁹⁵Pt-¹¹⁹Sn) and ²J(¹¹⁷Sn-¹¹⁹Sn) satellites due to isotopologues **G2** and **4**, agree well with previously published data obtained by Koch,⁶⁹ Table 3.3.

Table 3.2: The NSA's calculated for the respective isotopologues of the $[Pt(SnCl_3)_5]^{3-}$ complex anion compared to the ^{119}Sn NMR signal areas experimentally obtained for the $^1J(^{195}Pt-^{119}Sn)$ and $^2J(^{117}Sn-^{119}Sn)$ satellites due to the respective isotopologues.

1J Sat	Isotopologue	NSA ^a		^{119}Sn NMR signal areas ^d	
		Stat. ^b	Normalized ^c	Stat.	Exp.
G1	$[^iPt(^iSnCl_3)_n(^{119}SnCl_3)_{5-n}]^{3-}$	0.173	1.00	1.00	1.00
a G2	$[^{195}Pt(^iSnCl_3)_n(^{119}SnCl_3)_{5-n}]^3$	0.086	0.497	0.249	0.25 ± 0.01
b 3	$[^{195}Pt(^iSnCl_3)_3(^{117}SnCl_3)(^{119}SnCl_3)]^3$	0.026	0.148	0.037	0.03 ± 0.003
c 4	$[^iPt(^iSnCl_3)_3(^{117}SnCl_3)(^{119}SnCl_3)]^{3-}$	0.051	0.296	0.148	$0.16^e \pm 0.01$
				5	
d 6	$[^iPt(^iSnCl_3)_2(^{117}SnCl_3)_2(^{119}SnCl_3)]^{3-}$	0.01	0.040	0.010	- ^f

^a Natural Statistical Abundance of the respective isotopologues. Note, 67.7 % of the NSA's given in Table A1 in Appendix A are due to isotopologues that contain a magnetically-inactive iPt isotope, and 33.3 % are due to isotopologues that contain the magnetically-active ^{195}Pt isotope. ^b NSA's calculated using Equation 3.1. ^c Normalized values of NSA's for ease of comparing ^{119}Sn NMR signal areas and should be equal to the sum of the satellites. ^d ^{119}Sn signal areas of each respective satellites. ^e Note, isotopologues **4** and **5** have the same splitting pattern, thus both these isotopologues contribute to the signal areas of satellites (b2), Figure 3.2. ^f Not reliably interpretable.

Table 3.3: Experimentally obtained ^{119}Sn NMR data^a compared to values reported in Literature.

Parameter	Experimental Values	Literature Values ^b
$\delta(^{119}Sn)$ / ppm	-123.4	- 126.4
$^1J(^{195}Pt-^{119}Sn)$ / Hz	15 868	15 791
$^2J(^{117}Sn-^{119}Sn)$ / Hz	6060	6057

^aChemical shifts in ppm relative to Me_4Sn (neat). ^bThese values were obtained by K. R. Koch.⁶⁹

Thus, all the $^1J(^{195}Pt-^{119}Sn)$ and $^2J(^{117}Sn-^{119}Sn)$ satellites observed in the ^{119}Sn NMR spectrum of the $[Pt(SnCl_3)_5]^{3-}$ complex anion, indicated by symbols (a) to (d) in Figure 3.2, are unambiguously assigned to isotopologues **G2** to **6** shown in Scheme 3.5. The $^1J(^{195}Pt-^{119}Sn)$ and $^2J(^{117}Sn-^{119}Sn)$ satellites due to isotopologues **3**, **5** and **6** have to our knowledge not been identified to date. The isotopologues of the $[Pt(SnCl_3)_5]^{3-}$ complex anion listed in Table A1 in Appendix A that are not considered here are not abundant enough to be observed with ^{119}Sn

NMR in a reasonable experimental time. As expected, due to rapid Berry-pseudo rotation, isotopomers of the homoleptic chlorido species are not observed in the ^{119}Sn NMR spectrum.

3.2.2. ^{119}Sn NMR of the homoleptic $[Pt(\text{SnBr}_3)_5]^{3-}$ complex anion

In contrast to the sharp ^{119}Sn NMR signals of the homoleptic chlorido $[Pt(\text{SnCl}_3)_5]^{3-}$ species, the ^{119}Sn NMR spectrum of $[Pt(\text{SnBr}_3)_5]^{3-}$ extracted into chloroform-*d* (20% (v/v) Aliquat-336), shown in Figure 3.3, shows broad peaks with an average width at half peak height of 1 500 Hz or more. Several attempts to get sharper ^{119}Sn resonances were not successful, for reasons not entirely clear. It is possible that either chemical exchange rates are slow²⁹ or some radicals (Sn^\cdot) are present in solution. The main ^{119}Sn NMR signal at $\delta(^{119}\text{Sn}) = \pm -232$ ppm compares well with the chemical shift reported by Koch⁶⁹ ($\delta(^{119}\text{Sn}) = \pm -234.3$ ppm) and are tentatively assigned to isotopologue **GI** of the $[Pt(\text{SnBr}_3)_5]^{3-}$ complex anion, Scheme 3.7.[‡]

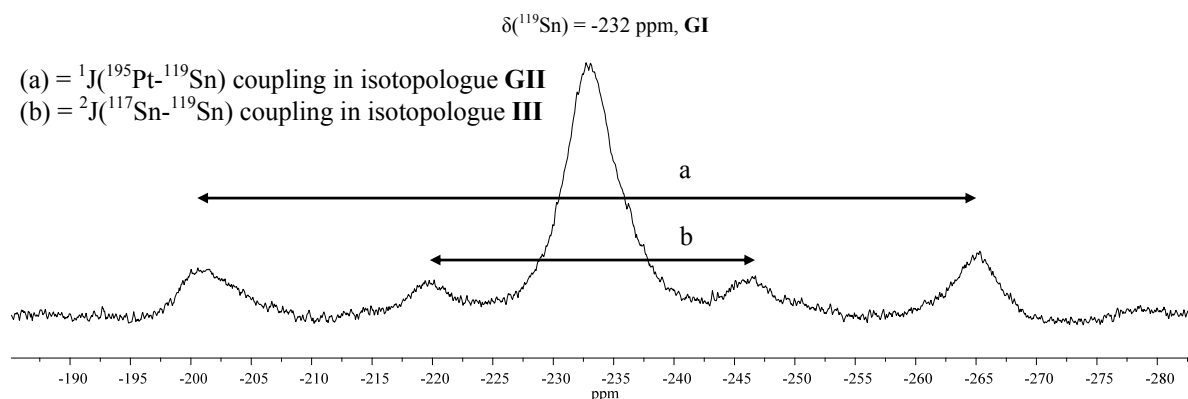
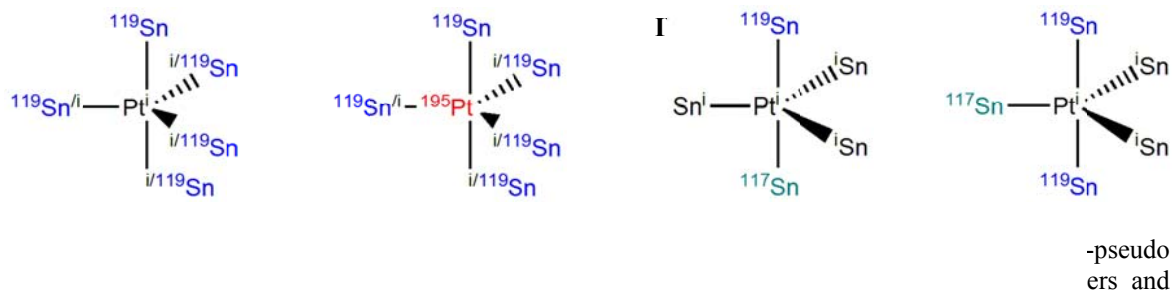


Figure 3.3: ^{119}Sn NMR spectrum obtained for $[Pt(\text{SnBr}_3)_5]^{3-}$ in CDCl_3 (20% AQ-336(Br) at 293 K. Chemical shifts in ppm relative to Me_4Sn (neat).

From the unambiguous assignments of the $^1J(^{195}\text{Pt}-^{119}\text{Sn})$ and $^2J(^{119}\text{Sn}-^{117}\text{Sn})$ satellites obtained in the ^{119}Sn NMR spectrum of the $[Pt(\text{SnCl}_3)_5]^{3-}$ species, it is reasonable to assign the satellites indicated by (a) in Figure 3.3 to $^1J(^{195}\text{Pt}-^{119}\text{Sn})$ coupling in isotopologue **GII** shown in Scheme 3.7. By the same reasoning, the satellites indicated by (b) in Figure 3.3 are assigned to $^2J(^{117}\text{Sn}-^{119}\text{Sn})$ coupling in isotopologues **IV** and **V**, Scheme 3.7.

[‡] In order to distinguish between isotopologues containing Cl^- and Br^- , Roman numerals are used for Br^- containing isotopologues.

Moreover, the $^1J(^{195}Pt-^{119}Sn) = \pm 14\,257$ Hz and $^2J(^{119}Sn-^{117}Sn) = \pm 6\,076$ Hz coupling constants compare well to that reported by Koch for this species, $^1J(^{195}Pt-^{119}Sn) = 14852$ Hz and $^2J(^{119}Sn-^{117}Sn) = 6035$ Hz.⁶⁹



The ^{119}Sn NMR signals of the $[Pt(SnBr_3)_5]^{3-}$ complex anion are shifted ‘upfield’ with respect to the $[Pt(SnCl_3)_5]^{3-}$ complex. Substitution of Cl^- with Br^- thus results in a more shielded ^{119}Sn nucleus, presumably due to Br^- being less electronegative than Cl^- .²⁹

3.2.3. ^{195}Pt NMR of the homoleptic $[Pt(SnCl_3)_5]^{3-}$ complex anions

All ^{195}Pt NMR resonance frequencies are reported relative to a 1 mm coaxial insert tube containing 0.1 M $[PtCN_4]^{2-}$ as a secondary reference solution. Due to the very large shielding range of ^{195}Pt NMR, the use of $[PtCl_6]^{2-}$ as an external reference may result in uncertain $\delta(^{195}Pt)$ measurements. Thus $K_2Pt(CN)_4$ which allows measuring the reference in the same spectral window as the ^{195}Pt NMR spectra of $[Pt(SnCl_3)_5]^{3-}$ was used. The $\delta^{195}Pt$ chemical shift of $[PtCN_4]^{2-}$ is -4 700 ppm relative to $[PtCl_6]^{2-}$ ($\delta^{195}Pt = 0.0$ ppm). The ^{195}Pt NMR spectrum of $[Pt(SnCl_3)_5]^{3-}$ extracted into chloroform-*d* (20% (v/v) Aliquat-336) is shown in Figure 3.4 shows a central ^{195}Pt NMR signal at -5 904.6 ppm ($\Delta\nu_{1/2} = 42.1$ Hz) and is flanked by several nJ coupling satellites. The central ^{195}Pt NMR signal is normalized to a relative signal area of 1 and is assigned to isotopologue 7, Scheme 3.8, which contains the magnetically-active ^{195}Pt isotope, but no magnetically-active tin nuclei, ^{119}Sn , ^{117}Sn or ^{115}Sn .

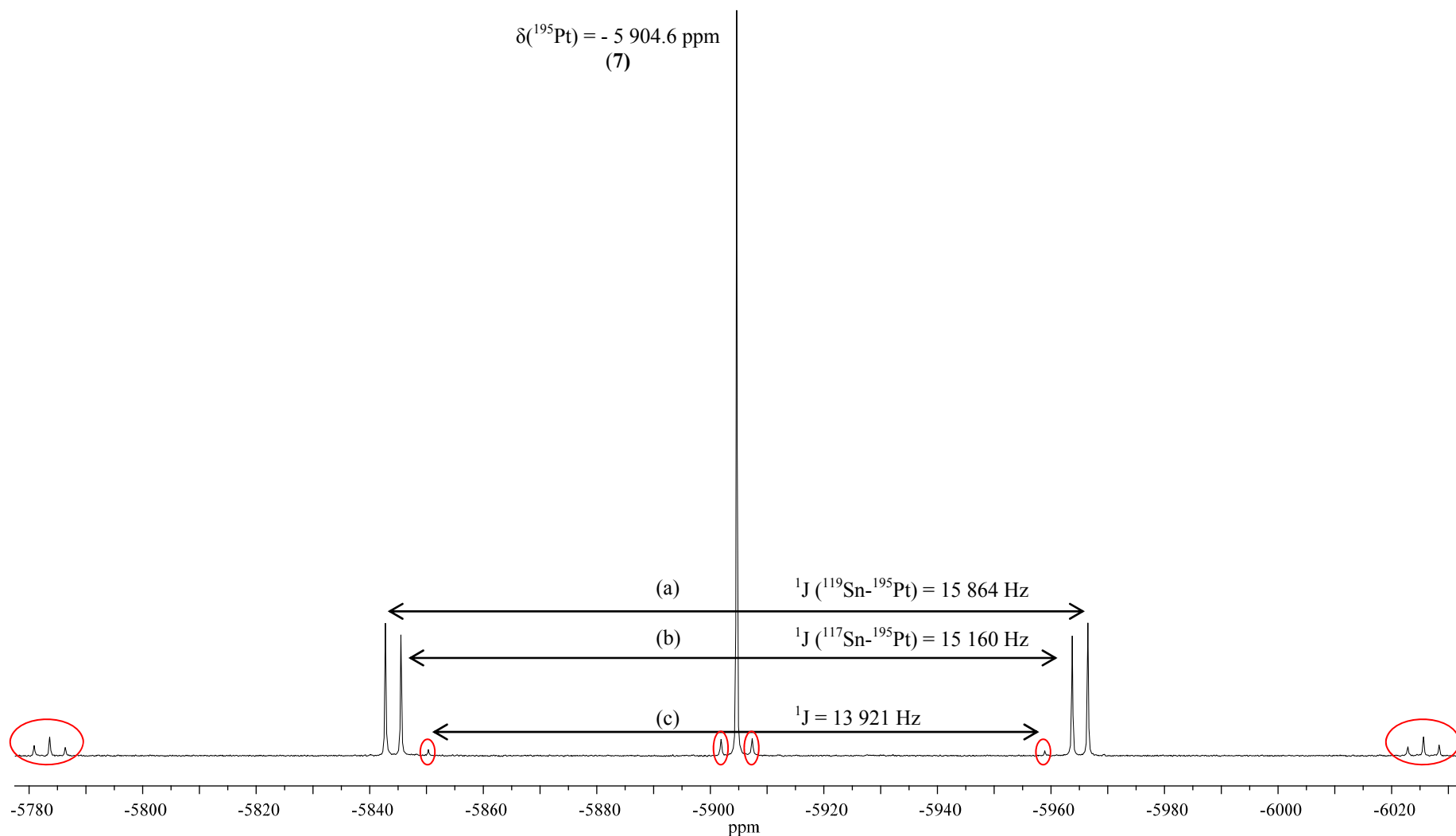
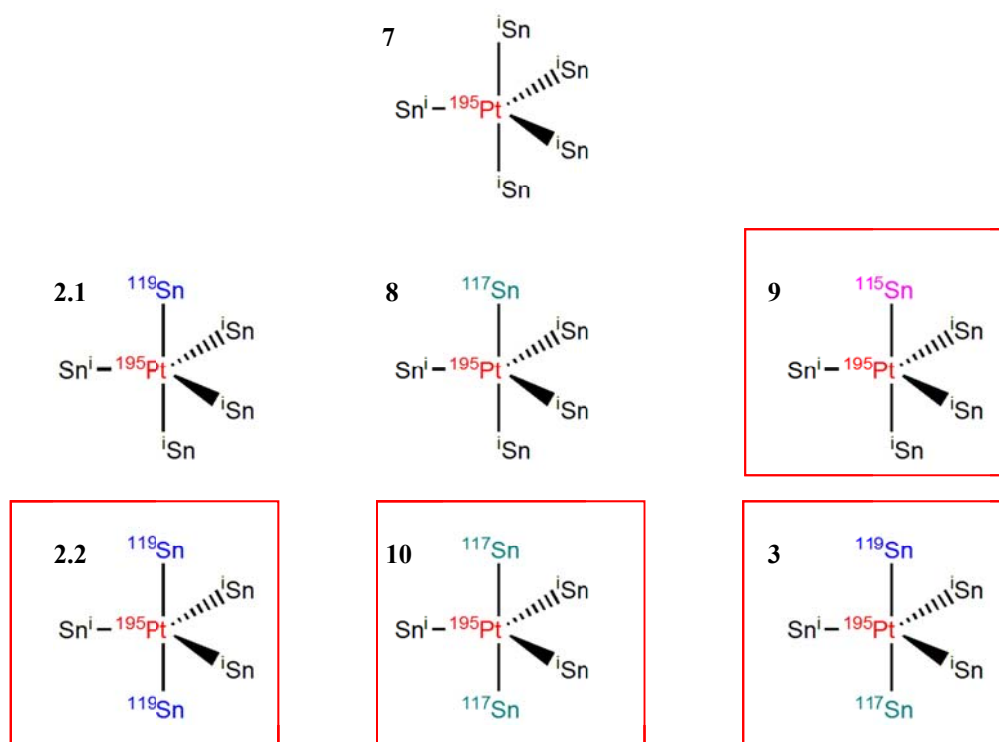


Figure 3.4: ^{195}Pt NMR spectrum obtained for $[\text{Pt}(\text{SnCl}_3)_5]^{3-}$ in CDCl_3 (20% AQ-336) at 293 K. Chemical shifts in ppm relative to K_2PtCN_4 (in D_2O) at $\delta^{195}\text{Pt} = -4\,700.0\text{ ppm}$. Where (a) and (b) represent the respective $^1J(^{195}\text{Pt}-^{119}\text{Sn})$ and $^1J(^{195}\text{Pt}-^{117}\text{Sn})$ satellites observed for isotopologues **1.1** and **8** in Scheme 3.7. The encircled signals have not been reported in literature.



Scheme 3.8: Isotopologues of $[Pt(SnCl_3)_5]^{3-}$ observed with ^{195}Pt NMR. Due to the rapid Berry-pseudo rotations, it is not possible to distinguish isotopomers from isotopologues. All Cl^- were left out for clarity. The bordered isotopologues **2.2**, **3**, **9** and **10** have not been reported in literature.

The satellites indicated by the symbols (a) and (b) in Figure 3.4 have previously been assigned to $^1J(^{119}Sn-^{195}Pt)$ and $^1J(^{117}Sn-^{119}Sn)$ satellites respectively.^{2,27,29} In addition to these satellites, the ^{195}Pt NMR signals indicated by circles in Figure 3.4 have to our knowledge not been reported in literature. To determine the identity of the isotopologues responsible for all the $^1J(^{119/117/115}Sn-^{195}Pt)$ satellites observed in the ^{195}Pt NMR spectrum shown in Figure 3.4 the relative ^{195}Pt NMR signal areas of the respective satellites, as well as the corresponding coupling constants, were measured and reported in Tables 3.4 and 3.5 respectively. The relative area of each $^1J(^{119}Sn-^{195}Pt)$ satellite indicated by the symbol (a) in Figure 3.4 is 0.24, giving a sum of 0.48. This signal area agrees remarkably well with the NSA calculated for isotopologue **2.1** (Schemes 3.6 and 3.8), listed in Table 3.4, and are assigned to the $^1J(^{119}Sn-^{195}Pt)$ coupling expected for isotopologue **2.1**.[§] Similarly, the relative signal areas measured for the set of $^1J(^{117}Sn-^{195}Pt)$ satellites illustrated by (b) in Figure 3.4 agree well with the NSA calculated for isotopologue **8** in Scheme 3.8, Table 3.4, and are due to $^1J(^{117}Sn-^{195}Pt)$ coupling. These assignments are confirmed when comparing the ratio of the coupling

[§] The relative ^{119}Sn NMR signal areas of the $^1J(^{195}Pt-^{119}Sn)$ satellites observed in Figure 3.2 are equal to the sum of the NSA's of the isotopologues shown in Scheme 3.6, whereas the relative ^{195}Pt NMR signal areas of the $^1J(^{119}Sn-^{195}Pt)$ satellites observed in Figure 3.4 are equal to the NSA of isotopologue **2.1** specifically, illustrated in Scheme 3.8.

constants of satellites (a) to (b), Table 3.5, to the $\gamma(^{119}\text{Sn})/\gamma(^{117}\text{Sn})$ ratio. Moreover, the assignment of these two sets of satellites to $^1\text{J}(^{119}\text{Sn}-^{195}\text{Pt})$ and $^1\text{J}(^{117}\text{Sn}-^{195}\text{Pt})$ couplings is in accordance with the assignments given in the literature.^{2,27,29} In addition to the $^1\text{J}(^{119}\text{Sn}-^{195}\text{Pt})$ and $^1\text{J}(^{117}\text{Sn}-^{195}\text{Pt})$ satellites a third set of relatively low intensity satellites indicated by (c) in Figure 3.4, $^1\text{J} = 13\,920.5$ Hz, is observed. These signals have not been previously reported in the literature to our knowledge! The relative ^{195}Pt NMR signal area of each satellite is 0.01 and the sum of the satellite areas is equal to the NSA of isotopologue **9** illustrated in Scheme 3.8, Table 3.4. Moreover, the ratio of the coupling constants of satellites (b) to (c) is equal to the $\gamma(^{117}\text{Sn})/\gamma(^{115}\text{Sn})$ ratio as shown in Table 3.5, confirming that the ^1J satellites indicated by the symbol (c) in Figure 3.4 are due to $^1\text{J}(^{115}\text{Sn}-^{195}\text{Pt})$ coupling in isotopologue **9**, not previously reported.

Table 3.4: Comparison of the ^{195}Pt NMR signal areas obtained experimentally with those of the calculated NSA's of the possible isotopologues of the $[\text{Pt}(\text{SnCl}_3)_5]^{3-}$ complex anion

^1J sat	Isotopologue	NSA ^a		^{195}Pt NMR signal areas ^d	
		Statistical ^b	Normalized ^c	Statistical	Experimental
7	$[\text{Pt}(^i\text{SnCl}_3)_5]^{3-}$	0.139	1.00	1.00	1.00
a	2.1 $[\text{Pt}(^i\text{SnCl}_3)_4(^{119}\text{SnCl}_3)]^{3-}$	0.072	0.512	0.256	0.24±0.01
b	8 $[\text{Pt}(^i\text{SnCl}_3)_4(^{117}\text{SnCl}_3)]^{3-}$	0.063	0.454	0.227	0.21±0.01
c	9 $[\text{Pt}(^i\text{SnCl}_3)_3(^{115}\text{SnCl}_3)]^{3-}$	0.003	0.020	0.010	0.01±0.002
d	2.2 $[\text{Pt}(^i\text{SnCl}_3)_3(^{119}\text{SnCl}_3)_2]^{3-}$	0.014	0.105	0.026	0.024±0.01
e	10 $[\text{Pt}(^i\text{SnCl}_3)_3(^{117}\text{SnCl}_3)_2]^{3-}$	0.011	0.082	0.021	0.02±0.001
f	3 $[\text{Pt}(^i\text{SnCl}_3)_3(^{119}\text{SnCl}_3)(^{117}\text{SnCl}_3)]^{3-}$	0.026	0.186	0.046	0.04±0.003
	5 $[\text{Pt}(^i\text{SnCl}_3)_2(^{119}\text{SnX}_3)_2(^{117}\text{SnCl}_3)]^{3-}$	0.004	0.029	0.005	-
	6 $[\text{Pt}(^i\text{SnCl}_3)_2(^{119}\text{SnX}_3)(^{117}\text{SnCl}_3)_2]^{3-}$	0.003	0.025	0.004	-

^a Natural Statistical Abundance of the respective isotopologues. ^b The NSA of the isotopologues calculated using Eq. 3.1 does not take into account that ^{195}Pt is magnetically-active, thus only 33.7 % of the NSA's calculated for the isotopologues using Eq. 3.1 are observed with ^{195}Pt NMR. ^c Normalized values of NSA's for ease of comparing ^{195}Pt NMR signal areas and should be equal to the sum of the satellites. ^d Area of each respective ^{195}Pt NMR signal.

Table 3.5: Comparison of the ratio of ¹J coupling constants of respective ¹J satellites to the ratio of gyromagnetic ratios of magnetically-active Sn isotopes present in respective isotopologues

¹ J sat	Isotopologue	¹ J(^{119/117/115} Sn- ¹⁹⁵ Pt) / Hz	¹ J ratios	γ(^x Sn)/γ(^y Sn)
a	2.1 [¹⁹⁵ Pt(ⁱ SnCl ₃) ₄ (¹¹⁹ SnCl ₃) ₃] ³⁻	15 864		
b	8 [¹⁹⁵ Pt(ⁱ SnCl ₃) ₄ (¹¹⁷ SnCl ₃) ₃] ³⁻	15 160	1.046 ^a	1.046 ^c
c	9 [¹⁹⁵ Pt(ⁱ SnCl ₃) ₄ (¹¹⁵ SnCl ₃) ₃] ³⁻	13 921	1.089 ^b	1.089 ^d

^a Ratio of ¹J coupling constants of satellites (a) to (b) illustrated in Figure 3.4. ^b Ratio of ¹J coupling constants of satellites (b) to (c) illustrated in Figure 3.4. ^c ^xSn = ¹¹⁹Sn and ^ySn = ¹¹⁷Sn. ^d ^xSn = ¹¹⁷Sn and ^ySn = ¹¹⁵Sn. The uncertainties on coupling constants are estimated to be ± 15 Hz

Each set of ¹⁹⁵Pt NMR signals indicated by a circle in Figure 3.5A at first appears to resemble a set of ‘triplets’ with signal area ratios of 1:2:1. However, after careful and accurate integration it was found that these sets of signals are not consistent with a simple 1st order ‘triplet’ structure. Rather, these are sets of satellites which originate from isotopologues with more than one magnetically-active tin nuclei, illustrated in Scheme 3.8. First consider isotopologue **2.2** shown in Scheme 3.8 which contains two ¹¹⁹Sn isotopes and the ¹⁹⁵Pt nucleus. Applying the method of successive splitting, the ¹⁹⁵Pt NMR signal is split into a doublet by one ¹¹⁹Sn isotope, ¹J(¹¹⁹Sn-¹⁹⁵Pt) = 15 864.2 Hz, as indicated by the symbol (a) in Figure 3.5B. The doublet is split again by a second ¹¹⁹Sn isotope with the same ¹J(¹¹⁹Sn-¹⁹⁵Pt) coupling constant 15 864.2 Hz, and results in the triplet indicated by the symbol (d) in Figure 3.5C. The central line of the triplet overlaps exactly with the ¹⁹⁵Pt signal due to isotopologue **7**, which prevents the integration of thereof. Nevertheless, as this is a 1st order triplet**, the relative ¹⁹⁵Pt NMR signal area ratio of the triplet indicated by (d) in Figure 3.5C is estimated to be 0.024:0.048:0.024, giving a sum total of 0.096 which is quantitatively consistent with the NSA calculated for isotopologue **2.2** shown in Scheme 3.8 and thus assigned accordingly. Similarly, the sum of the relative ¹⁹⁵Pt NMR signal areas of the triplet indicated by the symbol (e) in Figure 3.5C agree remarkably well with the NSA calculated for isotopologue **10** illustrated in Scheme 3.8 and is thus assigned to isotopologue **10**. The sum of the relative ¹⁹⁵Pt NMR signal areas indicated by the symbol (f) in Figure 3.5C agree exceptionally well with the NSA calculated for isotopologue **3**, Scheme 3.8. The doublet of doublets indicated by the symbol (f) in Figure 3.5C is due to both ¹J(¹¹⁹Sn-¹⁹⁵Pt) and ¹J(¹¹⁷Sn-¹⁹⁵Pt) coupling in isotopologue **3**.

** Using the method of successive splitting J coupling between ^{119/117/115}Sn and ¹⁹⁵Pt follow by definition 1st order rules, hence it is a ‘true’ triplet.

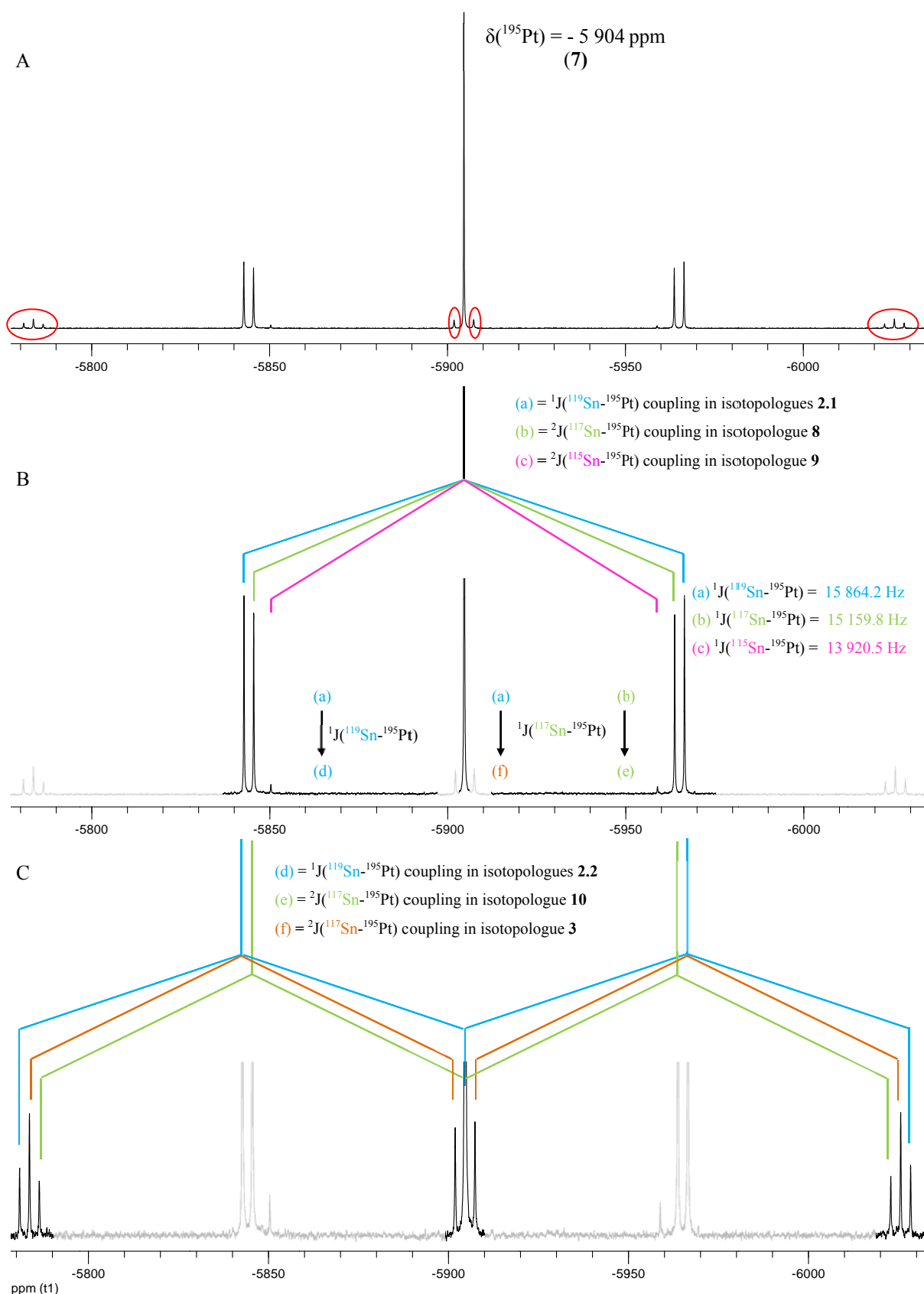


Figure 3.5: ^{195}Pt NMR spectrum obtained for $[Pt(\text{SnCl}_3)_5]^{3-}$ in CDCl_3 (30% AQ-336(Br)) at 293 K. Chemical shifts in ppm relative to K_2PtCN_4 (in D_2O) at $\delta(^{195}\text{Pt}) = -4\,700.0\text{ ppm}$. The 1J satellites indicated by the symbols (a) to (f) are assigned to the $^1J(^{119/117/115}\text{Sn}-^{195}\text{Pt})$ couplings of the respective isotopologues shown in Scheme 3.8. The $^1J(^{119/117}\text{Sn}-^{195}\text{Pt})$ satellites shown in C, (d), (e) and (f), resulted from successive splitting of the $^1J(^{119/117}\text{Sn}-^{195}\text{Pt})$ satellite signals in B by either $^1J(^{119}\text{Sn}-^{195}\text{Pt})$ or $^1J(^{117}\text{Sn}-^{195}\text{Pt})$ coupling.

To summarize, all the respective $^1J(^{119/117/115}\text{Sn}-^{195}\text{Pt})$ satellites observed in the ^{195}Pt NMR spectrum of the $[\text{Pt}(\text{SnCl}_3)_5]^{3-}$ complex anion, indicated by (a) to (f) in Figure 3.5, have been unambiguously assigned to the respective isotopologues shown in Scheme 3.8. To our knowledge, ^{195}Pt NMR signals of isotopologues **2.2**, **3**, **9** and **10** have not been reported in the literature and this shows the value and sensitivity of ^{195}Pt NMR compared to ^{119}Sn NMR for such structural assignments in solution.

3.2.4. ^{195}Pt NMR of the homoleptic $[\text{Pt}(\text{SnBr}_3)_5]^{3-}$ complex anions

The corresponding ^{195}Pt NMR spectrum of $[\text{Pt}(\text{SnBr}_3)_5]^{3-}$ extracted into chloroform-*d* (20% (v/v) Aliquat-336) is shown in Figure 3.6. Compared to the ^{119}Sn NMR spectrum (Figure 3.3) which is broad, the ^{195}Pt NMR spectrum shows a remarkable resemblance to the ^{195}Pt NMR spectrum of the $[\text{Pt}(\text{SnCl}_3)_5]^{3-}$ species (Figure 3.4). The central ^{195}Pt NMR signal at $\delta(^{195}\text{Pt}) = -5483.5$ ppm has a width at half peak height of 63.72 Hz and is flanked by several 1J satellites. Note that due to relatively small amounts of chloride unavoidably in the sample (see experimental Chapter 2.1.2, p 15) species such as $[\text{Pt}(\text{SnBr}_3)_4(\text{SnBr}_2\text{Cl})]^{3-}$ are also present in this solution and give rise to the ^{195}Pt NMR signals encircled in Figure 3.6. A detailed discussion of the heteroleptic species will be done in Chapter 4.

The same methodology used to elucidate the ^{195}Pt NMR spectrum of the homoleptic chlorido species in Section 3.2.3 was used to assign the spectrum and identify the possible NMR active isotopologues of the $[\text{Pt}(\text{SnBr}_3)_5]^{3-}$ complex anion. The central ^{195}Pt NMR signal is assigned to isotopologue **VII**, Table 3.6, which does not contain any $^{119/117/115}\text{Sn}$ nuclei, summarized in Scheme 3.9. From the good agreement between the NSA's of the respective isotopologues given in Scheme 3.9 and the relative ^{195}Pt NMR signal areas of each set of $^1J(^{119/117/115}\text{Sn}-^{195}\text{Pt})$ satellites (Table 3.6), assignments were made accordingly as illustrated in Figure 3.6. Moreover, confirmation of assignments of isotopologues **X.1**, **VIII** and **IX** is obtained from the excellent agreement of the ratios of the $^1J(^{119/117/115}\text{Sn}-^{195}\text{Pt})$ coupling constants with the $\gamma(^{119/117}\text{Sn})/\gamma(^{117/115}\text{Sn})$ ratios, Table 3.7. As for the $[\text{Pt}(\text{SnCl}_3)_5]^{3-}$ complex anion, the assignment of the triplets indicated by symbols (d) and (e) are ascribed to $^1J(^{119/119}\text{Sn}-^{195}\text{Pt})$ and $^1J(^{117/117}\text{Sn}-^{195}\text{Pt})$ satellites due to isotopologues **II.2** and **X** respectively, and the doublet of doublet indicated by the symbol (f) is assigned satellites due to $^1J(^{119/117}\text{Sn}-^{195}\text{Pt})$ coupling in isotopologue **III** as shown in Figure 3.6.

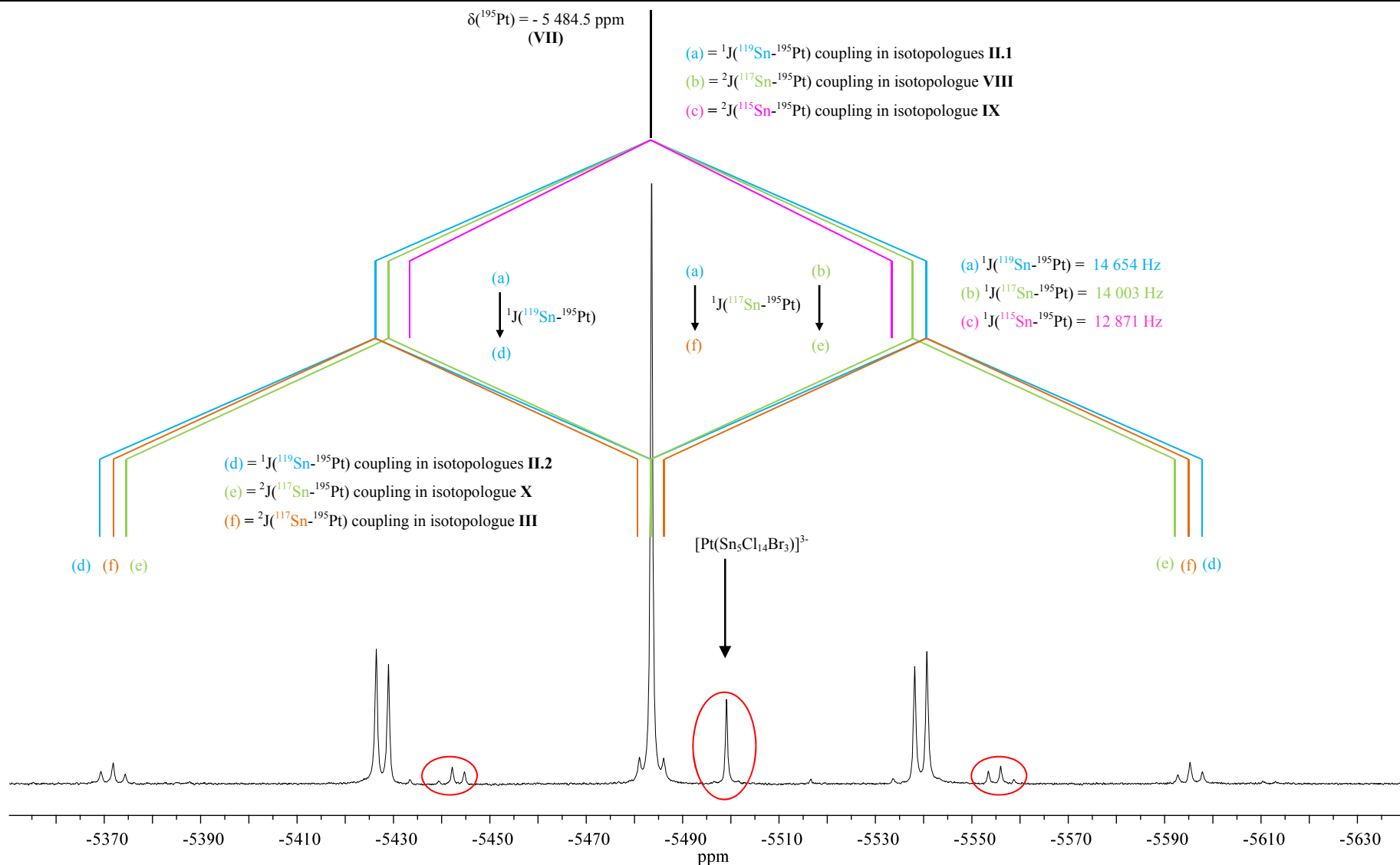
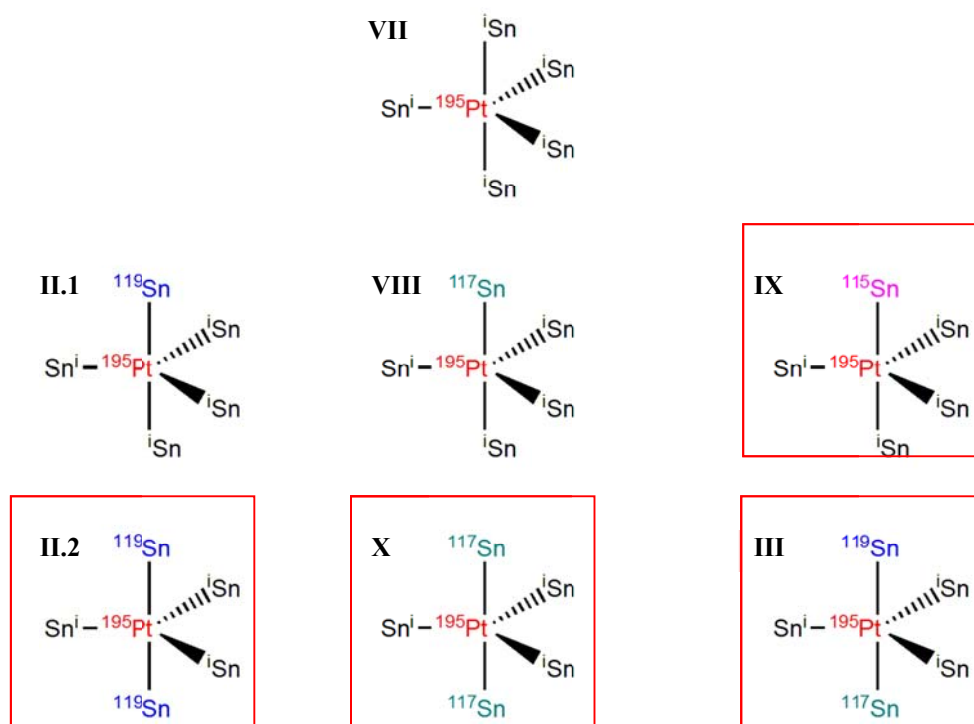


Figure 3.6: ^{195}Pt NMR spectrum obtained for $[Pt(SnBr_3)_5]^{3-}$ in $CDCl_3$ (20% AQ-336(Br)) at 293 K. The 1J satellites indicated by (a) to (f) is assigned to $^1J(^{119/117/115}Sn-^{195}Pt)$ couplings of the isotopologues shown in Scheme 3.9. Similarly to the analogous chlorido species, the $^1J(^{119/117}Sn-^{195}Pt)$ satellites obtained for isotopologues II.2, X and III result from successive splitting. The encircled ^{195}Pt NMR signals are due to the $[Pt(Sn_5Cl_4Br)_3]^{3-}$ complex anion.



Scheme 3.9: Isotopologues of $[Pt(SnBr_3)_5]^{3-}$ observed with ^{195}Pt NMR. The bordered isotopologues **IX**, **II.2**, **X** and **III** have not been reported in literature.

Table 3.6: Comparison of the ^{195}Pt NMR signal areas experimentally obtained with ^{195}Pt NMR to calculated NSA's of the possible isotopologues of the $[Pt(SnBr_3)_5]^{3-}$ complex anion

$^1J_{sat}$	Isotopologue	NSA ^a		^{195}Pt NMR signal areas ^d	
		Statistical ^b	Normalized ^c	Statistical	Experimental
	VII $[^{195}Pt(iSnBr_3)_5]^{3-}$	0.139	1.00	1.00	1.00
a	II.1 $[^{195}Pt(iSnBr_3)_4(^{119}SnBr_3)]^{3-}$	0.072	0.512	0.256	0.25±0.01
b	VIII $[^{195}Pt(iSnBr_3)_4(^{117}SnBr_3)]^{3-}$	0.063	0.454	0.227	0.21±0.01
c	IX $[^{195}Pt(iSnBr_3)_4(^{115}SnBr_3)]^{3-}$	0.003	0.020	0.010	0.01±0.002
d	II.2 $[^{195}Pt(iSnBr_3)_3(^{119}SnBr_3)_2]^{3-}$	0.014	0.105	0.026	0.02±0.002
e	X $[^{195}Pt(iSnBr_3)_3(^{117}SnBr_3)_2]^{3-}$	0.011	0.082	0.021	0.02±0.001
f	III $[^{195}Pt(iSnBr_3)_3(^{119}SnBr_3)(^{117}SnBr_3)]^{3-}$	0.026	0.186	0.046	0.04±0.004
	V $[^{195}Pt(iSnBr_3)_2(^{119}SnBr_3)_2(^{117}SnBr_3)]^{3-}$	0.004	0.029	0.005	-
	VI $[^{195}Pt(iSnBr_3)_2(^{119}SnBr_3)(^{117}SnBr_3)_2]^{3-}$	0.003	0.025	0.004	-

^a Natural Statistical Abundance of the respective isotopologues. ^b The NSA of the isotopologues calculated using Eq. 3.1 does not take into account that only ^{195}Pt is magnetically-active, and thus only 33.7 % of the NSA's calculated for the isotopologues using Eq. 3.1 are observable with ^{195}Pt NMR. ^c Normalized values of NSA's for ease of comparing ^{195}Pt NMR signal areas and should be equal to the sum of the satellites. ^d Area of each respective ^{195}Pt NMR signal.

Table 3.7: Comparison of the ratio of 1J coupling constants of respective 1J satellites to the ratio of gyromagnetic ratios of magnetically-active Sn isotopes present in respective isotopologues

1J sat	Isotopologue	$^1J(^{119/117/115}Sn-^{195}Pt)$ / Hz	1J ratios	$\gamma(^xSn)/\gamma(^ySn)$
a	II.1 $[^{195}Pt(^iSnBr_3)_4(^{119}SnBr_3)]^{3-}$	14 654	1.046 ^a	1.046 ^c
b	VIII $[^{195}Pt(^iSnBr_3)_4(^{117}SnBr_3)]^{3-}$	14 003		
c	IX $[^{195}Pt(^iSnBr_3)_4(^{115}SnBr_3)]^{3-}$	12 871	1.089 ^b	1.089 ^d

^a Ratio of 1J coupling constants of satellites (a) to (b) illustrated in Figure 3.6. ^b Ratio of 1J coupling constants of satellites (b) to (c) illustrated in Figure 3.6. ^c $^xSn = ^{119}Sn$ and $^ySn = ^{117}Sn$. ^d $^xSn = ^{117}Sn$ and $^ySn = ^{115}Sn$. The uncertainties on coupling constants are estimated to be ± 15 Hz

All the respective $^1J(^{119/117/115}Sn-^{195}Pt)$ satellites observed in the ^{195}Pt NMR spectrum of the $[Pt(SnBr_3)_5]^{3-}$ complex anion, indicated by (a) to (f) in Figure 3.6, are unambiguously assigned to the respective isotopologues shown in Scheme 3.9. Isotopologues **II.2**, **III**, **IX** and **X** have, to our knowledge, not been reported in the literature.

There are several apparent differences when comparing the ^{195}Pt NMR spectrum of the $[Pt(SnBr_3)_5]^{3-}$ complex anion to that of the chlorido analogue. Firstly, a downfield shift of 421 ± 3 ppm is obtained when comparing the chemical shift of the ^{195}Pt NMR signal of isotopologue **VII** to **7**, Table 3.8. Secondly, the value of the $^1J(^{119/117/115}Sn-^{195}Pt)$ coupling constants of the $Pt(SnX_3)_5]^{3-}$ complex anions decreases by *ca.* 8% on passing from $X = Cl^-$ to Br^- , Table 3.8.

Table 3.8: ^{195}Pt NMR data obtained for the $[Pt(SnCl_3)_5]^{3-}$ and the $[Pt(SnBr_3)_5]^{3-}$ complex anions^a

	$\delta^{195}Pt$ (ppm)	$^1J(^{119}Sn-^{195}Pt)$ / Hz	$^1J(^{117}Sn-^{195}Pt)$ / Hz	$^1J(^{115}Sn-^{195}Pt)$ / Hz
$[Pt(SnCl_3)_5]^{3-}$	-5904.6	15864	15160	13921
$[Pt(SnBr_3)_5]^{3-}$	-5483.5	14659	14009	12862

^a Chemical shifts in ppm relative to K_2PtCN_4 (in D_2O). The uncertainties on chemical shifts and coupling constants are estimated to be ± 3 ppm and ± 10 Hz, respectively.

In a study of the $[Pt(X_n(SnX_3)_{4-n})]^{2-}$ ($X = Cl/Br^-$, $n = 1 - 4$) and $[Pt(SnX_3)_5]^{3-}$ ($X = Cl/Br^-$) complex anions by means of ^{119}Sn NMR, ^{195}Pt NMR as well as X-ray diffraction, Nelson *et al*²⁹ showed that the Pt-Sn bond lengths increased in the order *cis*- $[PtCl_2(SnCl_3)_2]^{2-} < [Pt(Br_3(SnBr_3))]^{2-} < cis$ - $[PtBr_2(SnBr_3)_2]^{2-}$. It thus appears as though elongation of the Pt-Sn bond occurs upon substitution of Cl with Br in Pt-Sn complexes. Extrapolating this ‘trend’ to

the [Pt(SnX₃)₅]³⁻ (X = Cl⁻/Br⁻) species studied here, one would expect the Pt-Sn bond to elongate upon substitution of Cl⁻ with Br⁻, which supports the trend observed in ¹J coupling constants seen here. However, further studies are needed to confirm whether this is the only reason for the trend.

Preliminary DFT calculations^{††} (using the Amsterdam density functional, ADF, software package) performed on the [Pt(SnX₃)₅]³⁻ (X = Cl⁻/Br⁻) species does show an elongation of the Pt-Sn bond length upon substitution of Cl⁻ by Br⁻, Table 3.9. This is consistent with the prediction derived from the trend observed by Nelson *et al.*²⁹ The ¹⁹⁵Pt nucleus thus becomes less shielded for the homoleptic bromido complex anion, yielding the ‘downfield’ shift of the ¹⁹⁵Pt NMR signals as shown in Table 3.8. Furthermore, the elongated Pt-Sn bond length of the homoleptic bromido species also explains the decrease in ¹J(^{119/117/115}Sn-¹⁹⁵Pt) coupling constants, Table 3.8.

Table 3.9: Comparative Pt-Sn and Sn-X bond lengths for [Pt(SnX₃)₅]³⁻ (X = Cl⁻ or Br⁻) determined by DFT calculations

	Pt-Sn bond length / Å				Sn-X bond length / Å			
	Exp. ^a		DFT calc.		Exp. ^a		DFT calc.	
	axial	equatorial	axial	equatorial	ax.	eq.	ax.	eq.
[Pt(SnCl ₃) ₅] ³⁻	2.553	2.577	2.561	2.585	2.363 ^b		2.364	2.393
[Pt(SnBr ₃) ₅] ³⁻			2.573	2.597			2.517	2.549

^a The experimental Pt-Sn and Sn-Cl bond lengths were obtained by Nelson *et al.*²⁹ ^b Nelson *et al* only reported an average Sn-Cl bond length.

Finally, greater ¹⁹⁵Pt NMR signal line widths are obtained for the [Pt(SnBr₃)₅]³⁻ species compared to the [Pt(SnCl₃)₅]³⁻ species which suggests that the intra-molecular site-exchange process mentioned previously (by a Berry-pseudo mechanism) occurs slower on the ¹⁹⁵Pt NMR acquisition time-scale for the homoleptic bromido species.

^{††} The basic parameters used for the DFT calculations performed by Dr. W. J. Gerber: the Local Density Approximation (LDA) was used as Exchange Correlation functional in the SCF calculations for Geometry optimization. Vibrational Frequency calculations confirmed that the optimized geometries are a true minimum on the potential energy surface. The QZ4P basis set was used for all atoms. Moreover, scalar relativistic effects were taken into account as set out in the ZORA formalism.

3.3. Conclusion

Comparison of the NSA's calculated for each possible isotopologue to the areas of the ¹¹⁹Sn or ¹⁹⁵Pt NMR signals, together with the comparison of the ¹J/¹J ratios of respective ¹J satellites to the ratio of gyromagnetic ratios of the related magnetically-active tin nuclei and the application of the method of successive splitting allowed for the unambiguous identification of 20 isotopologues of the [Pt(SnX₃)₅]³⁻ (X = Cl⁻/Br⁻) complex anions, Schemes 3.5, 3.7, 3.8 and 3.9. Moreover, high-resolution ¹¹⁹Sn and ¹⁹⁵Pt NMR facilitated the identification of ten isotopologues, **2.2**, **3**, **5**, **6**, **9**, **10**, **II.2**, **III**, **IX** and **X**, that have never been reported in literature.

Replacement of all the Cl⁻ with Br⁻ in the [Pt(SnX₃)₅]³⁻ (X = Cl⁻/Br⁻) complex anions resulted in an 'upfield' shift of 110 ppm of the ¹¹⁹Sn NMR signals compared to the 'downfield' shift of 421 ppm of the ¹⁹⁵Pt NMR signals. This is indicative of the chemical shift of the ¹⁹⁵Pt NMR signals being much more sensitive to a change in the electronic environment compared to ¹¹⁹Sn NMR signals. As was expected, no isotopomers were observed in either the ¹¹⁹Sn or the ¹⁹⁵Pt NMR spectrum, confirming that the Berry-pseudo rotation of these trigonal bipyramidal species occurs rapidly on the NMR acquisition time-scale. Furthermore, the ¹¹⁹Sn NMR spectrum of the [Pt(SnBr₃)₅]³⁻ complex anion only resulted in only very broad ¹¹⁹Sn NMR signals that could not be elucidated. The ¹⁹⁵Pt NMR spectrum of the same solution reveals the presence of a heteroleptic species, [Pt(Sn₅Cl₁₄Br)]³⁻, in solution. From the separate ¹⁹⁵Pt NMR signals observed, the broad ¹¹⁹Sn NMR signal cannot be ascribed to *intra-* or *inter-* molecular halide scrambling occurring in solution as suggested in literature, and might rather be due to overlap of the ¹¹⁹Sn NMR signals of the two respective species. However, further investigation is required. It is thus clear that high resolution ¹⁹⁵Pt NMR by comparison to ¹¹⁹Sn NMR is a much more powerful tool to assign these structures as (1) shielding of the ¹⁹⁵Pt nucleus shows much higher sensitivity to small changes in the SnX₃⁻ (X = Cl⁻/Br⁻) ligand and (2) narrower ¹⁹⁵Pt NMR lines are obtained.

Having fully assigned the ¹¹⁹Sn and ¹⁹⁵Pt NMR spectra obtained for the homoleptic chlorido and bromido species, the next chapter will concentrate on a detailed study of the much more complex heteroleptic [Pt(Sn₅Cl_nBr_{15-n})]³⁻ (n = 0 – 15) complex anions by means of high resolution ¹⁹⁵Pt NMR and ¹¹⁹Sn NMR.

Chapter IV

Characterization of the heteroleptic $[Pt(Sn_5Cl_nBr_{15-n})]^{3-}$ ($n = 0 - 15$) species by means of ^{119}Sn and high resolution ^{195}Pt NMR

4.1. Introduction

The heteroleptic $[Pt(SnCl_nBr_{3-n})_5]^{3-}$ ($n = 0 - 3$) complex anions have not received much attention in the literature unlike the analogous homoleptic chlorido and bromido species. However, mixed halide tin(IV) species⁷⁶ and trihalostannato anions⁷⁷ have been investigated to some degree. Burke and Lauterbur⁷⁶ were the first to study mixed halide tin(IV) $SnCl_nBr_{4-n}$ ($n = 1 - 3$) species by means of ^{119}Sn NMR obtained from mixtures of $SnCl_4$ and $SnBr_4$, as well as similar results for mixtures of $SnCl_4$ and SnI_4 and of $SnBr_4$ and SnI_4 . These mixed halide complexes are formed by halogen scrambling. The trihalogenotin SnX_3^- ($X = Cl/Br^-$) group is a well known ligand in transition-metal compounds as it formally has a 'lone' pair of electrons that can act as a σ -donor. Coddington and Taylor⁷⁷ investigated diethyl ether extracts containing the trihalogenostannate(II) anions $[SnX_3]^-$, $[SnX_2Y]^-$, $[SnXY_2]^-$, $[SnY_3]^-$ and $[SnX(Y)Z]^-$ (where X, Y, and Z = Cl, Br or I) and with $(H_3O)^+$ as cation by means of ^{119}Sn NMR. At $-60^\circ C$ the ^{119}Sn chemical shifts of all ten trihalogenostannate(II) anions, $[SnCl_xBr_yI_z]^-$ ($x + y + z = 3$) could be assigned. Garralda *et al*⁷⁸ and Koch⁶⁹ both observed halogen scrambling within transition-metal tin(II)halide complexes. Garralda *et al*⁷⁸ studied the five-coordinate $[Rh(SnCl_nBr_{(3-n)})(norborene)(tertiary phosphine)_2]$ complexes by means of ^{31}P and ^{119}Sn NMR spectroscopy. The NMR data Garralda *et al* obtained showed the existence of a mixture of complexes containing $SnCl_3^-$, $SnCl_2Br^-$, $SnClBr_2^-$ and $SnBr_3^-$ ligands bound to Rh(I). Moreover, the ^{119}Sn NMR spectrum showed that the complexes with the mixed halide ligands, $SnCl_2Br^-$, $SnClBr_2^-$, had $\delta(^{119}Sn)$ shifts between the $\delta(^{119}Sn)$ shifts of the complexes with $SnCl_3^-$ and $SnBr_3^-$ as ligands respectively. Similar results were obtained by Koch⁶⁹ by ^{119}Sn NMR of the series of $[Pt(SnCl_xBr_y)_5]^{3-}$ ($x + y = 3$) complex anions extracted into chloroform with 20% (v/v) Aliquat-336. The ^{119}Sn spectrum reported from mixing equal volumes of solutions containing the $[Pt(SnCl_3)_5]^{3-}$ and $[Pt(SnBr_3)_5]^{3-}$ complexes is shown in Figure 4.1. Four sets of resonances, each set consisting out of 5 – 8 resolved ^{119}Sn lines, were obtained. These were

assigned to four sets of resonances corresponding to $[\text{PtSn}_5\text{Cl}_{15-n}\text{Br}_n]^{3-}$, $[\text{PtSn}_5\text{Cl}_{10-n}\text{Br}_{5+n}]^{3-}$ and $[\text{PtSn}_5\text{Cl}_{5-n}\text{Br}_{10+n}]^{3-}$ ($n = 0, 5$) as heteroleptic species, with the resolution increasing for species with more bromido ligand bound to Sn(II).⁶⁹ However, due to low S/N ratios and relatively poor resolution, each individual line within the respective sets of resonances could not completely be assigned. In this chapter the objective is to re-examine this series of heteroleptic species with both ^{119}Sn and ^{195}Pt NMR.

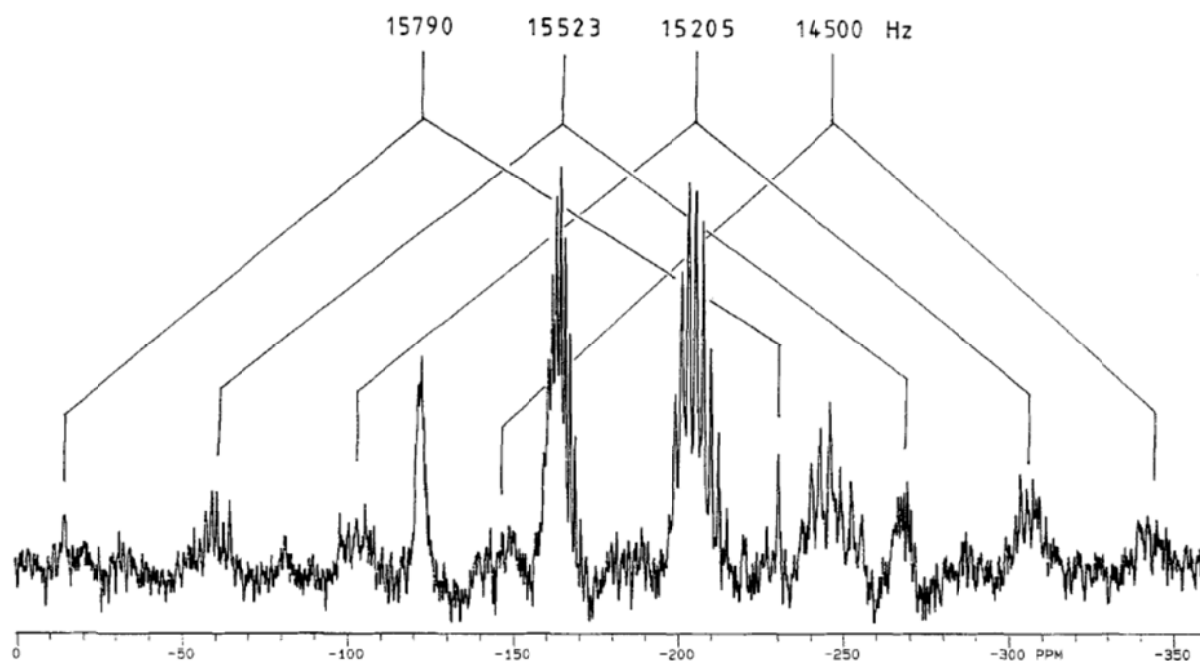
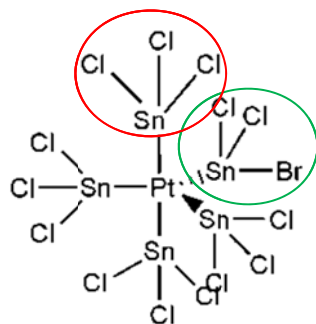


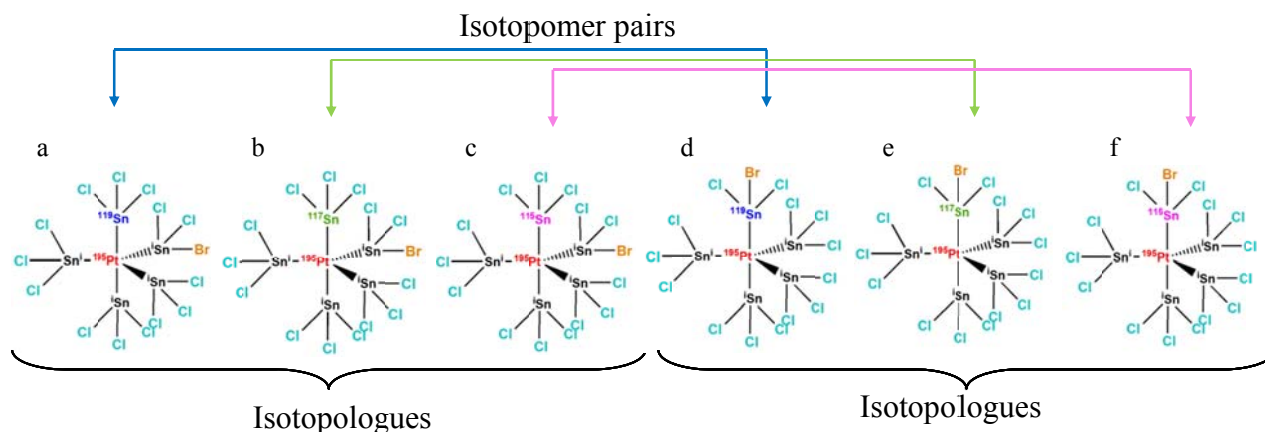
Figure 4.1: ^{119}Sn NMR spectrum obtained by Koch⁶⁹ for a solution containing equal volumes of $[\text{Pt}(\text{SnCl}_3)_5]^{3-}$ and $[\text{Pt}(\text{SnBr}_3)_5]^{3-}$ in Aliquat 336 at 25 °C

The detailed investigation of the possible isotopologues of the $[\text{Pt}(\text{SnX}_3)_5]^{3-}$ ($X = \text{Cl}^-/\text{Br}^-$) complex anions in Chapter 3 illustrated the power of ^{195}Pt NMR and this led to the unambiguous identification and assignment of 20 possible isotopologues. However, isotopomers of the homoleptic chlorido and bromido species could not be observed. For the heteroleptic species various isotopomers, in addition to the isotopologues discussed in Chapter 3, are possible. Consider the heteroleptic species wherein one Cl^- is substituted with Br^- . The $[\text{Pt}(\text{Sn}_5\text{Cl}_{14}\text{Br})]^{3-}$ complex anion has two possible coordinating tin ligands, namely SnCl_3^- and SnCl_2Br^- , as illustrated in Scheme 4.1. If rapid *intra-* or *inter-*molecular *halide exchange* occurs on the ^{195}Pt NMR acquisition time scale, it may be expected that the $\delta(^{195}\text{Pt})$ and the $^1J(^{119/117/115}\text{Sn} - ^{195}\text{Pt})$ satellites for each respective isotopomer pair, Scheme 4.2,

would rapidly interchange. On the other hand, if slow halide exchange takes place, two separate sets ^{195}Pt NMR peaks and two sets of $^1J(^{119/117/115}Sn - ^{195}Pt)$ satellites should be observed for the respective isotopomer pairs.



Scheme 4.1: Structure of the heteroleptic $[Pt(Sn_3Cl_{14}Br)]^{3-}$ species, showing the two types of coordinating tin ligands, $SnCl_3^-$ and $SnCl_2Br^-$.



Scheme 4.2: Structures of the various isotopologues and isotopomers possible for the $[Pt(Sn_3Cl_{14}Br)]^{3-}$ complex anion. Only isotopologues with one spin-active Sn nucleus is shown. Structures a to c, and d to f are isotopologues of each other, whereas a and d, b and e, c and f are isotopomer pairs.

In view of this, the heteroleptic $[Pt(SnCl_xBr_y)]^{3-}$ ($x + y = 3$) complex anions were re-investigated by means of high-resolution ^{195}Pt NMR in conjunction with ^{119}Sn NMR, with the objective to fully elucidate all the possible isotopologues of the $[Pt(SnCl_xBr_y)]^{3-}$ ($x + y = 3$) complex anions extracts in chloroform-*d* (20 % v/v Aliquat-336). From the studies relating to the homoleptic species in Chapter III it is clear that ^{195}Pt NMR spectroscopy shows significantly higher resolution and much narrower line-widths compared to ^{119}Sn NMR.

4.2. Results and Discussion

4.2.1. ^{195}Pt NMR of the series of $[Pt(Sn_5Cl_nBr_{15-n})]^{3-}$ ($n = 0 - 15$) complex anions

In previous studies^{57,69} it was shown that when homoleptic transition-metal (Pt and Rh) tin(II)halide (halide = Cl^- and Br^-) complexes are mixed, halide exchange occurs to form the corresponding heteroleptic species. In this study therefore equimolar $(R_3NCH_3^+)_3-$ $[Pt(SnCl_3)_5]^{3-}$ and $(R_3NCH_3^+)_3[Pt(SnBr_3)_5]^{3-}$ ($R = (CH_2)_7CH_3$) solutions in $CDCl_3$ were mixed in several volume ratios and left for one day to equilibrate before acquiring the ^{195}Pt NMR spectra.^{‡‡} Shown in Figure 4.2 are the ^{195}Pt NMR spectra of the ‘pure’ homoleptic complexes $[Pt(SnCl_3)_5]^{3-}$ and $[Pt(SnBr_3)_5]^{3-}$ together with representative mixtures of the heteroleptic species. The ^{195}Pt NMR spectra are truly remarkable showing groups of highly resolved and complex spectra. Due to halide scrambling in these mixed $[Pt(SnCl_3)_5]^{3-}$ and $[Pt(SnBr_3)_5]^{3-}$ extract solutions there are now four possible trihalostannato ligands ($SnCl_3^-$, $SnCl_2Br^-$, $SnClBr_2^-$, $SnBr_3^-$) which appear to coordinate to Pt(II). Thus 14 heteroleptic $[Pt(Sn_5Cl_nBr_{15-n})]^{3-}$ ($n = 1 - 14$) species are possible in addition to the 2 homoleptic species. The ^{195}Pt NMR spectra of the homoleptic chlorido and bromido species are shown in Figures 4.2 (A) and (E) respectively, whereas the ^{195}Pt NMR spectra of the heteroleptic species, $[Pt(Sn_5Cl_nBr_{15-n})]^{3-}$ ($n = 1 - 14$) are shown in Figures 4.2 (B), (C) and (D).

A total of sixteen separate sets of ^{195}Pt NMR signals with a complex set of satellites due to J coupling and relatively high intensity are observed in Figure 4.2, numbered 1 – 16 for clarity. Signals 1 and 16 are clearly assigned to the homoleptic isotopologues **7** and **VII** as discussed in Chapter 3. In several previous hetero-nuclear NMR studies it was shown that the resonance frequencies of the heteroleptic species are expected to occur between those of the homoleptic species.^{48,57,74} It is thus reasonable to suggest that the 14 ^{195}Pt NMR signals, numbered 2 – 15 in Figure 4.2, originate from the 14 possible heteroleptic $[Pt(Sn_5Cl_nBr_{15-n})]^{3-}$ ($n = 1 - 14$) complex anions corresponding to the isotopologues that contain the ^{195}Pt nucleus but no magnetically-active Sn nuclei, illustrated in Scheme 4.3.

^{‡‡} Detailed experimental procedure in Chapter 2, Section 2.1.3, p 16

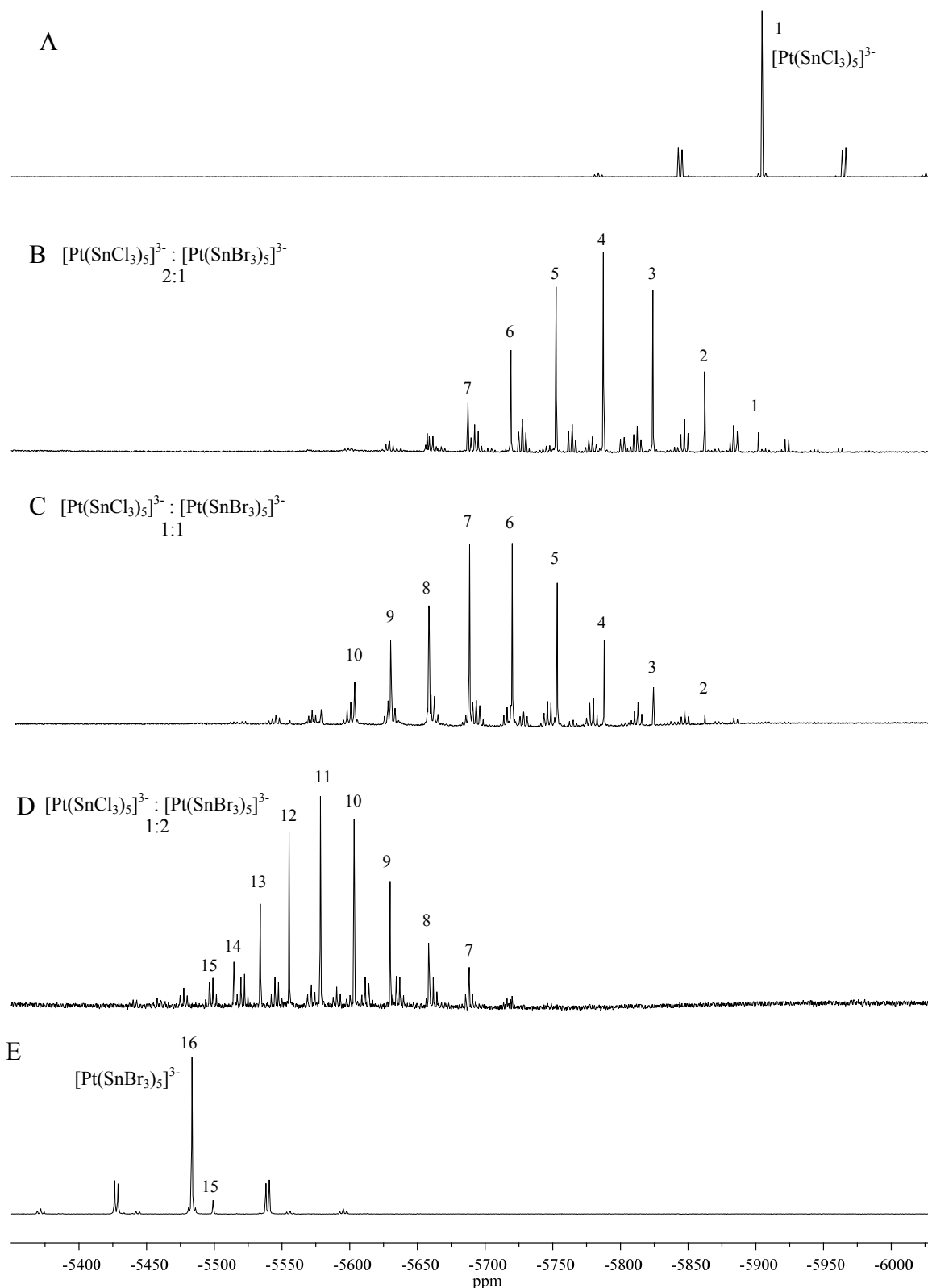
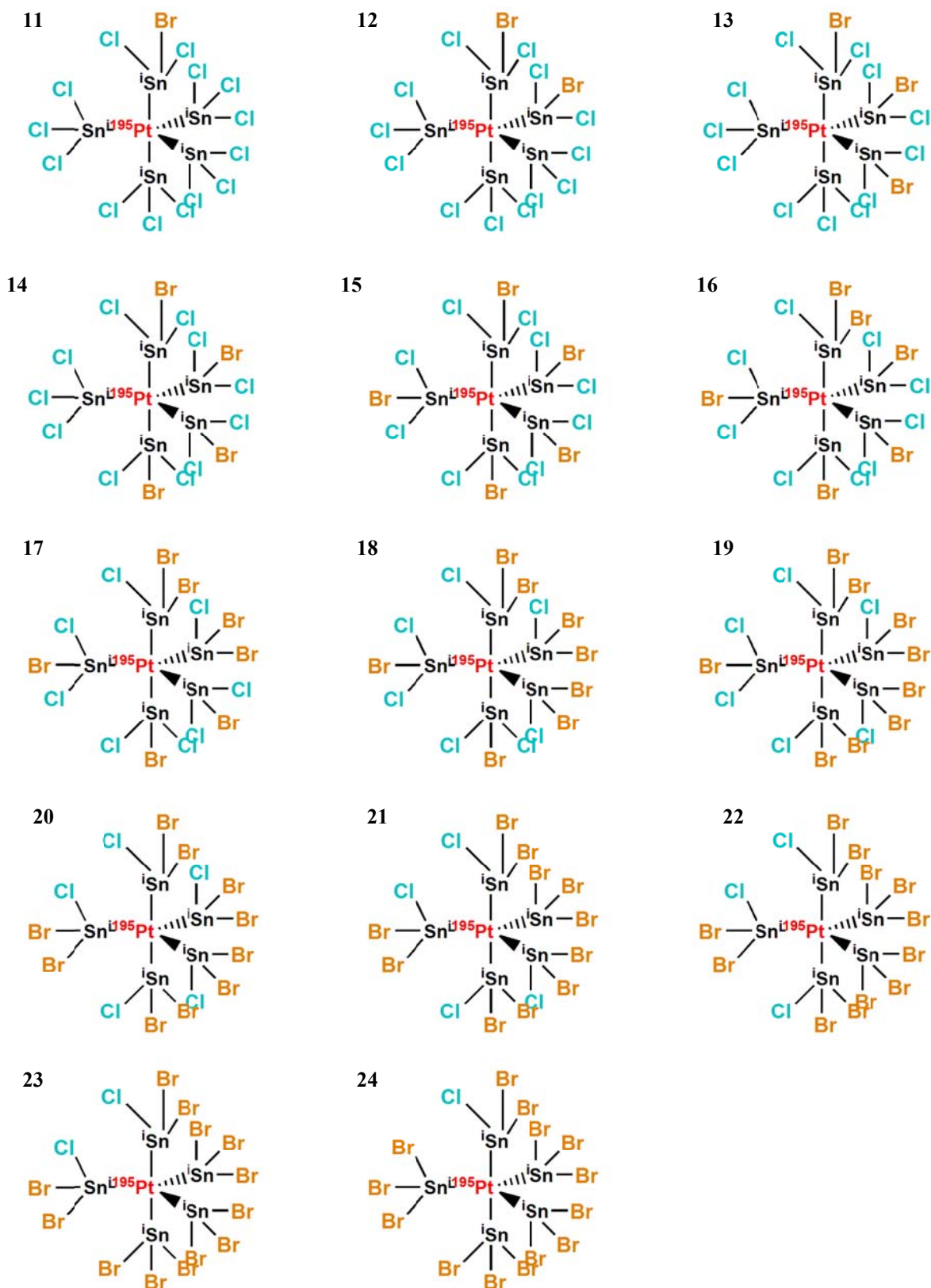


Figure 4.2: ^{195}Pt NMR spectra (128.93 MHz) obtained at 20 °C for (A) $[\text{Pt}(\text{SnCl}_3)_5]^{3-}$ and (E) $[\text{Pt}(\text{SnBr}_3)_5]^{3-}$ in CDCl_3 (20% AQ-336). The spectra shown in (B), (C) and (D) are those of the mixtures of $[\text{Pt}(\text{SnCl}_3)_5]^{3-}$ and $[\text{Pt}(\text{SnBr}_3)_5]^{3-}$ with volume ratios of 2:1, 1:1 and 1:2 respectively. Expansions of these ^{195}Pt NMR spectra are given in Appendix C.



Scheme 4.3: The isotopologues of the 14 heteroleptic species assigned tentatively to the major ^{195}Pt NMR signals numbered 2 – 15 in Figure 4.2. All the isotopologues contain ^{195}Pt and no magnetically-active Sn nuclei. Several isotopomers are also possible for these species and are illustrated in Appendix B. These 14 particular isotopologues/isotopomers are encircled in Appendix B.

The above mentioned proposition is supported by excellent second order correlation obtained when plotting the $\delta(^{195}\text{Pt})$ as a function of the number of Br^- ligands present in each $[Pt(Sn_5Cl_nBr_{15-n})]^{3-}$ ($n = 0 - 15$) species, Figure 4.3. Such systematic ^{195}Pt chemical shift trends have been observed by Kramer and Koch for the $[PtCl_{6-n}Br_n]^{2-}$ complex anions as a function of halide substitution.⁴⁸ The tentative assignments of the 16 $\delta(^{195}\text{Pt})$ NMR signals shown in Figure 4.2, are listed in Table 4.1.

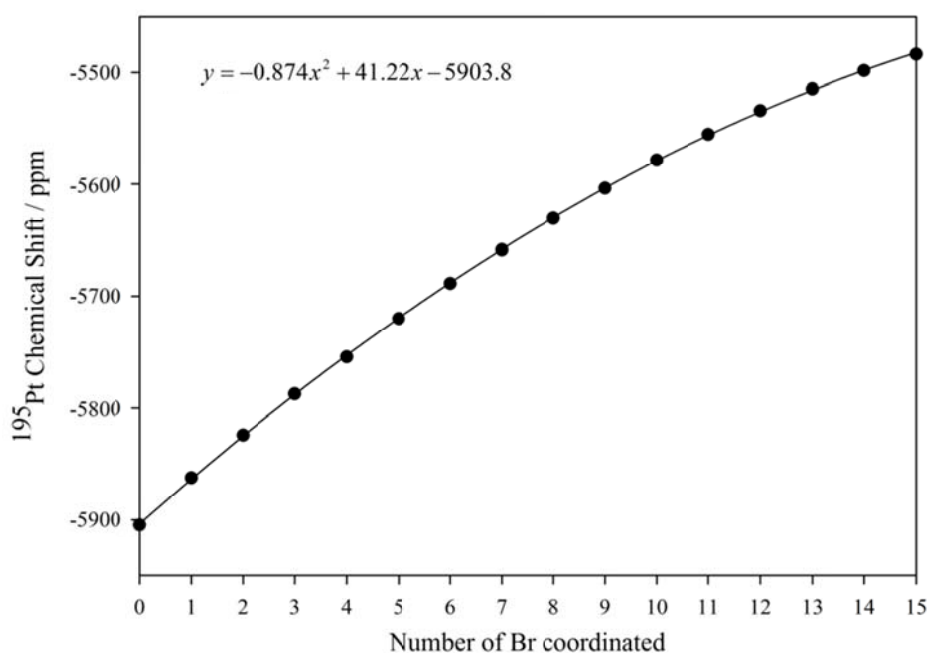


Figure 4.3: Plot of the ^{195}Pt NMR chemical shifts of the 16 $[Pt(Sn_5Cl_nBr_{15-n})]^{3-}$ ($n = 0 - 15$) species as a function of the number of Br^- ligands present in the complex anion. An excellent second order correlation is obtained.

Table 4.1: ^{195}Pt NMR Chemical shifts and tentative assignments of the $[Pt(SnCl_nBr_{15-n})]^{3-}$ ($n = 0 - 15$) species ^a

^{195}Pt NMR signal	$\delta(^{195}Pt)/ppm$	Tentative assignments	Isotopologue
1	-5904.64	$[^{195}Pt(iSnCl_3)_5]^{3-}$	7
2	-5862.16	$[^{195}Pt(iSn_5Cl_{14}Br)]^{3-}$	11
3	-5823.98	$[^{195}Pt(iSn_5Cl_{13}Br_2)]^{3-}$	12
4	-5787.40	$[^{195}Pt(iSn_5Cl_{12}Br_3)]^{3-}$	13
5	-5754.37	$[^{195}Pt(iSn_5Cl_{11}Br_4)]^{3-}$	14
6	-5719.98	$[^{195}Pt(iSn_5Cl_{10}Br_5)]^{3-}$	15
7	-5688.59	$[^{195}Pt(iSn_5Cl_9Br_6)]^{3-}$	16
8	-5658.49	$[^{195}Pt(iSn_5Cl_8Br_7)]^{3-}$	17
9	-5630.58	$[^{195}Pt(iSn_5Cl_7Br_8)]^{3-}$	18
10	-5603.75	$[^{195}Pt(iSn_5Cl_6Br_9)]^{3-}$	19
11	-5578.44	$[^{195}Pt(iSn_5Cl_5Br_{10})]^{3-}$	20
12	-5555.32	$[^{195}Pt(iSn_5Cl_4Br_{11})]^{3-}$	21
13	-5534.02	$[^{195}Pt(iSn_5Cl_3Br_{12})]^{3-}$	22
14	-5514.59	$[^{195}Pt(iSn_5Cl_2Br_{13})]^{3-}$	23
15	-5498.16	$[^{195}Pt(iSn_5ClBr_{14})]^{3-}$	24
16	-5483.54	$[^{195}Pt(iSnBr_3)_5]^{3-}$	VII

^a All the ^{195}Pt NMR resonance frequencies are reported relative to a 1 mm co-axial insert containing 0.1 M K_2PtCN_4 as reference solution ($\delta(^{195}Pt) = -4700.0$ ppm). The uncertainties on ^{195}Pt chemical shifts are estimated to be ± 3 ppm.

However, for the unambiguous identification and confirmation of the assignment of all 14 heteroleptic species a detailed analysis of the $^1J(^{119/117/115}Sn-^{195}Pt)$ coupling constants and $^1J(^{119/117/115}Sn-^{195}Pt)$ satellite signal areas of isotopologues is required. Moreover, assignment of the heteroleptic species is made more challenging due to the presence of isotopomers (*vide infra*) in addition to isotopologues as illustrated in Scheme 4.2.^{§§}

Figure 4.4 shows an expansion of the set of ^{195}Pt NMR signals tentatively assigned to the $[Pt(Sn_5Cl_{14}Br)]^{3-}$ heteroleptic species (**11**) showing the numerous coupling satellites. The isotopologues and isotopomers possible for this species are illustrated in Scheme 4.4. The ^{195}Pt NMR signal at $\delta(^{195}Pt) = -5862.2$ ppm is assigned to the isotopologue of the $[Pt(Sn_5Cl_{14}Br)]^{3-}$ complex anion which contains a ^{195}Pt nucleus but no magnetically-active Sn isotopes and therefore is the most abundant isotopologue, **11** in Scheme 4.4. The respective $^1J(^{119/117/115}Sn - ^{195}Pt)$ satellites, encircled in Figure 4.4, are due to the isotopologues and isotopomers which contain a ^{195}Pt nucleus and one magnetically-active tin isotope, **25 – 30** in

^{§§} In order to avoid multiple numbering schemes, numbering of each new isotopologue and isotopomer of the heteroleptic species continues with the numbering scheme used for the isotopologues of the homoleptic species.

Scheme 4.4. Interestingly, in addition to the 3 three sets of $^1J(^{119/117/115}\text{Sn}-^{195}\text{Pt})$ satellites observed in the ^{195}Pt NMR spectrum of the $[\text{Pt}(\text{SnCl}_3)_5]^{3-}$ complex anion, shown in Figure 3.5 in Chapter 3, a fourth set of $^1J(^x\text{Sn}-^{195}\text{Pt})$ satellites with a coupling constant of 14 562 Hz (Table 4.2) is observed and is indicated by the symbol (c) in Figure 4.4. The ratio of the coupling constants of 1J satellites (a) to (b) (15 933 Hz/15 228 Hz = 1.046) is equal to the $\gamma(^{119}\text{Sn})/\gamma(^{117}\text{Sn})$ ratio (1.046), shown in Table 4.2. Similarly, the ratio of the coupling constants of 1J satellites (b) to (d) (15 228 Hz/14 079 Hz = 1.089) is equal to the $\gamma(^{117}\text{Sn})/\gamma(^{115}\text{Sn})$ ratio (1.089), Table 4.2. The satellites indicated by (a), (b) and (d) (Figure 4.4) are therefore clearly assigned to $^1J(^{119}\text{Sn}-^{195}\text{Pt})$, $^1J(^{117}\text{Sn}-^{195}\text{Pt})$ and $^1J(^{115}\text{Sn}-^{195}\text{Pt})$ couplings and correspond (*vide infra*) to the isotopologues listed in Table 4.2. Furthermore, the ratio of coupling constants of satellites (b) to (c) (15 228 Hz/14 562 Hz = 1.046) (Figure 4.4) is equal to the $\gamma(^{119}\text{Sn})/\gamma(^{117}\text{Sn})$ ratio (1.046), Table 4.2. This implies that the satellites indicated by (b) in Figure 4.4 originates from both $^1J(^{119}\text{Sn}-^{195}\text{Pt})$ and $^1J(^{117}\text{Sn}-^{195}\text{Pt})$ couplings and the satellites indicated by (c) originates from $^1J(^{117}\text{Sn}-^{195}\text{Pt})$ coupling. Taking into consideration that there are two tin ligands (SnCl_3^- , SnCl_2Br^-) it is reasonable to suggest that two different $^1J(^{119}\text{SnCl}_3^- - ^{195}\text{Pt})$ and $^1J(^{119}\text{SnCl}_2\text{Br}^- - ^{195}\text{Pt})$ couplings should be observed, which can be attributed to isotopomers **25** and **28**, shown in Scheme 4.4. If this is the case, it implies that the relative chemical shift difference between the two chemical shifts of the exchanging species ($\nu_A - \nu_B$) relative to the actual reaction rate constant (κ) is larger than 2.2 ($\kappa/\Delta\nu > 2.2$) and thus that *intra*- and *inter*- molecular halide exchange is slow on the ^{195}Pt NMR acquisition time-scale. Similarly, it is possible to observe two different $^1J(\text{Sn}-^{195}\text{Pt})$ couplings for isotopomers **26** and **29** and for isotopomers **27** and **30**. This should be reflected in the relative signal peak areas of the respective $^1J(^{119/117/115}\text{Sn}-^{195}\text{Pt})$ satellites as the $[\text{Pt}(\text{Sn}_5\text{Cl}_{14}\text{Br})]^{3-}$ complex anion has four SnCl_3^- ligands and one SnCl_2Br^- ligand. In Figure 4.4 it is clearly seen that the relative $^1J(^{119}\text{Sn}-^{195}\text{Pt})$ satellite signal areas are now lower in intensity than the $^1J(^{117}\text{Sn}-^{195}\text{Pt})$ satellites. The relative experimental ^{195}Pt NMR signal areas and the NSA's calculated for each isotopologue and isotopomer are listed in Table 4.3. The excellent agreement of the experimental $^1J(^{119/117/115}\text{Sn}-^{195}\text{Pt})$ satellite signal areas with the NSA's of isotopologues/ isotopomers (Table 4.3) confirms that the 1J satellite indicated by the symbols (a), (b), (c) and (d) in Figure 4.4 are due to the isotopologues and isotopomers **25**, **26/28**, **29** and **27** in Scheme 4.4, respectively. Moreover, the data in Table 4.3 is in agreement with the notion that *intra*- and *inter*- molecular halide exchange is slow on the ^{195}Pt NMR acquisition time-scale.

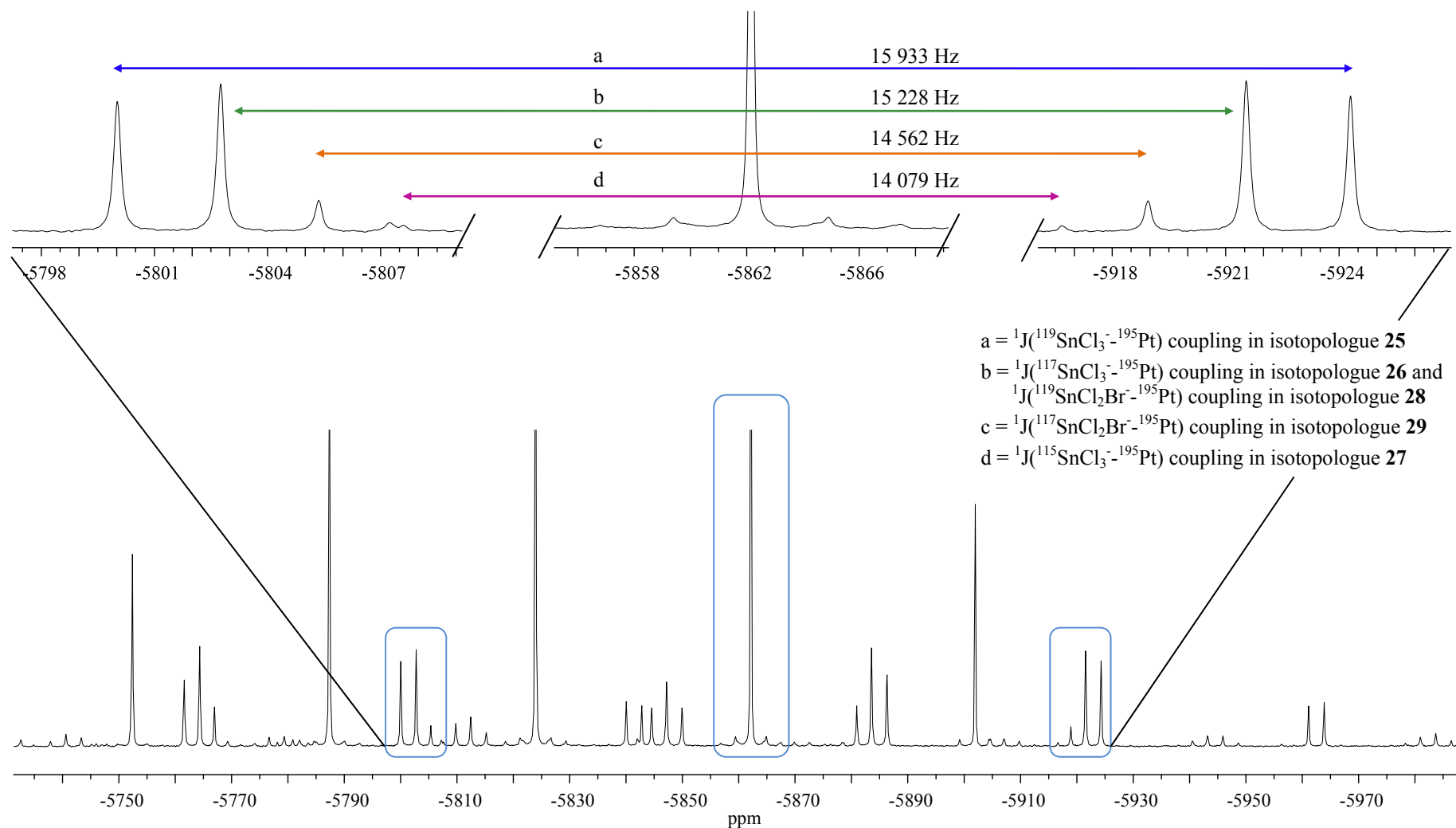
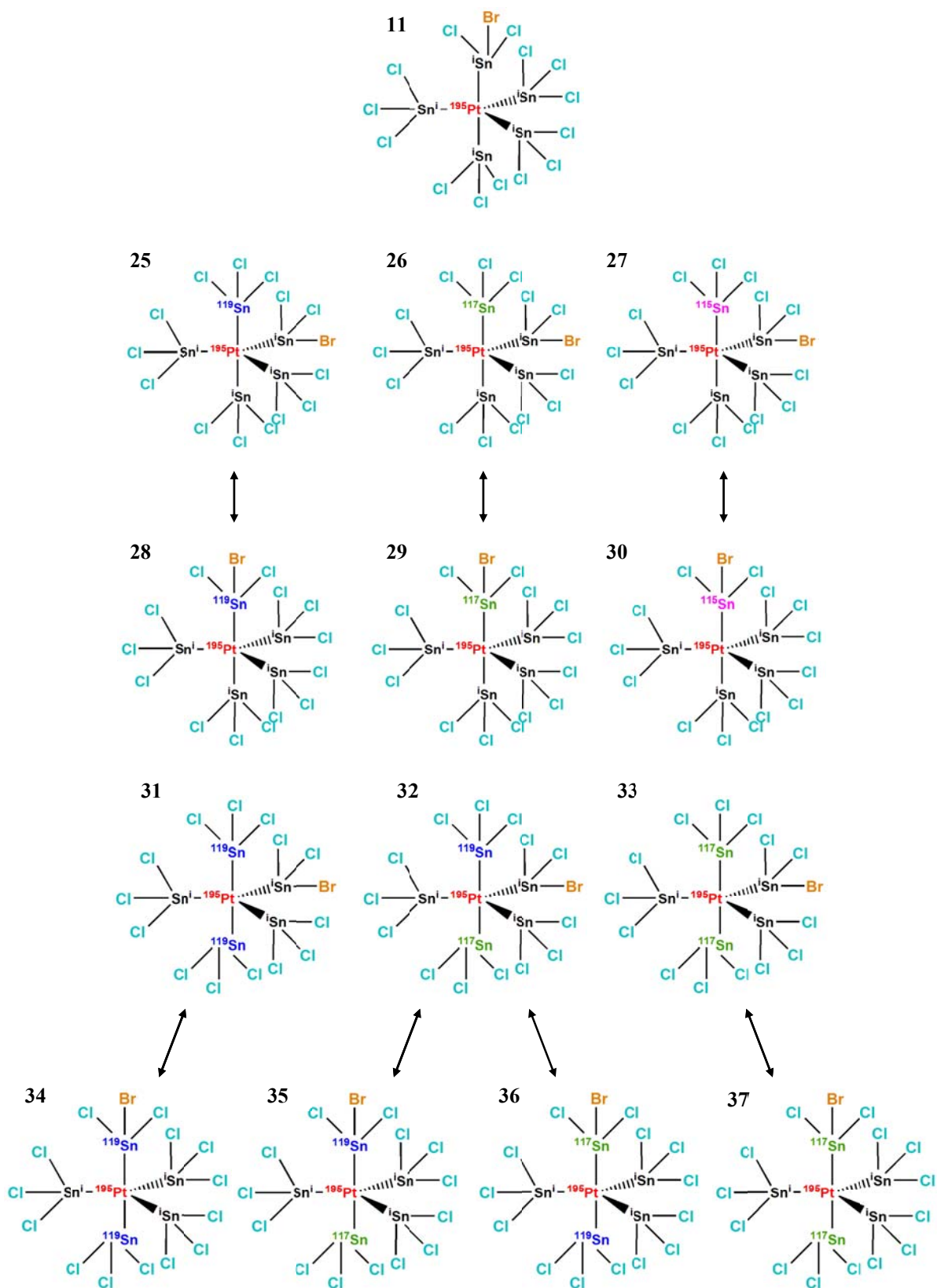


Figure 4.4: ^{195}Pt NMR spectrum obtained for solution with $[Pt(\text{SnCl}_3)_5]^{3-}$ to $[Pt(\text{SnBr}_3)_5]^{3-}$ ratio of 2:1. Only a partial part of the spectrum is shown as to focus specifically on the ^{195}Pt NMR signal obtained for $[Pt(\text{Sn}_5\text{Cl}_4\text{Br})]^{3-}$ ($\delta(^{195}\text{Pt}) = -5862$ ppm) and its respective 1J satellites. The main resonance signals, as well as the 1J satellites observed due to coupling in isotopologues/isotopomers with one magnetically active tin nucleus, are encircled. The expansion focuses specifically on these 1J satellites.



Scheme 4.4: The 14 isotopologues and isotopomers possible for the $[Pt(Sn_5Cl_{14}Br)]^{3-}$ complex anion. The double headed arrows show isotopomers associated with a particular isotopologue. For example 28 is an isotopomer of 25 in the sense that in 25 three Cl^- are bonded to ^{119}Sn compared to the two Cl^- and one Br^- bonded to ^{119}Sn in 28.

Table 4.2: Comparison of the ratio of 1J coupling constants of respective 1J satellites to the ratio of gyromagnetic ratios of magnetically-active Sn isotopes present in respective isotopologues

1J sat.	Isotopologue/isotopomer	$^1J(^{119/117/115}Sn-^{195}Pt)$ / Hz	1J ratios	$\gamma(^xSn)/\gamma(^ySn)$
a	25 $[^{195}Pt(^{119}SnCl_3)(^iSnCl_3)_3(^iSnCl_2Br)]^{3-}$	15 933		
b	26 $[^{195}Pt(^{117}SnCl_3)(^iSnCl_3)_3(^iSnCl_2Br)]^{3-}$	15 228	1.046 ^a	1.046 ^d
b	28 $[^{195}Pt(^{119}SnCl_2Br)(^iSnCl_3)_4]^{3-}$	15 228	1.046 ^a	1.046 ^d
c	29 $[^{195}Pt(^{117}SnCl_2Br)(^iSnCl_3)_4]^{3-}$	14 562	1.046 ^b	1.046 ^d
d	27 $[^{195}Pt(^{115}SnCl_3)(^iSnCl_3)_3(^iSnCl_2Br)]^{3-}$	14 079	1.089 ^c	1.089 ^e
	30 $[^{195}Pt(^{115}SnCl_2Br)(^iSnCl_3)_4]^{3-}$	- ^f		

^a Ratio of 1J coupling constants of satellites (a) to (b) illustrated in Figure 4.4. ^b Ratio of 1J coupling constants of satellites (b) to (c) illustrated in Figure 4.4. ^c Ratio of 1J coupling constants of satellites (b) to (d) illustrated in Figure 4.4. ^d $\gamma(^xSn) = \gamma(^{119}Sn)$ and $\gamma(^ySn) = \gamma(^{117}Sn)$. ^e $\gamma(^xSn) = \gamma(^{117}Sn)$ and $\gamma(^ySn) = \gamma(^{115}Sn)$. ^f Due to the low NSA of isotopologue/isotopomer **30**, the $^1J(^{115}SnCl_2Br-^{195}Pt)$ satellites could not be observed.

Table 4.3: Comparison of the ^{195}Pt NMR signal areas experimentally obtained for $[Pt(SnCl_3)_5]^{3-}$ and $[Pt(SnCl_3)_4(SnCl_2Br)]^{3-}$ with ^{195}Pt NMR to the calculated NSA's of the possible isotopologues/isotopomers of the species

1J sat.	Isotopologue/Isotopomer	$[Pt(SnCl_3)_5]^{3-}$		$[Pt(SnCl_3)_4(SnCl_2Br)]^{3-}$	
		NSA ^a	^{195}Pt signal area	NSA ^b	^{195}Pt signal area
	11 $[^{195}Pt(^iSnCl_3)_4(^iSnCl_2Br)]^{3-}$	1.00	1.00	1.00	1.00
a	25 $[^{195}Pt(^{119}SnCl_3)(^iSnCl_3)_3(^iSnCl_2Br)]^{3-}$	0.256	0.24	0.20	0.19
b	26 $[^{195}Pt(^{117}SnCl_3)(^iSnCl_3)_3(^iSnCl_2Br)]^{3-}$	0.227	0.21	0.18	} 0.212 ^c
b	28 $[^{195}Pt(^{119}SnCl_2Br)(^iSnCl_3)_4]^{3-}$	-	-	0.056	
c	29 $[^{195}Pt(^{117}SnCl_2Br)(^iSnCl_3)_4]^{3-}$	-	-	0.047	0.042
d	27 $[^{195}Pt(^{115}SnCl_3)(^iSnCl_3)_3(^iSnCl_2Br)]^{3-}$	0.01	0.01	0.008	0.006
	30 $[^{195}Pt(^{115}SnCl_2Br)(^iSnCl_3)_4]^{3-}$	-	-	-	- ^d

^a NSA calculated for respective isotopologues divided by 2 for ease of comparison to the ^{195}Pt NMR signal area.

^b 80% of the NSA calculated for the isotopologues of the homoleptic chlorido species with 5 $SnCl_3^-$ ligands.

^c Note, isotopologues 26 and 28 have the same splitting pattern, thus both these isotopologues/isotopomers contribute to the signal areas of satellites indicated by (c) in Figure 4.4. ^d Due to the low NSA of isotopologue/isotopomer **30**, the $^1J(^{115}SnCl_2Br-^{195}Pt)$ satellites could not be observed.

When the [Pt(Sn₅Cl₁₄Br)]³⁻ complex anion contains a ¹⁹⁵Pt nucleus and two magnetically-active tin nuclei an even more complex ¹J splitting pattern is expected, as shown in Figure 4.5. In this case the two magnetically-active Sn nuclei can either both be present in the SnCl₃⁻ ligands or one can be present in the SnCl₃⁻ ligand and the other in the SnCl₂Br⁻ ligand. This result in the seven possible combinations of isotopologues and isotopomers listed in Table 4.4. In order to unambiguously assign the respective ¹J(^{119/117}Sn-¹⁹⁵Pt) satellites the method of successive splitting was applied, as illustrated in Figure 4.5. As established above the respective ¹J coupling constants decrease in the order ¹J(¹¹⁹SnCl₃-¹⁹⁵Pt) > ¹J(¹¹⁷SnCl₃-¹⁹⁵Pt) = ¹J(¹¹⁹SnCl₂Br-¹⁹⁵Pt) > ¹J(¹¹⁷SnCl₂Br-¹⁹⁵Pt). In view of this, the ¹J coupling in isotopologues **31**, **33** and **35** (Scheme 4.4) result in triplet splitting patterns, shown by (e), (i) and (j) in Figure 4.5, respectively. Moreover, the ¹J couplings of isotopologues/ isotopomers **32**, **34**, **36** and **37** (Scheme 4.4) result in doublet of doublets splitting patterns, shown by (f), (g), (h) and (k) in Figure 4.5. However, as the ¹J(¹¹⁷SnCl₃-¹⁹⁵Pt) and ¹J(¹¹⁹SnCl₂Br-¹⁹⁵Pt) coupling constants are equal the ¹J satellites due to isotopologues **32** (f) and **34** (g) overlap. This is also the case for the ¹J satellites due to isotopologues **33** (i) and **35** (j) as illustrated in Figure 4.5. Unfortunately, the ¹⁹⁵Pt NMR signals of these ¹J(^{119/117}Sn-¹⁹⁵Pt) satellites are too low to accurately measure the areas which prevents the comparison thereof to the NSA's of the isotopologues/isotopomers.

Table 4.4: Coupling constants measured for the ¹J(^{119/117}Sn-¹⁹⁵Pt) satellites of isotopologues/isotopomers **7** to **13** of the [Pt(Sn₅Cl₁₄Br)]³⁻ complex anion

¹ J Sat.	Isotopologue/ Isotopomer	X ^a	¹ J(X- ⁹⁵ Pt) / Hz	Y ^b	¹ J(Y- ⁹⁵ Pt) / Hz
e	3 [Pt(¹¹⁹ SnCl ₃) ₂ (¹¹⁷ SnCl ₃) ₂ (¹¹⁹ SnCl ₂ Br)] ³⁻	¹¹⁹ SnCl ₃	15933	¹¹⁹ SnCl ₃	15933
	1] ³⁻				
f	3 [Pt(¹¹⁹ SnCl ₃)(¹¹⁷ SnCl ₃)(¹¹⁹ SnCl ₂ Br)] ³⁻	¹¹⁹ SnCl ₃	15933	¹¹⁷ SnCl ₃	15228
	2 (¹¹⁷ SnCl ₂ Br)] ³⁻				
i	3 [Pt(¹¹⁷ SnCl ₃) ₂ (¹¹⁹ SnCl ₃) ₂ (¹¹⁷ SnCl ₂ Br)] ³⁻	¹¹⁷ SnCl ₃	15228	¹¹⁷ SnCl ₃	15228
	3] ³⁻				
g	3 [Pt(¹¹⁹ SnCl ₃)(¹¹⁹ SnCl ₂ Br)(¹¹⁷ SnCl ₃)] ³⁻	¹¹⁹ SnCl ₃	15933	¹¹⁹ SnCl ₂ B	15228
	4] ³⁻			r	
j	3 [Pt(¹¹⁷ SnCl ₃)(¹¹⁹ SnCl ₂ Br)(¹¹⁹ SnCl ₃)] ³⁻	¹¹⁷ SnCl ₃	15228	¹¹⁹ SnCl ₂ B	15228
	5] ³⁻			r	
h	3 [Pt(¹¹⁹ SnCl ₃)(¹¹⁷ SnCl ₂ Br)(¹¹⁷ SnCl ₃)] ³⁻	¹¹⁹ SnCl ₃	15933	¹¹⁷ SnCl ₂ B	14562
	6] ³⁻			r	
k	3 [Pt(¹¹⁷ SnCl ₃)(¹¹⁹ SnCl ₂ Br)(¹¹⁷ SnCl ₃)] ³⁻	¹¹⁷ SnCl ₃	15228	¹¹⁷ SnCl ₂ B	14562
	7] ³⁻			r	

^a X represents the tin ligand that ¹⁹⁵Pt couples to, resulting in the first splitting of the main resonance signal into a doublet. ^b Y represents the second tin ligand that ¹⁹⁵Pt couples to, resulting in further splitting into either a triplet (t) or a doublet of doublet (dd).

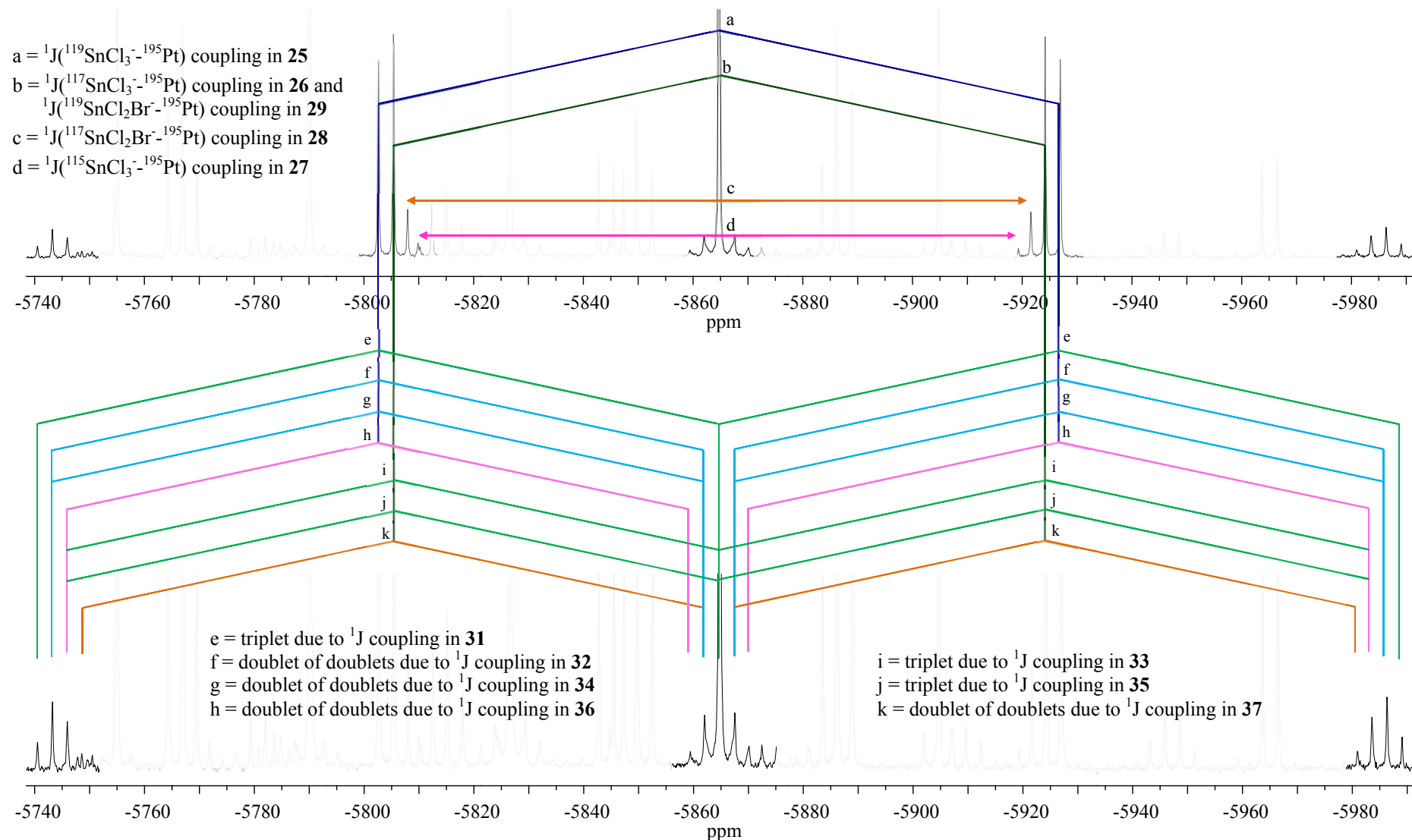


Figure 4.5: ${}^{195}\text{Pt}$ NMR spectrum obtained for solution with $[Pt(\text{SnCl}_3)_5]^{3-}$ to $[Pt(\text{SnBr}_3)_5]^{3-}$ ratio of 2:1. Only a partial part of the spectrum is shown as to focus specifically on the ${}^{195}\text{Pt}$ NMR signal obtained for $[Pt(\text{Sn}_5\text{Cl}_{14}\text{Br})]^{3-}$ ($\delta({}^{195}\text{Pt}) = -5862$ ppm) and its respective 1J satellites.

In this way the respective $^1J(^{119/117/115}\text{Sn}-^{195}\text{Pt})$ satellites indicated by the symbols (a) – (k) in the ^{195}Pt NMR spectrum shown in Figure 4.5 are thus unambiguously assigned to isotopologues and isotopomers **11** and **25 – 37** of the $[\text{Pt}(\text{Sn}_5\text{Cl}_{14}\text{Br})]^{3-}$ complex anion (Scheme 4.4).

The same methodology was used to assign all the ^{195}Pt NMR signals numbered 3 – 15 in Figure 4.2 to the remaining 13 heteroleptic $[\text{Pt}(\text{SnCl}_n\text{Br}_{15-n})]^{3-}$ ($n = 1 - 13$) species (Appendix B lists the possible isotopologues and isotopomers of the $[\text{Pt}(\text{SnCl}_n\text{Br}_{15-n})]^{3-}$ ($n = 10 - 13$) species and the splitting patterns obtained with ^{195}Pt NMR for the $[\text{Pt}(\text{SnCl}_n\text{Br}_{15-n})]^{3-}$ ($n = 11 - 13$) species are shown in Appendix C). The $^1J(^{119/117}\text{Sn}-^{195}\text{Pt})$ coupling constants measured for the respective isotopologues and isotopomers (containing the ^{195}Pt nucleus and one spin-active tin nucleus) of each heteroleptic species are listed in Table 4.5.^{***} Regardless of the fact that there are four possible trihalostannato ligands (SnCl_3^- , SnCl_2Br^- , SnClBr_2^- , SnBr_3^-) which may coordinate to the Pt(II) centre in the heteroleptic species, a maximum of five $^1J(^{119/117}\text{Sn}-^{195}\text{Pt})$ satellites for any given species is observed (^{195}Pt NMR signals numbered 4 – 10 in Figure 4.2). It was shown for the $[\text{Pt}(\text{Sn}_5\text{Cl}_{14}\text{Br})]^{3-}$ complex anion that due to slow *intra*- and *inter*- molecular halide exchange on the ^{195}Pt NMR acquisition time-scale, the 1J satellites for the respective isotopomers are *not* averaged.

Moreover, at 128.7 MHz (14.03 T) the satellites obtained due to $^1J(^{117}\text{SnCl}_3-^{195}\text{Pt})$ and $^1J(^{119}\text{SnCl}_2\text{Br}-^{195}\text{Pt})$ couplings of the respective isotopologues (**26** and **28**) are not resolved and are considered to have equal coupling constants. However, at higher magnetic field strengths one might be able to distinguish between the two sets of satellites. With this in mind, it is reasonable to suggest that the $^1J(^{119/117}\text{Sn}-^{195}\text{Pt})$ satellites of the ^{195}Pt NMR signals numbered 3 – 15 in Figure 4.2 arise from 1J couplings that decrease in the order $^1J(^{195}\text{Pt}-^{119}\text{SnCl}_3) > ^1J(^{195}\text{Pt}-^{117}\text{SnCl}_3) = ^1J(^{195}\text{Pt}-^{119}\text{SnCl}_2\text{Br}) > ^1J(^{195}\text{Pt}-^{117}\text{SnCl}_2\text{Br}) = ^1J(^{195}\text{Pt}-^{119}\text{SnClBr}_2) > ^1J(^{195}\text{Pt}-^{117}\text{SnClBr}_2) = ^1J(^{195}\text{Pt}-^{119}\text{SnBr}_3) > ^1J(^{195}\text{Pt}-^{117}\text{SnBr}_3)$. In confirmation of the assignments of the satellites shown in Table 4.6, and thus also the proposed trend of the satellites, the $^1J(^{119}\text{Sn}-^{195}\text{Pt})/^1J(^{117}\text{Sn}-^{195}\text{Pt})$ ratios calculated for each isotopologue/isotopomer given in Table 4.6 and show excellent agreement to the $\gamma(^{119}\text{Sn})/\gamma(^{117}\text{Sn})$ ratio, 1.046.

^{***} Due to the low NSA of the $^{195}\text{Pt}-^{115}\text{Sn}$ isotopologues the $^1J(^{115}\text{Sn}-^{195}\text{Pt})$ satellites will not be discussed in this section.

Table 4.5: ^{195}Pt NMR $\delta(^{195}Pt)$ and $^1J(^xSn-^{195}Pt)$ parameters and assignments of the $[Pt(SnCl_nBr_{15-n})]^{3-}$ ($n = 0 - 15$) signals

			$\delta^{195}Pt$ / ppm	$^1J(^{119}Sn-^{195}Pt)$ / Hz				$^1J(^{117}Sn-^{195}Pt)$ / Hz			
				$^{119}SnCl_3$	$^{119}SnCl_2Br$	$^{119}SnClBr_2$	$^{119}SnBr_3$	$^{117}SnCl_3$	$^{117}SnCl_2Br$	$^{117}SnClBr_2$	$^{117}SnBr_3$
1	7	$[Pt(SnCl_3)_5]^{3-}$	-5905	15864				15160			
2	11	$[PtSn_5Cl_{14}Br]^{3-}$	-5862	15933	15228			15228	14563		
3	12	$[PtSn_5Cl_{13}Br_2]^{3-}$	-5824	15995	15295	14633		15295	14633	13983	
4	13	$[PtSn_5Cl_{12}Br_3]^{3-}$	-5787	16050	15351	14683	14057	15351	14683	14057	13451
5	14	$[PtSn_5Cl_{11}Br_4]^{3-}$	-5754	16105	15406	14738	14104	15406	14738	14105	13544
6	15	$[PtSn_5Cl_{10}Br_5]^{3-}$	-5720	16163	15464	14787	14144	15464	14787	14144	13539
7	16	$[PtSn_5Cl_9Br_6]^{3-}$	-5689	16228	15520	14840	14187	15520	14840	14187	13552
8	17	$[PtSn_5Cl_8Br_7]^{3-}$	-5659	16269	15584	14898	14198	15584	14898	14198	13581
9	18	$[PtSn_5Cl_7Br_8]^{3-}$	-5631	16332	15620	14955	14278	15620	14955	14278	13643
10	19	$[PtSn_5Cl_6Br_9]^{3-}$	-5603	16419	15685	14989	14326	15686	14989	14326	13678
11	20	$[PtSn_5Cl_5Br_{10}]^{3-}$	-5578	-	15753	15057	14376	15753	15057	14376	13728
12	21	$[PtSn_5Cl_4Br_{11}]^{3-}$	-5555	-	15822	15111	14435	15822	15111	14435	13781
13	22	$[PtSn_5Cl_3Br_{12}]^{3-}$	-5534	-	15825	15178	14482	15825	15178	14482	13841
14	23	$[PtSn_5Cl_2Br_{13}]^{3-}$	-5515		15911	15233	14548		15233	14548	13876
15	24	$[PtSn_5ClBr_{14}]^{3-}$	-5498			15302	14592			14592	13940
16	VII	$[Pt(SnBr_3)_5]^{3-}$	-5483				14659				14009

Table 4.6: Ratios calculated for respective $^1J(^{119}\text{Sn}-^{195}\text{Pt})/^1J(^{117}\text{Sn}-^{195}\text{Pt})$ to be compared to the $\gamma(^{119}\text{Sn})/\gamma(^{117}\text{Sn})$ ratio, 1.046.

	$^1J(^{119}\text{Sn}-^{195}\text{Pt})/(^1J(^{117}\text{Sn}-^{195}\text{Pt}))$			
	SnCl ₃	SnCl ₂ Br	SnClBr ₂	SnBr ₃
[Pt(SnCl ₃) ₅] ³⁻	1.046			
[PtSn ₅ Cl ₁₄ Br] ³⁻	1.046	1.046		
[PtSn ₅ Cl ₁₃ Br ₂] ³⁻	1.046	1.045	1.046	
[PtSn ₅ Cl ₁₂ Br ₃] ³⁻	1.046	1.045	1.045	1.045
[PtSn ₅ Cl ₁₁ Br ₄] ³⁻	1.045	1.045	1.045	1.041
[PtSn ₅ Cl ₁₀ Br ₅] ³⁻	1.045	1.046	1.045	1.045
[PtSn ₅ Cl ₉ Br ₆] ³⁻	1.046	1.046	1.046	1.047
[PtSn ₅ Cl ₈ Br ₇] ³⁻	1.044	1.046	1.049	1.045
[PtSn ₅ Cl ₇ Br ₈] ³⁻	1.046	1.045	1.047	1.046
[PtSn ₅ Cl ₆ Br ₉] ³⁻	1.047	1.046	1.046	1.047
[PtSn ₅ Cl ₅ Br ₁₀] ³⁻	-	1.046	1.047	1.047
[PtSn ₅ Cl ₄ Br ₁₁] ³⁻	-	1.047	1.047	1.047
[PtSn ₅ Cl ₃ Br ₁₂] ³⁻		1.043	1.048	1.046
[PtSn ₅ Cl ₂ Br ₁₃] ³⁻		1.045	1.047	1.048
[PtSn ₅ ClBr ₁₄] ³⁻			1.049	1.047
[Pt(SnBr ₃) ₅] ³⁻				1.046

Based on the above analysis and good agreement between $^1J(^{119/117}\text{Sn}-^{195}\text{Pt})$ values and $\gamma(^{119}\text{Sn})/\gamma(^{117}\text{Sn})$ ratios, the assignments of all the respective $^1J(^{119/117}\text{Sn}-^{195}\text{Pt})$ satellites observed for each of the many species support the assignments made earlier based on the ^{195}Pt NMR chemical shift trend obtained (Figure 4.3 and Table 4.1) and it is reasonable to conclude that ambiguity regarding the assignments of the 16 $[\text{Pt}(\text{SnCl}_n\text{Br}_{15-n})]^{3-}$ ($n = 0 - 15$) species has been eradicated, based on the well resolved ^{195}Pt NMR spectra.

Interestingly the systematic trends obtained by plotting the 1J coupling constants measured for each species against the corresponding $\delta(^{195}\text{Pt})$ of a given species, Figure 4.7, lends confidence to these assignments. Moreover, the trends observed show that the substitution of Cl⁻ by Br⁻ affects both the magnitude of the $^1J(^{119/117}\text{Sn}-^{195}\text{Pt})$ coupling constants measured and the $\delta(^{195}\text{Pt})$ of that particular species.

Firstly, with each addition of a Br^- to a spin-inactive tin nucleus, ^{119}Sn , the $^1J(^{119/117}SnCl_{3-n}Br_n-^{195}Pt)$ ($n = 0 - 3$) coupling constants increase with $\pm 0.4\%$. Secondly, the $^1J(^{119/117}SnCl_{3-n}Br_n-^{195}Pt)$ ($n = 0 - 3$) coupling constants decrease with $\pm 4.5\%$ on going from $n = 0$ to 1, 2 and 3. This decrease in the $^1J(^{119/117}Sn-^{195}Pt)$ values suggests that $SnCl_3^-$ is a better σ -donor and/or π -acceptor toward Pt(II) than $SnBr_3^-$, as was suggested by Nelson *et al.*²⁹ At this stage it is cannot unambiguously be established why an increase of 0.4 % in the value of 1J is observed.

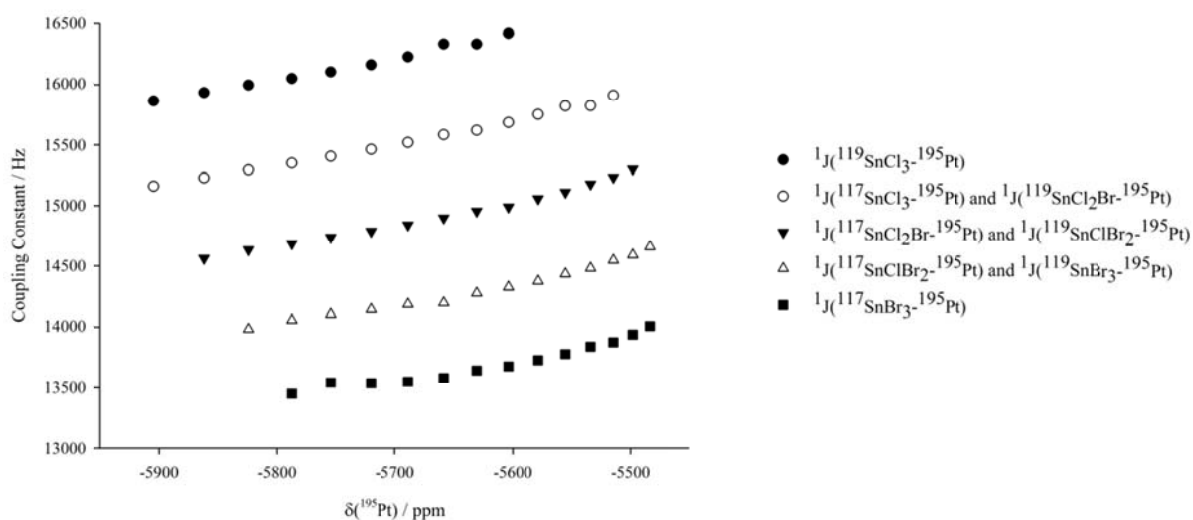


Figure 4.6: Trends obtained when plotting the coupling constants of the respective satellites against the chemical shift of the $[Pt(SnCl_nBr_{15-n})]^{3-}$ ($n = 0 - 15$) complex anions.

In conclusion the remarkable ^{195}Pt NMR spectra obtained have enabled the unambiguous characterization of all 16 $[Pt(SnCl_nBr_{15-n})]^{3-}$ ($n = 0 - 15$) species, together with their respective 1J satellites. Moreover it is shown that separate sets of $^1J(^{119/117/115}Sn-^{195}Pt)$ satellites are obtained for each different type of $(^{119/117/115}SnCl_{3-n}Br_n)^-$ ($n = 0 - 3$) ligand bound to Pt(II) in these complexes. This suggests that once equilibrium has been reached, *intra*- or *inter*-molecular halide exchange in the organic Aliquat-336-chloroform extracts of $[Pt(SnCl_nBr_{15-n})]^{3-}$ ($n = 0 - 15$) does not occur rapidly on the ^{195}Pt NMR acquisition time-scale, and allows for the spectroscopic visualization of the extreme complexity of the deceptively simple $[Pt(SnCl_nBr_{15-n})]^{3-}$ ($n = 0 - 15$) heteroleptic complex anions.

4.2.2. Revisiting the ^{119}Sn NMR Spectra acquired for the heteroleptic $[Pt(Sn_5Cl_nBr_{15-n})]^{3-}$ ($n = 0 - 15$) species

The corresponding ^{119}Sn NMR spectra acquired for the mixed $(\text{R}_3\text{NCH}_3^+)_3[\text{Pt}(\text{SnCl}_3)_5]^{3-}$ and $(\text{R}_3\text{NCH}_3^+)_3[\text{Pt}(\text{SnBr}_3)_5]^{3-}$ ($\text{R} = (\text{CH}_2)_7\text{CH}_3$) extracts are shown in Figure 4.7, where (A) and (D) show the ^{119}Sn NMR spectra of the homoleptic chlorido and bromido species respectively, and (B) and (C) show the ^{119}Sn NMR spectra of the heteroleptic species, $[Pt(\text{SnCl}_n\text{Br}_{15-n})]^{3-}$ ($n = 1 - 14$). Four main sets of ^{119}Sn NMR signals observed with each set consisting of several individual resonances are shown in Figure 4.7. The ^{119}Sn NMR chemical shifts of these sets of signals compare well to the chemical shifts of the sets of ^{119}Sn NMR signals tentatively assigned to the $[Pt(\text{SnCl}_3)_5]^{3-}$, $[Pt(\text{SnCl}_2\text{Br})_5]^{3-}$, $[Pt(\text{SnClBr}_2)_5]^{3-}$ and $[Pt(\text{SnBr}_3)_5]^{3-}$ complex anions by Koch⁶⁹ (Figure 4.1). Unfortunately, elucidation of each individual ^{119}Sn NMR signal within the set of signals is made difficult by the low signal-to-noise ratio and the extent of signal-overlap obtained in the ^{119}Sn NMR spectrum. Since fortunately the high-resolution ^{195}Pt NMR described above has enabled the identification of each $[Pt(\text{SnCl}_n\text{Br}_{15-n})]^{3-}$ ($n = 0 - 15$) species present in these solutions, this knowledge can now be used to re-interpret the ^{119}Sn NMR spectra acquired for these solutions.

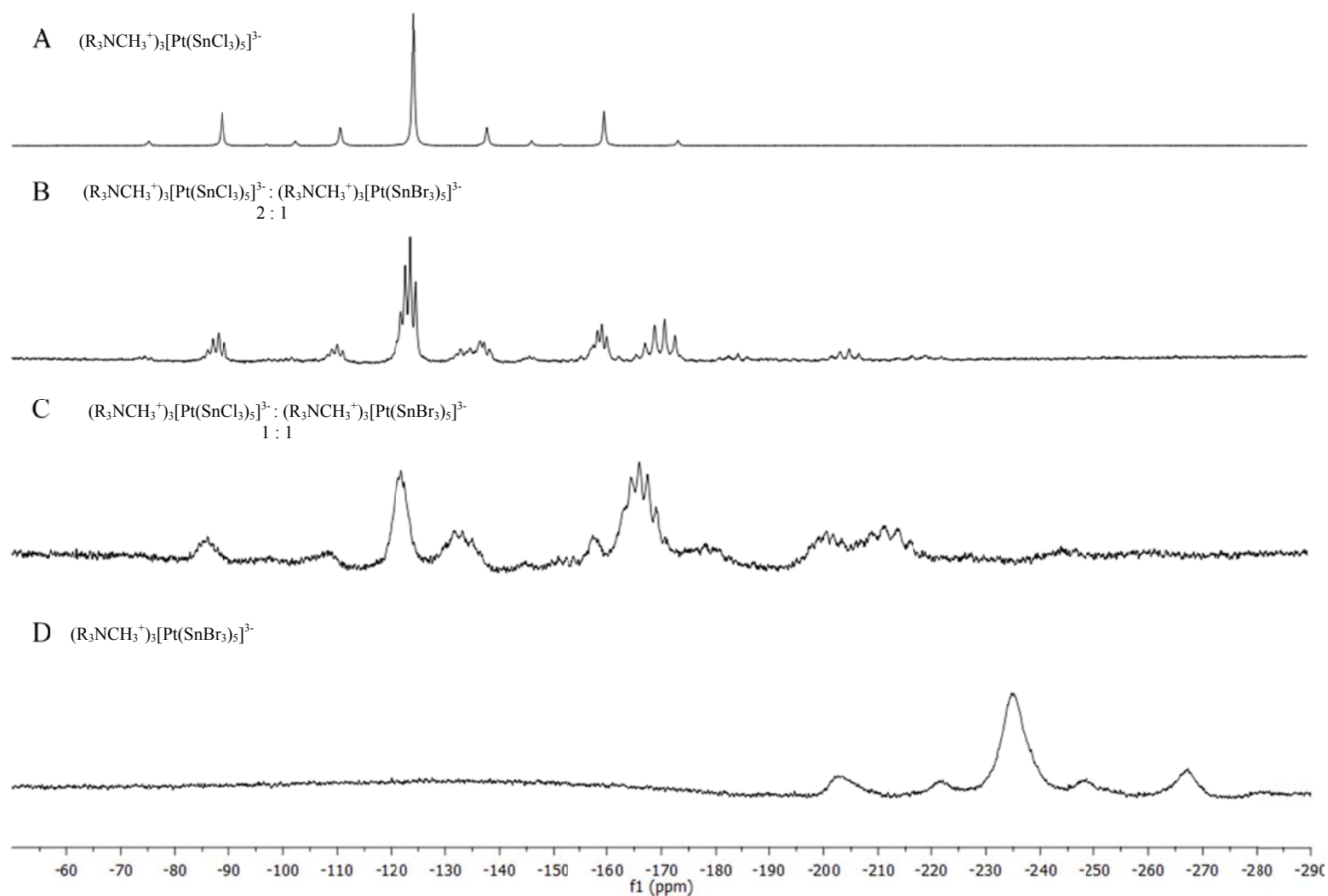


Figure 4.7: ^{119}Sn NMR spectra (223.7 MHz) obtained at 20 °C for (A) $[\text{Pt}(\text{SnCl}_3)_5]^{3-}$ and (D) $[\text{Pt}(\text{SnBr}_3)_5]^{3-}$ in CDCl_3 (20% AQ-336). The spectra shown in (B) and (C) are those of the mixtures of $[\text{Pt}(\text{SnCl}_3)_5]^{3-}$ and $[\text{Pt}(\text{SnBr}_3)_5]^{3-}$ with volume ratios of 2:1 and 1:1 respectively.

An expansion of the ^{119}Sn NMR spectrum of the solution with a to $(\text{R}_3\text{NCH}_3^+)_3[\text{Pt}(\text{SnBr}_3)_5]^{3-}$ ratio of 2:1 (v/v) is shown in Figure 4.8.

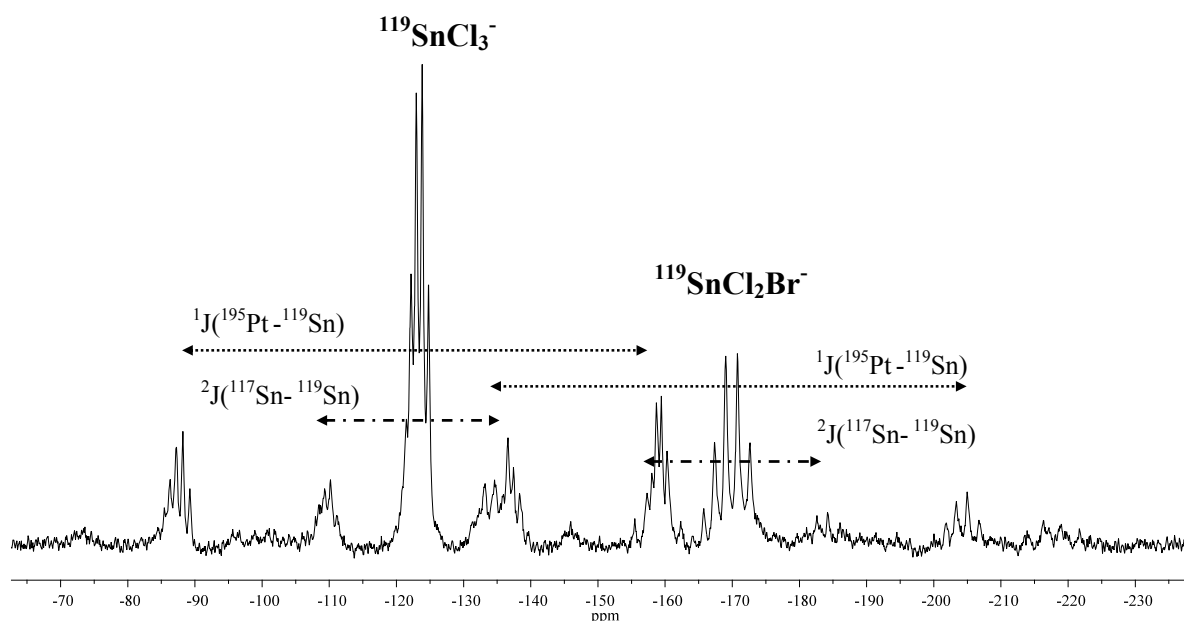
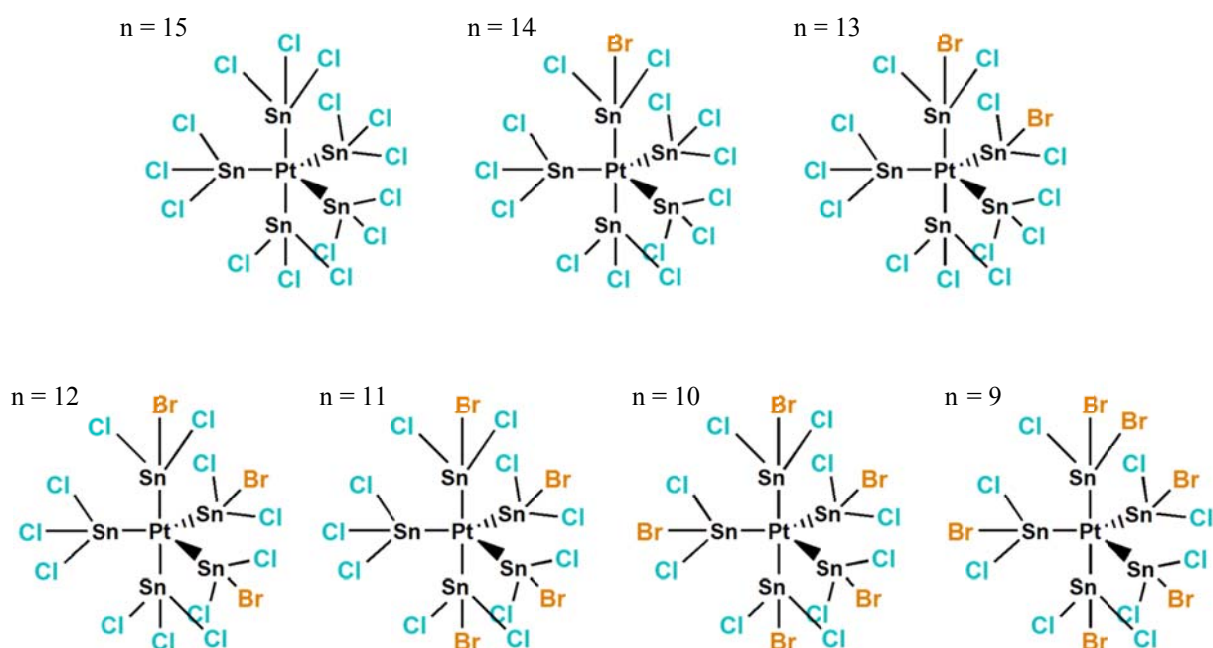


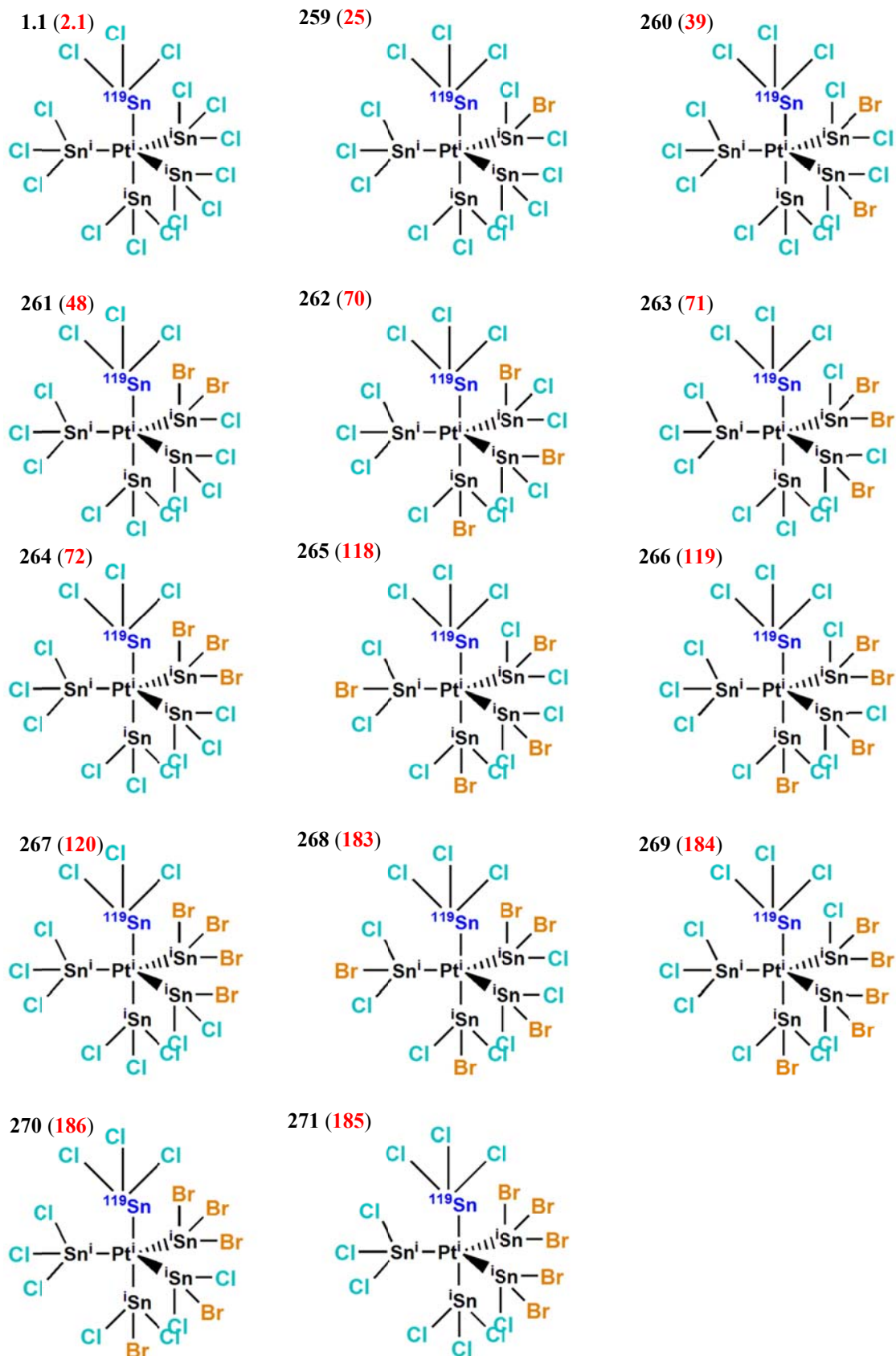
Figure 4.8: ^{119}Sn NMR spectrum recorded for the solution with a $[\text{Pt}(\text{SnCl}_3)_5]^{3-}$ to $[\text{Pt}(\text{SnBr}_3)_5]^{3-}$ volume ratio of 2 to 1. The arrows represent the 1J and 2J couplings obtained for the $^{119}\text{SnCl}_3^-$ and $^{119}\text{SnCl}_2\text{Br}^-$ ligands, respectively.

The main features of this spectrum are two sets of signals centred at $\delta(^{119}\text{Sn}) = -123$ ppm and -170 ppm respectively, each set flanked by its respective $^1J(^{195}\text{Pt}-^{119}\text{Sn})$ and $^2J(^{117}\text{Sn}-^{119}\text{Sn})$ satellites. Moreover, each set of signals, as well as its corresponding 1J and 2J satellites, consist of approximately 5 to 6 individually resolved ^{119}Sn NMR signals. From the ^{195}Pt NMR spectrum recorded for this solution, Figure 4.2 B, it is known that the 7 heteroleptic $[\text{Pt}(\text{SnCl}_n\text{Br}_{15-n})]^{3-}$ ($n = 8 - 15$) species shown in Scheme 4.5 are present in this solution. Therefore the ^{119}Sn NMR signals observed in the ^{119}Sn NMR spectrum acquired for this solution, Figure 4.8, are most likely to originate from these 7 species.

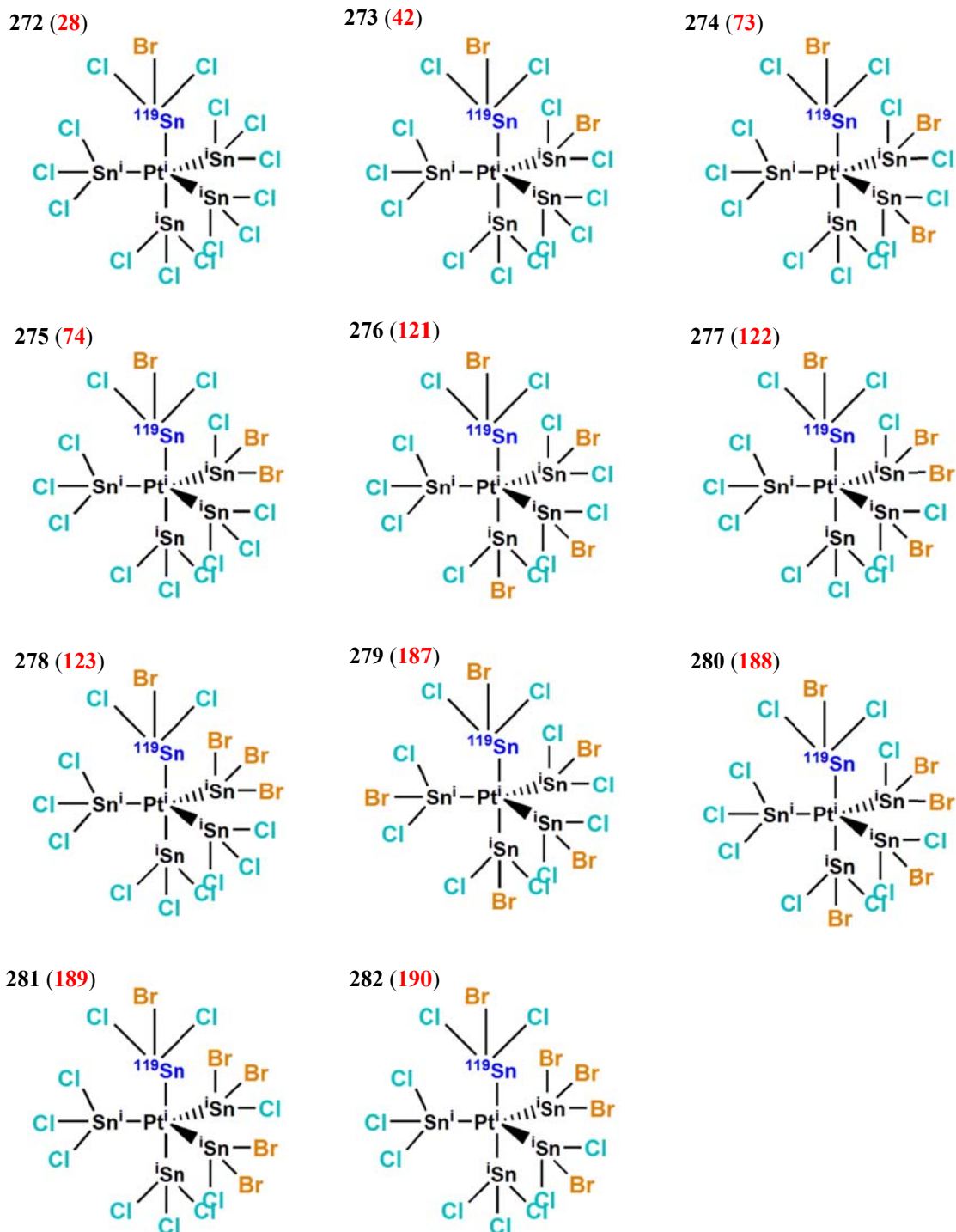


Scheme 4.5: The 7 mixed halide complex anions, known from the ^{195}Pt NMR spectrum, to be present in the solution with a $[\text{Pt}(\text{SnCl}_3)_5]^{3-}$ to $[\text{Pt}(\text{SnBr}_3)_5]^{3-}$ ratio of 2 to 1. It should be noted that only one representative isomer of each species is shown here, though many more are possible as shown in Appendix B.

Moreover, there are 72 isotopologues and isotopomers that contain the magnetically-active ^{119}Sn nucleus and either a magnetically-inactive ^{195}Pt isotope or a magnetically-active ^{195}Pt isotope possible for the $[\text{Pt}(\text{SnCl}_n\text{Br}_{15-n})]^{3-}$ ($n = 10 - 15$) species (Schemes 4.6, 4.7 and Appendix B).



Scheme 4.6: Isotopomers of the 6 $[Pt(Sn_5Cl_nBr_{15-n})]^{3-}$ ($n = 10 - 15$) heteroleptic complex anions with the general formula $[Pt(^{119}SnCl_3)(Sn_4Cl_nBr_{12-n})]^{3-}$ ($n = 7 - 12$). In parenthesis are given the corresponding isotopologues that contain the magnetically-active ^{195}Pt nucleus and are illustrated in Schemes 3.6, 4.4 and the Schemes shown in Appendix B.



Scheme 4.7: Isotopomers of the 5 $[Pt(Sn_5Cl_nBr_{15-n})]^{3-}$ ($n = 11 - 15$) heteroleptic complex anions with the general formula $[Pt(^{119}SnCl_2Br)(Sn_4Cl_nBr_{12-n})]^{3-}$ ($n = 8 - 12$). In parenthesis are given the corresponding isotopologues that contain the magnetically-active ^{195}Pt nucleus and are illustrated in Scheme 4.4 and the Schemes shown in Appendix B.

An expansion of the main set of ¹¹⁹Sn NMR signals centred at -123 ppm, flanked by its ¹J(¹⁹⁵Pt-¹¹⁹Sn) satellites, is shown in Figure 4.9. Both the main set of signals and its ¹J satellites consist of 5 resolved individual ¹¹⁹Sn NMR signals.^{†††} The ¹J(¹⁹⁵Pt-¹¹⁹Sn) coupling constants measured for the satellites indicated by the symbols (a), (b), (c), (d) and (e) in Figure 4.9 compare very well to the ¹J(¹¹⁹SnCl₃-¹⁹⁵Pt) coupling constants obtained with ¹⁹⁵Pt NMR for isotopologues/isotopomers **2**, **25**, **39/48**, **70/71/72** and **118/119/120** (illustrated in Scheme 4.6) as shown in Table 4.7. Thus, each individual ¹¹⁹Sn NMR signal within the set of signals centred at -123 ppm (Figure 4.9) can be unambiguously assigned to an isotopologue/isotopomer which contains a magnetically-active ¹¹⁹Sn isotope and a magnetically-inactive ¹⁹⁵Pt isotope (**1** and **259 – 267** in Scheme 4.6) as shown in Table 4.8.

The same methodology is used to assign the individual resonances obtained in the set of resonances centred at δ(¹¹⁹Sn) = -170.4 ppm, which was tentatively assigned to the SnCl₂Br⁻ ligand by Koch.⁶⁹ Figure 4.10 shows an expansion of this set of ¹¹⁹Sn NMR signals, flanked by the ¹J(¹⁹⁵Pt-¹¹⁹Sn) satellites, the main set of signals consisting of 5 resolved individual ¹¹⁹Sn NMR signals. The respective ¹J(¹⁹⁵Pt-¹¹⁹Sn) satellites indicated by the symbols (f), (g), (h) and (i) in Figure 4.10 again agree well with the ¹J(¹⁹⁵Pt-¹¹⁹SnCl₂Br) coupling constants obtained with ¹⁹⁵Pt NMR for isotopologues/isotopomers **28**, **42**, **73/ 74** and **121/122/123** illustrated in Scheme 4.7 and are thus assigned accordingly (Table 4.9). In view of these assignments the individual ¹¹⁹Sn NMR signals within the set of signals centred at δ(¹¹⁹Sn) = -170.4 ppm are assigned to the respective isotopologues/isotopomers illustrated in Scheme 4.7 that contain the magnetically-active ¹¹⁹Sn isotope and the magnetically-inactive ¹⁹⁵Pt isotope and are listed in Table 4.10. Unfortunately the signal-to-noise ratio is too low to allow for accurate measurement of ¹J(¹⁹⁵Pt-¹¹⁹Sn) coupling constants due the satellites indicated by (j) in Figure 4.10. From the assignments listed in Table 4.10 it reasonable to tentatively assign the ¹¹⁹Sn NMR signal at δ(¹¹⁹Sn) = -165.9 ppm to isotopomers **279 – 282** illustrated in Scheme 4.7, however further studies are needed to confirm this.

^{†††} Unfortunately, due to signal-overlap and the low signal-to-noise ratio, accurate measurement of the ²J(¹¹⁷Sn-¹¹⁹Sn) couplings are not possible.

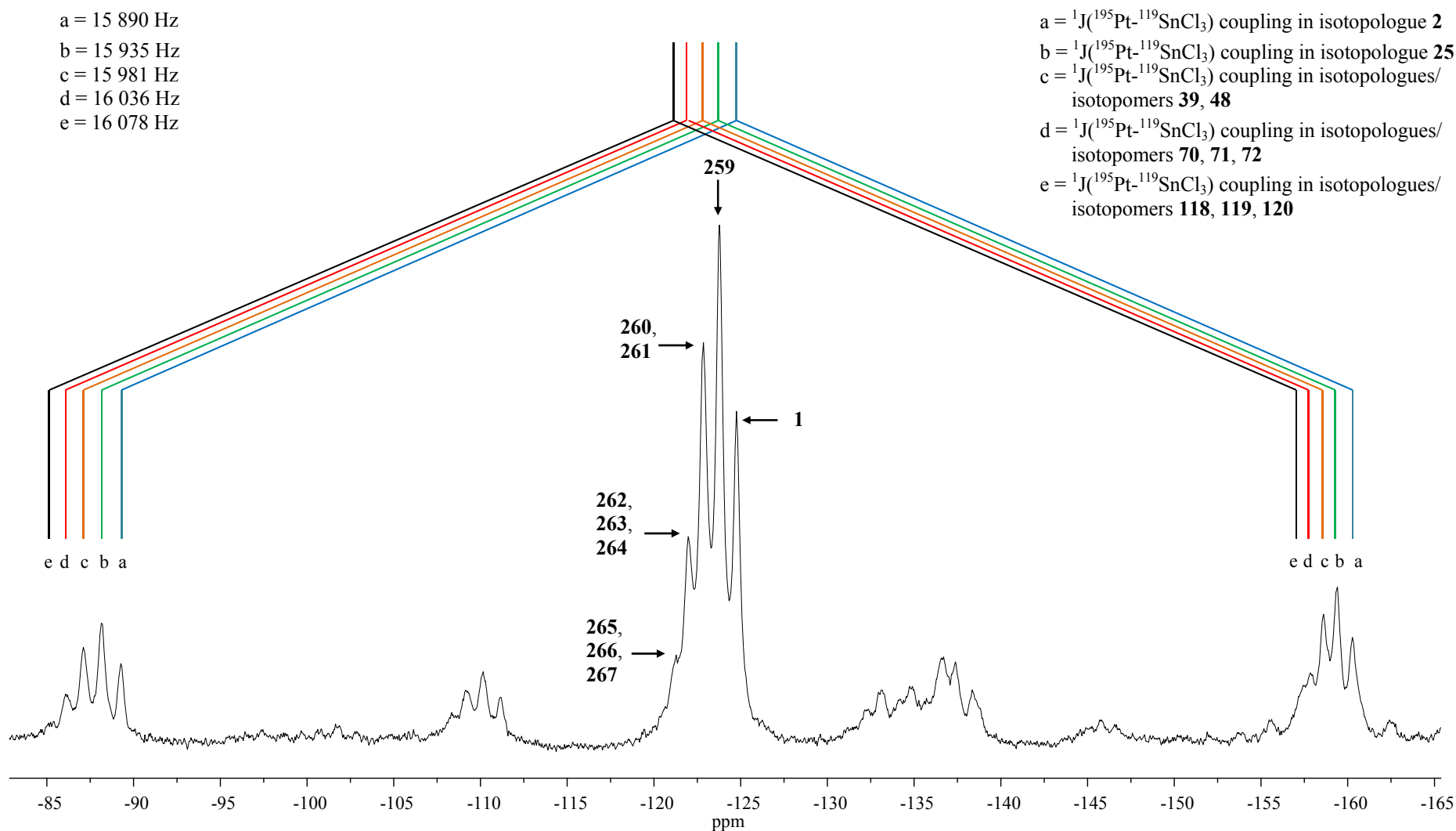


Figure 4.9: An expansion of the ^{119}Sn NMR spectrum recorded for the solution with a $[Pt(SnCl_3)_5]^{3-}$ to $[Pt(SnBr_3)_5]^{3-}$ volume ratio of 2 to 1 to focus on the ^{119}Sn NMR signals centred at -123 ppm. The symbols (a) to (e) indicate the ${}^1J(^{195}\text{Pt}-^{119}\text{Sn})$ satellites due to the respective isotopologues. The isotopologues/ isotopomers responsible for the individual ^{119}Sn NMR signals in the main set of signals are indicated by the arrows.

Table 4.7: ¹J(¹⁹⁵Pt-¹¹⁹Sn) coupling constants^a measured for ¹J satellites of the set of ¹¹⁹Sn NMR signals centred at -123 ppm obtained with ¹⁹⁵Pt NMR compared to those obtained with ¹¹⁹Sn NMR.

Isotopologue/ Isotopomer		¹⁹⁵ Pt NMR	¹¹⁹ Sn NMR	
		¹ J(¹⁹⁵ Pt- ¹¹⁹ Sn)/ Hz	¹ J(¹⁹⁵ Pt- ¹¹⁹ Sn)/ Hz	
a	2	[¹⁹⁵ Pt(¹¹⁹ SnCl ₃)(Sn ₄ Cl ₁₂)] ³⁻	15889	15890
b	25	[¹⁹⁵ Pt(¹¹⁹ SnCl ₃)(Sn ₄ Cl ₁₁ Br)] ³⁻	15933	15935
c	39, 48	[¹⁹⁵ Pt(¹¹⁹ SnCl ₃)(Sn ₄ Cl ₁₀ Br ₂)] ³⁻	15995	15981
d	70, 71, 72	[¹⁹⁵ Pt(¹¹⁹ SnCl ₃)(Sn ₄ Cl ₉ Br ₃)] ³⁻	16050	16036
e	118, 119, 120	[¹⁹⁵ Pt(¹¹⁹ SnCl ₃)(Sn ₄ Cl ₈ Br ₄)] ³⁻	16105	16078

^a The uncertainties on coupling constants are estimated to be ± 15 Hz.**Table 4.8:** Assignment of each individual ¹¹⁹Sn NMR signal in the set of signals centred at - 123.0 ppm to a isotopologue/isotopomer of the respective heteroleptic [Pt(Sn₅Cl_nBr_{15-n})]³⁻ (n = 11 - 15) species.

Isotopologue/ Isotopomer		δ(¹¹⁹ Sn)/ ppm ^a
1	[ⁱ Pt(¹¹⁹ SnCl ₃)(Sn ₄ Cl ₁₂)] ³⁻	- 124.8
259	[ⁱ Pt(¹¹⁹ SnCl ₃)(Sn ₄ Cl ₁₁ Br)] ³⁻	- 123.8
260, 261	[ⁱ Pt(¹¹⁹ SnCl ₃)(Sn ₄ Cl ₁₀ Br ₂)] ³⁻	- 123.0
262, 263, 264	[ⁱ Pt(¹¹⁹ SnCl ₃)(Sn ₄ Cl ₉ Br ₃)] ³⁻	- 122.2
265, 266, 267	[ⁱ Pt(¹¹⁹ SnCl ₃)(Sn ₄ Cl ₈ Br ₄)] ³⁻	- 121.4

^a The uncertainties on chemicals shifts are estimated to be ± 3 ppm.

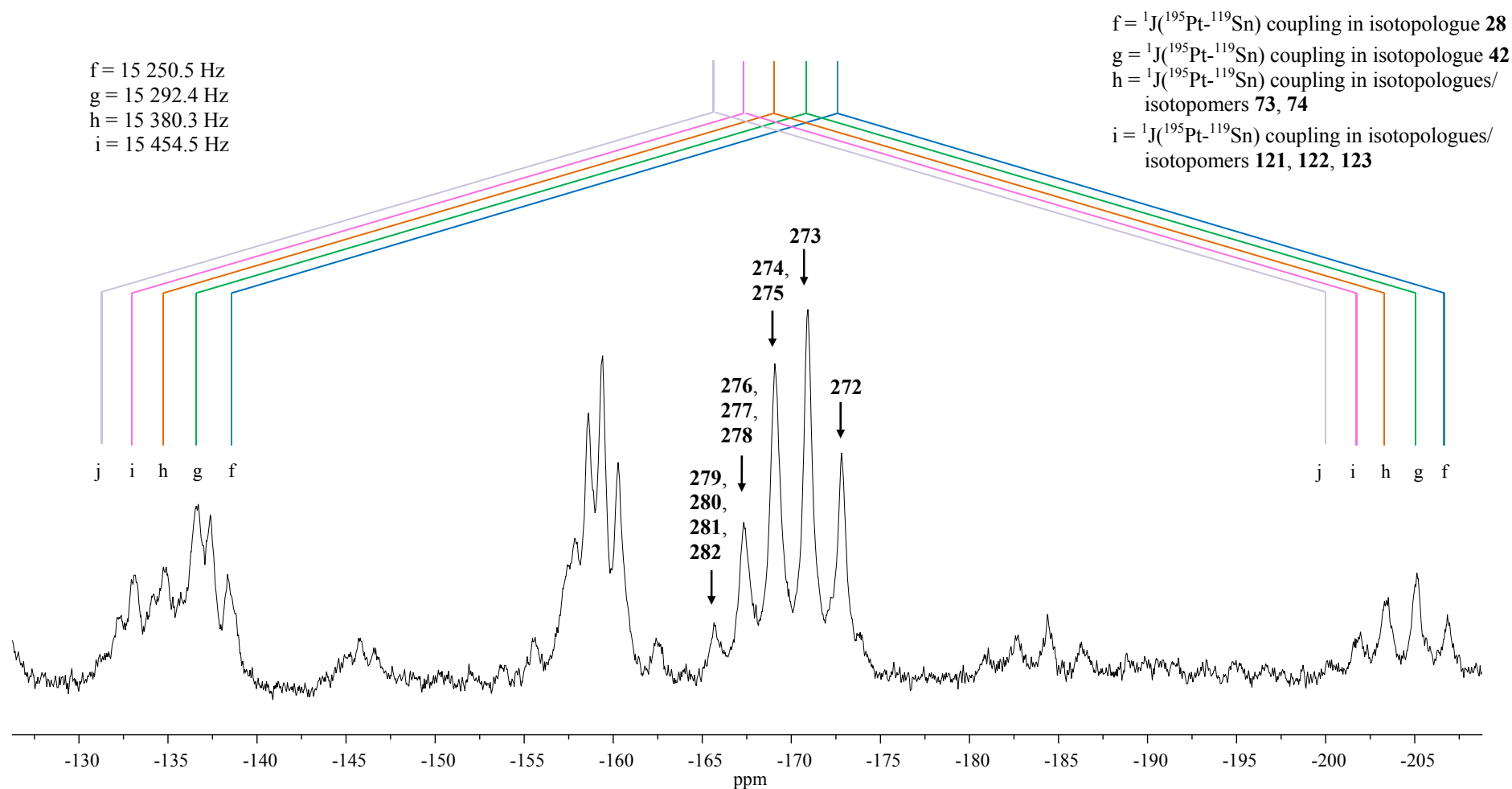


Figure 4.10: An expansion of the ^{119}Sn NMR spectrum recorded for the solution with a $[Pt(SnCl_3)_5]^{3-}$ to $[Pt(SnBr_3)_5]^{3-}$ volume ratio of 2 to 1 to focus on the ^{119}Sn NMR signals centred at -170 ppm. The symbols (f) to (j) indicate the ${}^1J(^{195}Pt-^{119}Sn)$ satellites due to the respective isotopologues. The isotopologues/ isotopomers responsible for the individual ^{119}Sn NMR signals in the main set of signals are indicated by the arrows.

Table 4.9: ¹J(¹⁹⁵Pt-¹¹⁹Sn) coupling constants^a measured for ¹J satellites of the set of ¹¹⁹Sn NMR signals centred at -170 ppm obtained with ¹⁹⁵Pt NMR compared to those obtained with ¹¹⁹Sn NMR.

	Isotopologue/ Isotopomer	¹⁹⁵ Pt NMR	¹¹⁹ Sn NMR
		¹ J(¹⁹⁵ Pt- ¹¹⁹ Sn)/ Hz	¹ J(¹⁹⁵ Pt- ¹¹⁹ Sn)/ Hz
f	28 [¹⁹⁵ Pt(¹¹⁹ SnCl ₂ Br)(Sn ₄ Cl ₁₂)] ³⁻	15 228	15 250
g	42 [¹⁹⁵ Pt(¹¹⁹ SnCl ₂ Br)(Sn ₄ Cl ₁₁ Br)] ³⁻	15 294	15 292
h	73, 74 [¹⁹⁵ Pt(¹¹⁹ SnCl ₂ Br)(Sn ₄ Cl ₁₀ Br ₂)] ³⁻	15 351	15 380
i	121, 122, 123 [¹⁹⁵ Pt(¹¹⁹ SnCl ₂ Br)(Sn ₄ Cl ₉ Br ₃)] ³⁻	15 406	15 405

^a The uncertainties for coupling constants are estimated to be ± 15 Hz.**Table 4.10:** Assignment of each individual ¹¹⁹Sn NMR signal in the set of signals centred at - 170.0 ppm to a isotopologue/isotopomer of the respective heteroleptic [Pt(Sn₅Cl_nBr_{15-n})]³⁻ (n = 11 - 14) species.

Isotopologue/ Isotopomer	δ(¹¹⁹ Sn)/ ppm ^a
272 [ⁱ Pt(¹¹⁹ SnCl ₂ Br)(Sn ₄ Cl ₁₂)] ³⁻	- 172.8
273 [ⁱ Pt(¹¹⁹ SnCl ₂ Br)(Sn ₄ Cl ₁₁ Br)] ³⁻	- 170.8
274, 275 [ⁱ Pt(¹¹⁹ SnCl ₂ Br)(Sn ₄ Cl ₁₀ Br ₂)] ³⁻	- 169.0
276, 277, 278 [ⁱ Pt(¹¹⁹ SnCl ₂ Br)(Sn ₄ Cl ₉ Br ₃)] ³⁻	- 167.2

^a The uncertainties for chemical shifts are estimated to be ± 3 ppm.

Each individual ¹¹⁹Sn NMR signal obtained within the set of signals centred at δ(¹¹⁹Sn) = - 123 and -170 ppm respectively, is thus unambiguously assigned to a specific isotopologue/isotopomer of the respective [Pt(SnCl_nBr_{15-n})]³⁻ (n = 10 - 15) species present in solution. From these assignments, listed in Tables 4.8 and 4.10, it is clear that the effect of substitution of Cl⁻ with Br⁻ on the chemical shift of the ¹¹⁹Sn signal depends on the position where the substitution occurs. For example, the substitution of a Cl⁻ with a Br⁻ on the ¹¹⁹SnCl₃⁻ ligand of isotopologue **1** to give isotopologue/isotopomer **272** results in an upfield shift of ± 48.3 ppm of the ¹¹⁹Sn NMR signal, Figure 4.11, which is indicative of the increased shielding experienced by the ¹¹⁹Sn nucleus. This is in agreement with Br⁻ being less electronegative than Cl⁻, and thus shielding the ¹¹⁹Sn nucleus to a greater extent. Conversely a downfield shift of ±1 ppm is observed when a Cl⁻ is substituted by a Br⁻ on the ⁱSnCl₃⁻ ligand of isotopologue **1** to give isotopologue/isotopomer **259**, which implies that the ¹¹⁹Sn nucleus

becomes less shielded. It is reasonable to suggest that this deshielding experienced by ^{119}Sn is due to Br^- being sterically more bulky than Cl^- which might cause an expansion of the coordination sphere of the complex anion. However, further investigations are needed to confirm this. Moreover, separate ^{119}Sn NMR signals are observed for isotopomers **259** and **272** which imply that *intra*- or *inter*- molecular halide exchange are too slow on the ^{119}Sn NMR acquisition time scale to be observed. This is in agreement with what was observed with ^{195}Pt NMR.

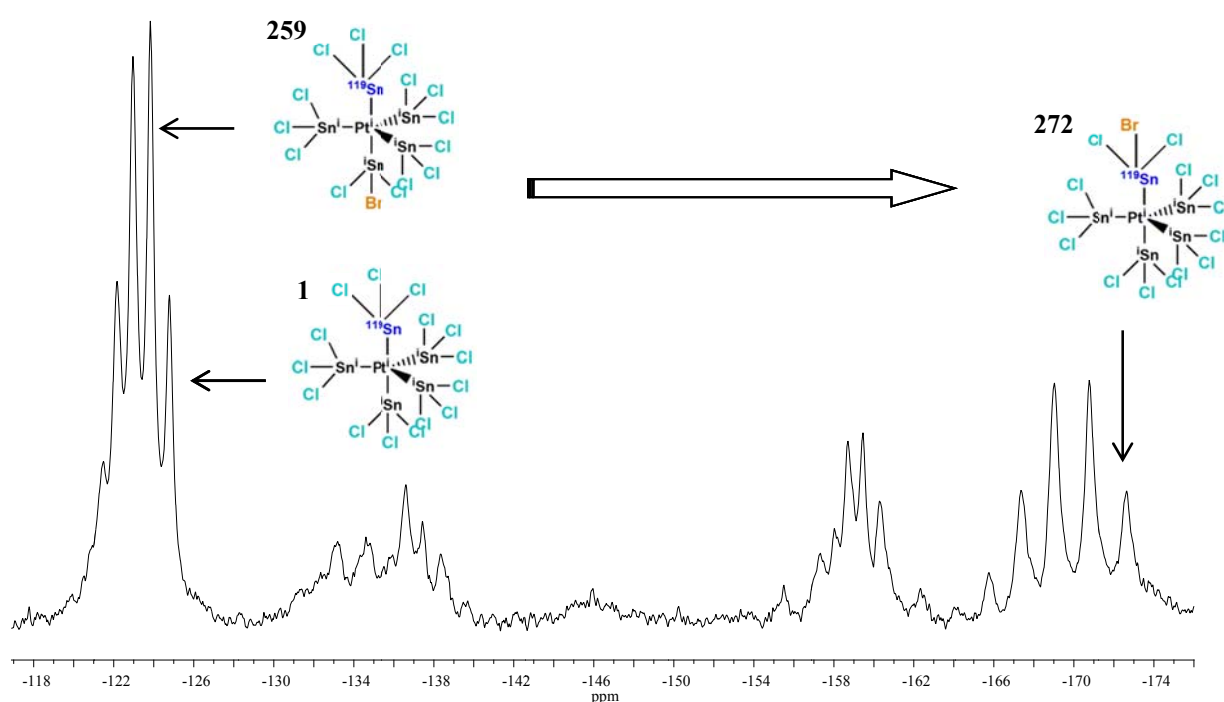


Figure 4.11: ^{119}Sn NMR spectrum of the solution with a $[\text{Pt}(\text{SnCl}_3)_5]^{3-}$ to $[\text{Pt}(\text{SnBr}_3)_5]^{3-}$ ratio of 2 to 1. Only a partial part of the spectrum is shown as to focus on the upfield shift obtained when Br^- adds to the NMR active ^{119}Sn ligand, as oppose to adding to an NMR inactive tin ligand.

Unfortunately, as the volume ratio of $(\text{R}_3\text{NCH}_3^+)_3[\text{Pt}(\text{SnBr}_3)_5]^{3-}$ to $(\text{R}_3\text{NCH}_3^+)_3[\text{Pt}(\text{SnCl}_3)_5]^{3-}$ increases, only broad, unresolved ^{119}Sn NMR signals are observed, shown in the ^{119}Sn NMR spectra given in Figures 4.7 (C) and (D).

This study has not only helped confirm the original assignments of the ^{119}Sn NMR spectra of Koch,⁶⁹ but has also shown that with the power of ^{195}Pt NMR at high magnetic fields (14.3 Tesla) significantly more detailed understanding of these systems has been obtained.

4.3. Conclusions

Excellent second order correlation is obtained when plotting the $\delta(^{195}\text{Pt})$ of the sixteen ^{195}Pt NMR signals observed for the mixed halide solutions as a function of the number of Br^- present in the $[\text{Pt}(\text{Sn}_5\text{Cl}_n\text{Br}_{15-n})]^{3-}$ ($n = 0 - 15$) complex. This suggests that 16 heteroleptic species can be identified by ^{195}Pt NMR signals in solution of which the 14 $[\text{Pt}(\text{Sn}_5\text{Cl}_n\text{Br}_{15-n})]^{3-}$ ($n = 1 - 14$) have not been identified in the literature. This proposal is supported by the good agreement obtained between the calculated NSA's for each possible isotopologue and isotopomer of the $[\text{Pt}(\text{Sn}_5\text{Cl}_{14}\text{Br})]^{3-}$ complex anion in particular and the experimental ^{195}Pt NMR peak integrals, as well as between the $^1\text{J}(^{119/117}\text{Sn}-^{195}\text{Pt})/^1\text{J}(^{117/115}\text{Sn}-^{195}\text{Pt})$ ratios of respective ^1J satellites and the $\gamma(^{119/117}\text{Sn})/\gamma(^{117/115}\text{Sn})$ ratios which allowed for the unambiguous assignment of all 14 possible isotopologues and isotopomers of this species (**11**, **25** – **36**). By applying the method of successive splitting to the remaining 13 main ^{195}Pt NMR signals (due to isotopologues/isotopomers **12** – **24**) of the heteroleptic species more than 500 isotopologues and isotopomers of the $[\text{Pt}(\text{Sn}_5\text{Cl}_n\text{Br}_{15-n})]^{3-}$ ($n = 2 - 14$) complex anions are observed and identified in the solution by means of ^{195}Pt NMR.

Compared to the unprecedented resolution obtained with ^{195}Pt NMR for these heteroleptic species, the corresponding ^{119}Sn NMR spectra showed four sets ^{119}Sn NMR signals, each set consisting of 5 – 7 individually resolved resonances. The knowledge of which $[\text{Pt}(\text{Sn}_5\text{Cl}_n\text{Br}_{15-n})]^{3-}$ ($n = 0 - 15$) complex anions are present in the solutions, as well as the magnitude of the respective $^1\text{J}(^{195}\text{Pt}-^{119}\text{SnCl}_3)$ and $^1\text{J}(^{195}\text{Pt}-^{119}\text{SnCl}_2\text{Br})$ coupling constants obtained with ^{195}Pt NMR allowed for the assignment of each individual ^{119}Sn NMR signals within the respective sets of signals to isotopologues/isotopomers **1.1**, **259** – **282** of the $[\text{Pt}(\text{Sn}_5\text{Cl}_n\text{Br}_{15-n})]^{3-}$ ($n = 10 - 15$) complex anions. High resolution ^{195}Pt NMR thus proved to be an indispensable tool for the unambiguous assignment of each resolved individual ^{119}Sn NMR signal observed in the ^{119}Sn NMR spectrum of this solution. These assignments made support the speculative assignments by Koch⁶⁹ in that each of the four sets of ^{119}Sn NMR signals are due to a particular $(\text{SnCl}_n\text{Br}_{3-n})^-$ ($n = 0 - 3$) ligand. However, in contrast to Koch⁶⁹ who assigned a the set of ^{119}Sn signals to a $[\text{Pt}(\text{SnCl}_n\text{Br}_{3-n})_5]^{3-}$ complex anion, it is showed in this study that each individual ^{119}Sn NMR signal within a set is due to a particular isotopomer of a $[\text{Pt}(\text{Sn}_5\text{Cl}_n\text{Br}_{15-n})]^{3-}$ ($n = 0 - 15$) species.

Chapter V

Conclusions

The detailed ^{119}Sn and high-resolution ^{195}Pt NMR study performed on the series of $[\text{Pt}(\text{Sn}_5\text{Cl}_n\text{Br}_{15-n})]^{3-}$ ($n = 0 - 15$) complex anions emphasized the power of ^{195}Pt NMR spectroscopy in that it provided data not obtainable by any other means.

The greater nuclear shielding range and sensitivity of ^{195}Pt NMR allow for much greater detail to be obtained with respect to the distribution of isotopomers and isotopologues of $[\text{Pt}(\text{Sn}_5\text{Cl}_n\text{Br}_{15-n})]^{3-}$ ($n = 0 - 15$) complex anions extracted into a relatively non-polar solvent such as CDCl_3 by Aliquat-336. While ^{119}Sn NMR suggests the extraordinary number and complexity of these species the ^{119}Sn NMR signals are too broad and the shielding range is too insensitive to allow for similar detailed analysis. This is clearly evidenced by all sixteen possible $[\text{Pt}(\text{Sn}_5\text{Cl}_n\text{Br}_{15-n})]^{3-}$ ($n = 0 - 15$) species being observed and identified by means of ^{195}Pt NMR compared to only the 6 $[\text{Pt}(\text{Sn}_5\text{Cl}_n\text{Br}_{15-n})]^{3-}$ ($n = 10 - 15$) species identified by means of ^{119}Sn NMR. ^{195}Pt NMR is thus an ideal method to study the speciation of these complex anions.

The unprecedented resolution obtained with ^{195}Pt NMR has allowed for the assignment of all the respective $^1\text{J}(^{119/117/115}\text{Sn}-^{195}\text{Pt})$ satellites of each of the 16 $[\text{Pt}(\text{Sn}_5\text{Cl}_n\text{Br}_{15-n})]^{3-}$ ($n = 0 - 15$) respective species. From these assignments it is clear that the $^1\text{J}(^{195}\text{Pt}-^{119/117/115}\text{Sn})$ coupling constants for each species depend on the configuration of the $\text{SnCl}_n\text{Br}_{3-n}^-$ ($n = 0 - 3$) ligand and decreases in the order $^1\text{J}(^{119/117/115}\text{SnCl}_3-^{195}\text{Pt}) > ^1\text{J}(^{119/117/115}\text{SnCl}_2\text{Br}-^{195}\text{Pt}) > ^1\text{J}(^{119/117/115}\text{SnClBr}_2-^{195}\text{Pt}) > ^1\text{J}(^{119/117/115}\text{SnBr}_3-^{195}\text{Pt})$ with $^1\text{J}(^{119}\text{SnCl}_3-^{195}\text{Pt})$ couplings for example ranges from 15 864 to 16 419 Hz compared to $^1\text{J}(^{119}\text{SnBr}_3-^{195}\text{Pt})$ couplings that ranges from 14 057 to 14659 Hz.

Moreover, *intra-* or *inter-* molecular halide scrambling/exchange does not occur on either the ^{195}Pt NMR or the ^{119}Sn NMR time scale as is confirmed by the separate sets of $^1\text{J}(^{119/117/115}\text{Sn}-^{195}\text{Pt})$ satellites obtained with ^{195}Pt NMR for respective isotopologues and isotopomers of each species and the separate ^{119}Sn NMR signals obtained for isotopomers a particular $[\text{Pt}(\text{Sn}_5\text{Cl}_n\text{Br}_{15-n})]^{3-}$ ($n = 0 - 15$) species.

The value of considering all possible magnetically-active isotopologues and isotopomers of deceptively simple complex anions such as $[\text{Pt}(\text{Sn}_5\text{Cl}_n\text{Br}_{15-n})]^{3-}$ ($n = 0 - 15$) is nicely demonstrated by this system, provided the species are not in fast chemical exchange and adequate resolution is obtained. This is achieved by extracting these trigonal-bipyramidal anions into an appropriate non-polar solvent as demonstrated here.

Further DFT computational work on these complexes is required to contribute to the question of why the coordination preference of the Pt(II) (d^8) metal centre, which are normally 4-coordinate square planar complexes, tends with $\text{SnCl}_3^-/\text{SnBr}_3^-$ ligands to form 5-coordinate homoleptic $[\text{Pt}(\text{SnCl}_3)_5]^{3-}$ or $[\text{Pt}(\text{SnBr}_3)_5]^{3-}$ and the numerous heteroleptic $[\text{Pt}(\text{Sn}_5\text{Cl}_n\text{Br}_{15-n})]^{3-}$ ($n = 0 - 15$) complexes.

References

1. W. H. Wollaston, *Philosophical Transactions*, 1804, 427
2. M. S. Holt, W. L. Wilson, and J. H. Nelson, *Chemical Reviews*, 1989, **89**, p 11.
3. K. F. G. Brackenbury, L. Jones, I. Nel, K. R. Koch, and J. M. Wyrley-Birch, *Polyhedron*, 1987, **6** (1), p 71.
4. C. R. Fresenius (Translated by C. E. Groves), *Qualitative Chemical Analysis*, 10th Edition, p 158, J. And A. Churchill, London, 1887.
5. A. H. Sexton, *Outlines of Qualitative Analysis*, 3rd Edition, p 45, C. Griffin, London, 1892.
6. H. Wölbing, Ber. 1934, **67**, p 773.^{***}
7. G. H. Ayres and A. S. Meyer, Jr., *Analytical Chemistry*, 1951, **23** (2), p 299.
8. G. H. Ayres, *Analytical Chemistry*, 1953, **25** (11), p 1622.
9. L. Wöhler, *Chemiker-Zeitung*, 1907, 31, p 938.^{***}
10. L. Wöhler and A. Spengel, *Z. Chem. Ind. Kolloide*, 1909, **7**, p 243.^{***}
11. F. P. Treadwell and W. T. Wall, '*Analytical Chemistry*', 6th English Edition, Vol. 1, p 284, New York, John Wiley and Sons, 1921.
12. E. Sandell, '*Colorimetric Determination of Traces of Metals*', 3rd Edition, Interscience, New York, 1959.
13. D. Hunter, R. Milton, and K. M. A. Perry, *British Journal of Industrial Medicine*, 1945, **2**, p 92.
14. O. I. Milner and G. F. Shipman, *Analytical Chemistry*, 1955, **27** (9), p 1476.
15. A. S. Meyer, Jr. and G. H. Ayres, *Journal of American Chemical Society*, 1955, **77** (10), p 2671.
16. G. L. Elizarova and L. G. Matvienko, *Russian Journal of Inorganic Chemistry*, 1970, **15** (6), p 823.
17. S. K. Shukla, *Annales des Chimie (France)*, 1961, **6**, p 1383.
18. M. Lederer and S. K. Shukla, *Journal of Chromatography*, 1961, **6**, p 353.
19. J. F. Young, R. D. Gillard, and G. Wilkinson, *Journal of Chemical Society*, 1964, p 5176.
20. A. G. Davies, G. Wilkinson, and J. F. Young, *Journal of the American Chemical Society*, 1963, **85**, p 1692.
21. Bonati and J. Wilkinson, *Journal of the American Chemical Society*, 1964, p 179.

^{***} These are secondary references of which the original papers could not be obtained.

22. R. D. Gorsich, *Journal of the American Chemical Society*, 1962, **84**, p 2486.
23. R. D. Cramer, E. L. Jenner, and R. V. Lindsey, Jr., U. G. Stolberg, *Journal of American Chemical Society*, 1963, **85**, p 1691.
24. R. D. Cramer, R. V. Lindsey, Jr., C. T. Prewitt, U. G. Stolberg, *Journal of American Chemical Society*, 1965, **87** (3), p 658.
25. R. V. Lindsey, Jr., G. W. Parshall, U. G. Stolberg, *Journal of American Chemical Society*, 1965, **87** (3), pp 658.
26. R. V. Parish and P. J. Rowbotham, *Journal of the Chemical Society, Dalton Transitions*, 1973, p 37.
27. J. H. Nelson, V. Cooper, R. W. Rudolph, *Inorganic Nuclear Chemical Letters*, 1980, **16**, p 263.
28. P. S. Pregosin and H. Rügger, *Inorganica Chimica Acta*, 1984, **86**, p 55.
29. J. H. Nelson, W. L. Wilson, L. W. Cary, N. W. Alcock, H. J. Clase, G. S. Jas, L. Ramsey-Tassin, and J. W. Kenney, *Inorganic Chemistry*, 1996, **35** (4), p 883.
30. K. G. Moodley and M. J. Nicol, *Journal of the Chemical Society, Dalton Transitions*, 1977, p 239.
31. Yu. N. Kukushkin, P. G. A. Antonov, K. I. Dubonos, and L. V. Konovalov, *Russian Journal of Inorganic Chemistry*, 1973, **18**, p 1604.
32. P. G. A. Antonov, Yu. N. Kukushkin, L. N. Mitronina, L. N. Vasil'ev, and V. P. Sass, *Russian Journal of Inorganic Chemistry*, 1979, **24** (4), p 557.
33. A. Albinati, P. S. Pregosin, and H. Rügger, *Inorganic Chemistry*, 1984, **23**, p 3223.
34. G. W. Parshall, *Journal of the American Chemical Society*, 1964, **86**, p 5367.
35. W. A. G. Graham, *Inorganic Chemistry*, 1968, **7**, p 315.
36. W. Jetz, P. B. Simons, J. A. J. Thompson, W. A. G. Graham, *Inorganic Chemistry*, 1966, **5**, p 2217.
37. F. A. Cotton and C. S. Kraihanzel, *Journal of the American Chemical Society*, 1962, **84**, p 443.
38. R. F. Bryan, P. T. Greene, G. A. Melson, and P. F. Stokely, *Chemical Communication*, 1969, p 722.
39. J. Chatt, L. A. Duncanson, and L. M. Venanzi, *Journal of the Chemical Society*, 1955, p 4456.
40. F. R. Hartley, *Chemical Society Reviews*, 1973, **2**, p 287.
41. J. E. Huheey, *Inorganic Chemistry*, Harper & Row, New York, 2nd Edition, 1978.
42. R. C. Taylor, J. F. Young, and G. Wilkinson, *Inorganic Chemistry*, 1966, **5**, p 20.
43. J. Chatt, L. A. Duncanson and B. L. Shaw, *Chemistry and Industry (London)*, 1958, p 859.
44. J. Chatt and B. L. Shaw, *Journal of the Chemical Society*, 1962, p 5057.
45. M. Kretschmer, P. S. Pregosin, and H. Rügger, *Journal of Organometallic Chemistry*, 1983, **241**, p 87.

46. A. Albinati, U. von Gunten, P. S. Pregosin, and H. J. Reugg, *Journal of Organometallic Chemistry*, 1985, **295**, p 239.
47. R. Hani and R. A. Geanangel, *Coordination Chemistry Reviews*, 1982, **44**, p 229.
48. J. Kramer, K. R. Koch, *Inorganic Chemistry*, 2007, **44**, p 7466
49. K. A. Ostoja Starzewski and P. S. Pregosin, *Angewandte Chemie*, 1980, **92** (4), p 323.
50. K. A. Ostoja Starzewski and P. S. Pregosin, *Advances in Chemistry*, 1982, **196**, p 23.
51. K. A. Ostoja Starzewski, H. Rügger and P. S. Pregosin, *Inorganica Chimica Acta*, 1979, **36**, L 445.
52. C. J. Jameson and H.-Jörg Osten, *Journal of the American Chemical Society*, 1986, **108** (10), p 2497.
53. W. McFarlane and N. H. Rees, *Journal of the Chemical Society, Dalton Transitions*, 1990, p 3211.
54. J.A. Pople and D.P. Santry, *Molecular Physics*, 1964, **8**, p 1.
55. P. S. Pregosin and S. N. Sze, *Helvetica Chimica Acta*, 1978, **61** (5), p 1848.
56. M. Kretschmer, P. S. Pregosin, *Inorganica Chimica Acta*, 1982, **61**, p 247.
57. M. Garralda, V. Garcia, M. Kretschmer, P. S. Pregosin, and H. Rügger, *Helvetica Chimica Acta*, 1981, **64** (4), p 1150.
58. M. Kretschmer, P. S. Pregosin, and M. Garralda, *Journal of Organometallic Chemistry*, 1983, **244**, p 175.
59. P. S. Pregosin and H. Rügger, *Inorganica Chimica Acta*, 1984, **86**, p 55.
60. J. H. Nelson and N. W. Alcock, *Inorganic Chemistry*, 1982, **21** (3), p 1196.
61. N. W. Alcock and J. H. Nelson, *Journal of the Chemical Society, Dalton Transitions*, 1982, p 2415.
62. A. Goel and S. Goel, *Inorganica Chimica Acta*, 1984, **82**, p 41.
63. M. C. Grossel, R. P. Moulding, and K. R. Seddon, *Inorganica Chimica Acta*, 1982, **64**, L275.
64. R. Pietropaolo, M. Graziani, and U. Belluco, *Inorganic Chemistry*, 1969, **8** (7), p 1506.
65. G. K. Anderson, H. C. Clark, J. A. Davies, *Inorganic Chemistry*, 1983, **22**, p 434.
66. G. K. Anderson, C. Billard, H. C. Clark, J. A. Davies, *Inorganic Chemistry*, 1983, **22**, p 439.
67. H. C. Clark and J. Halpern, *Inorganic Chemistry*, 1974, **13**, p 1541.
68. N. V. Borunova, P. G. Antonov, Yu. N. Kukushkin, L. Kh. Freidlin, N. D. Trink, V. m. Ignatov, and I. K. Shirshikova, *Zhurnal Obshchei Khimii*, 1980, **50** (8), p 1862.
69. K. R. Koch, *Magnetic Resonance in Chemistry*, 1992, **30**, p 158.
70. K. R. Koch, J. E. Yates, *Analytica Chimica Acta*, 1983, **147**, p 235.
71. R. Tarozaitė, A. Jagminiene, V. Jasulaitiene, and M Kurtinaitiene, *Chemija*, 2007, **18** (4), p 1.

72. A. B. Rossi, R. Hoffman, *Inorganic Chemistry*, 1975, **14**, p 365.
73. H. A. Bent, *Chemical Review*, 1961, **61**, p 275.
74. P. Murray, W. J. Gerber and K. R. Koch, *Dalton Transactions*, 2008, **31**, p 4113.
75. IUPAC. *Compendium of Chemical Terminology*, 2nd ed. (the "Gold Book"). Compiled by A. D. McNaught and A. Wilkinson. Blackwell Scientific Publications, Oxford, 1997
76. J. J. Burke and P. C. Lauterbur, *Journal of the American Chemical Society*, 1961, **83**, p 326.
77. J. M. Coddington and M. J. Taylor, *Journal of the Chemical Society, Dalton Transitions*, 1989, p 2223.

Appendix A

Calculated NSA's of isotopologues

The NSA's of the possible isotopologues of the $[\text{Pt}(\text{SnCl}_3)_5]^{3-}$ were calculated using Equation 3.1 where n_x is the number of isotope x present in the specific isotopologue and ρ_x is the natural abundance of isotope x .

$$\rho(n_1 n_2 \dots n_x) = \frac{(\sum_{i=1}^x n_i)!}{n_1! n_2! \dots n_x!} \rho_1^{n_1} \cdot \rho_2^{n_2} \cdot \rho_x^{n_x}$$

For example, the NSA of the $[\text{Pt}({}^i\text{SnCl}_3)_5]^{3-}$ isotopologue, where all 5 tin ligands contain magnetically-inactive ${}^i\text{Sn}$ isotopes, is calculated as follows:

— A1

Similarly the NSA's of isotopologues $[\text{Pt}({}^i\text{SnCl}_3)_4({}^{119}\text{SnCl}_3)]^{3-}$ and $[\text{Pt}({}^i\text{SnCl}_3)_3({}^{119}\text{SnCl}_3)-({}^{117}\text{SnCl}_3)]^{3-}$ are calculated as shown in Equations A2 and A3.

——A2

————A3

Moreover, each one of the 56 possible isotopologues listed in Table A1 contains either a magnetically-inactive ${}^i\text{Pt}$ isotope or the ${}^{195}\text{Pt}$ isotope, giving a total of 112 possible isotopologues of the $[\text{Pt}(\text{SnCl}_3)_5]^{3-}$ species. Note that 67.7 % of the NSA's listed in Table A1 are due to isotopologues that contain ${}^i\text{Pt}$ and 33.3 % are due to isotopologues that contain the ${}^{195}\text{Pt}$ isotope. For example the NSA of isotopologue **3**, $[{}^{195}\text{Pt}({}^i\text{SnCl}_3)_3({}^{119}\text{SnCl}_3)({}^{117}\text{SnCl}_3)]^{3-}$, is 33.3 % of 0.0769 which gives 0.026, whereas the NSA of isotopologue **4**, $[{}^i\text{Pt}({}^i\text{SnCl}_3)_3-({}^{119}\text{SnCl}_3)({}^{117}\text{SnCl}_3)]^{3-}$, is 66.7 % of 0.0769 which gives 0.051, shown in Table 3.2 in Chapter 3.2.1, p 29. Only the 9 highlighted isotopologues in Table A1 are high enough in abundance to be observed with ${}^{119}\text{Sn}$ and ${}^{195}\text{Pt}$ NMR.

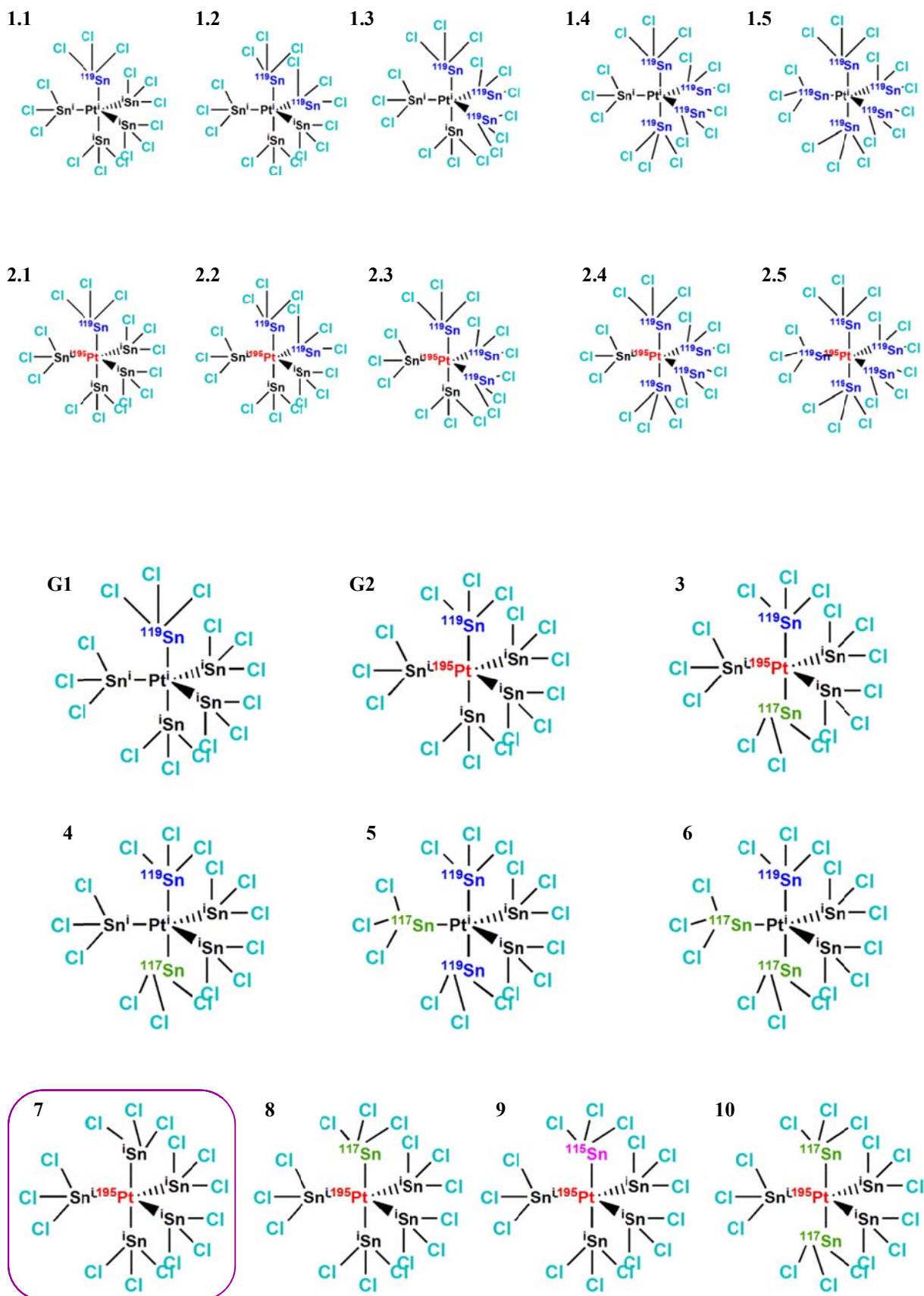
Table A1: Calculated NSA's of all 56 possible isotopologues of the $[\text{Pt}(\text{SnCl}_3)_5]^{3-}$ complex anion.

^{119}Sn	^{117}Sn	^{115}Sn	^iSn	NSA
5	0	0	0	4.65E-06
0	5	0	0	2.55E-06
0	0	5	0	4.54E-13
0	0	0	5	0.4135
4	1	0	0	2.06E-05
4	0	1	0	9.21E-07
4	0	0	1	2.27E-04
1	4	0	0	1.44E-05
1	0	4	0	5.73E-11
1	0	0	4	0.2117
0	4	1	0	5.70E-07
0	1	4	0	5.08E-11
0	1	0	4	0.1877
0	0	4	1	5.60E-10
0	0	1	4	0.0084
0	4	0	1	1.41E-04
3	2	0	0	3.66E-05
3	0	2	0	2.98E-05
3	0	0	2	4.44E-03
2	3	0	0	3.24E-05
2	0	3	0	2.89E-09
2	0	0	3	0.0433
0	3	2	0	5.09E-08
0	2	3	0	2.28E-09
0	0	3	2	2.76E-07
0	0	2	3	6.81E-05
0	2	0	3	0.0341
0	3	0	2	3.10E-03
3	1	1	0	3.27E-06
3	1	0	1	8.06E-04
3	0	1	1	3.60E-05
1	3	1	0	2.57E-06
1	3	0	1	6.34E-04
1	0	3	1	5.65E-08
1	0	1	3	3.43E-03
1	1	3	0	5.13E-09
1	1	0	3	0.0769
0	3	1	1	2.51E-05
0	1	3	1	5.01E-08

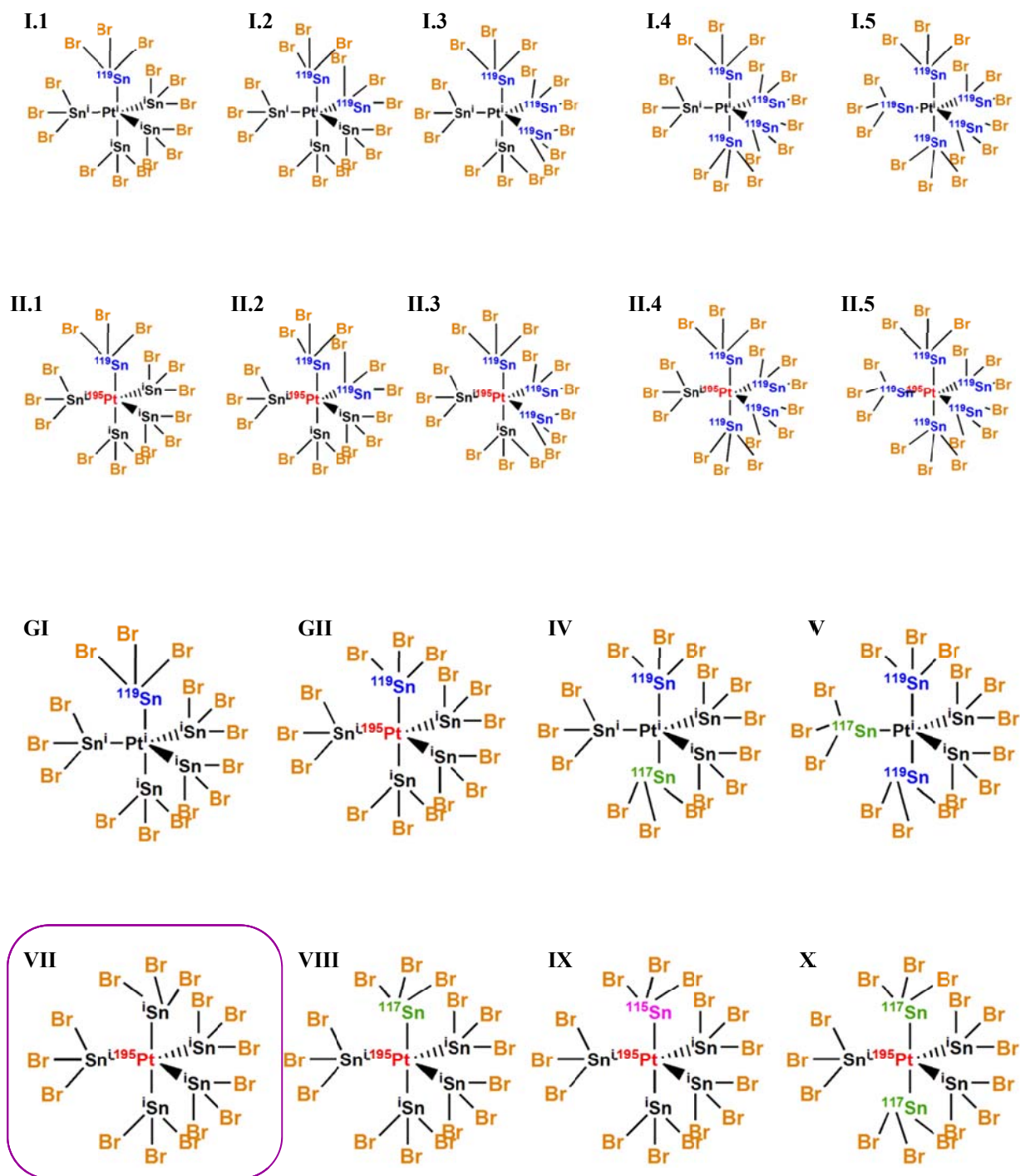
¹¹⁹ Sn	¹¹⁷ Sn	¹¹⁵ Sn	ⁱ Sn	NSA
0	1	1	3	3.05E-03
2	1	2	0	1.94E-07
2	1	0	2	0.0118
2	0	1	2	5.27E-04
2	0	2	1	2.14E-06
2	2	0	1	1.07E-03
2	2	1	0	4.35E-06
1	2	2	0	1.72E-07
1	2	0	2	0.0105
1	0	2	2	2.09E-05
0	2	2	1	1.68E-06
0	1	2	2	1.85E-05
0	2	1	2	4.15E-04
1	2	1	1	8.50E-05
1	1	2	1	3.80E-06
1	1	1	2	9.36E-04
2	1	1	1	9.58E-05

Appendix B

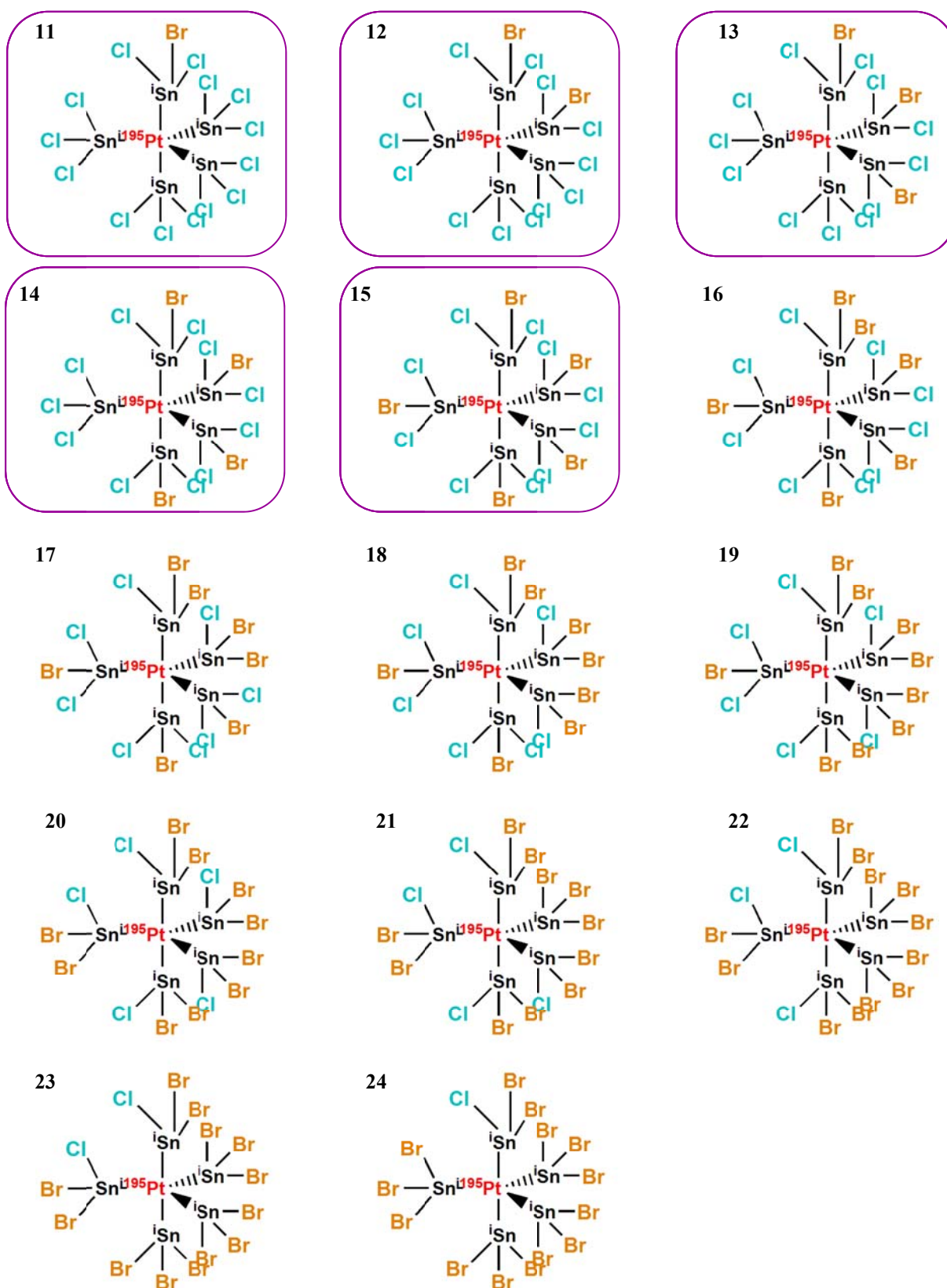
*Isotopologues and isotopomers of the $[Pt(SnCl_nBr_{15-n})]^{3-}$ ($n = 0, 10 - 15$)
heteroleptic complex anions*



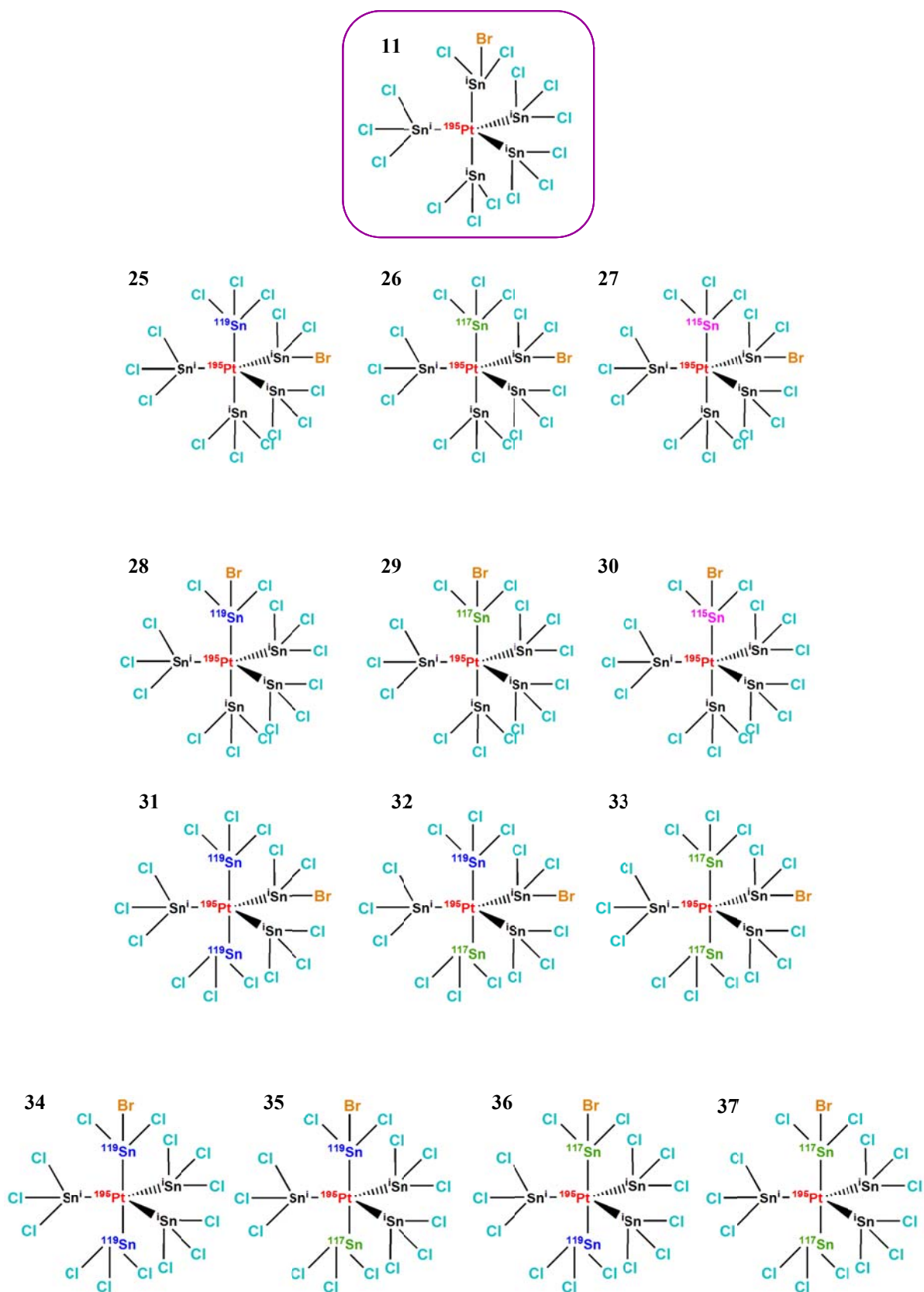
Scheme B1: Isotopologues of the $[\text{Pt}(\text{SnCl}_3)_5]^{3-}$ complex anion. Encircled is the isotopologue responsible for the ^{195}Pt NMR signal numbered 1 in Figure 4.2



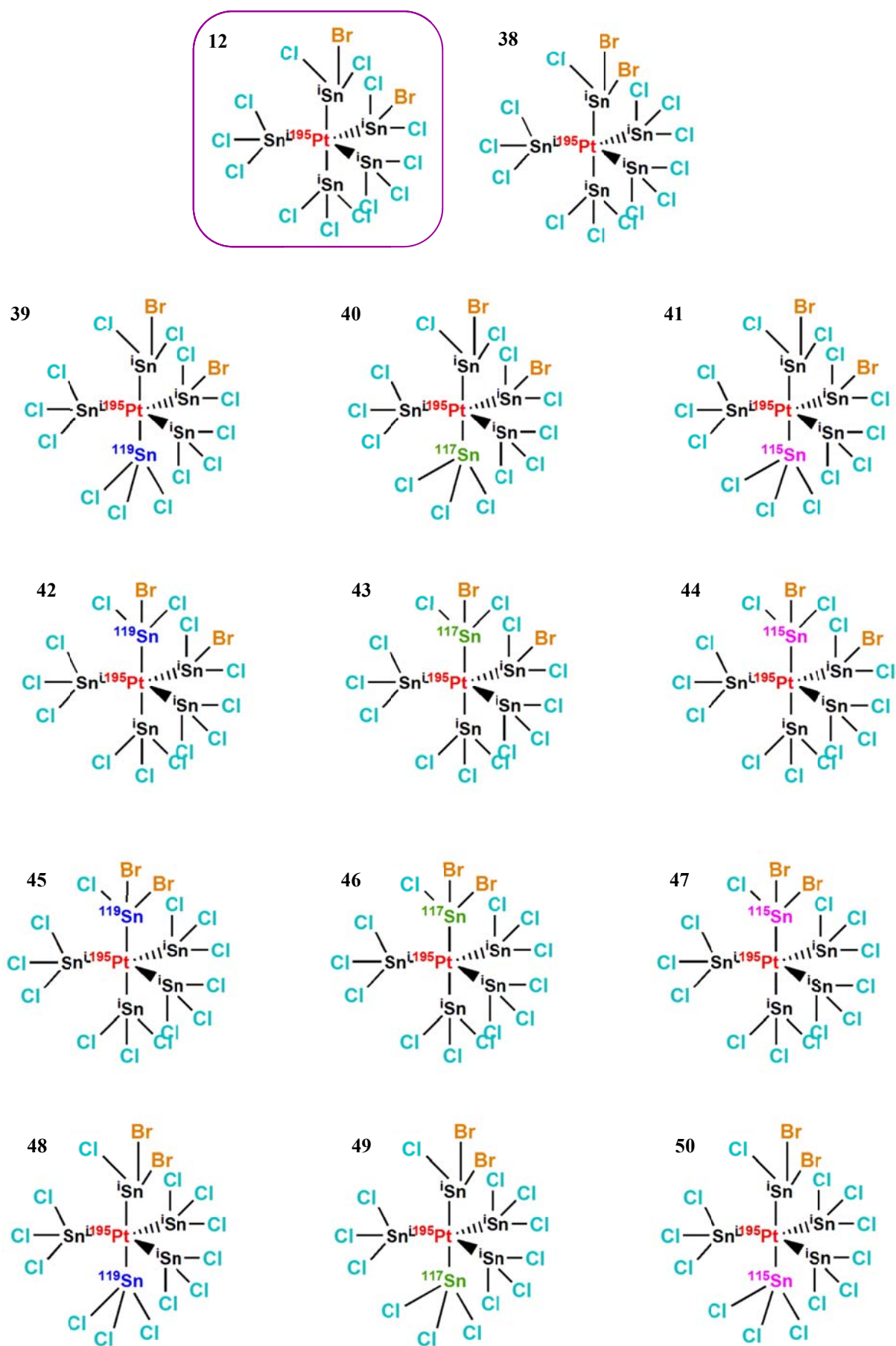
Scheme B2: Isotopologues of the $[\text{Pt}(\text{SnBr}_3)_5]^{3-}$ complex anion. Encircled is the isotopologue responsible for the ^{195}Pt NMR signal numbered 16 in Figure 4.2



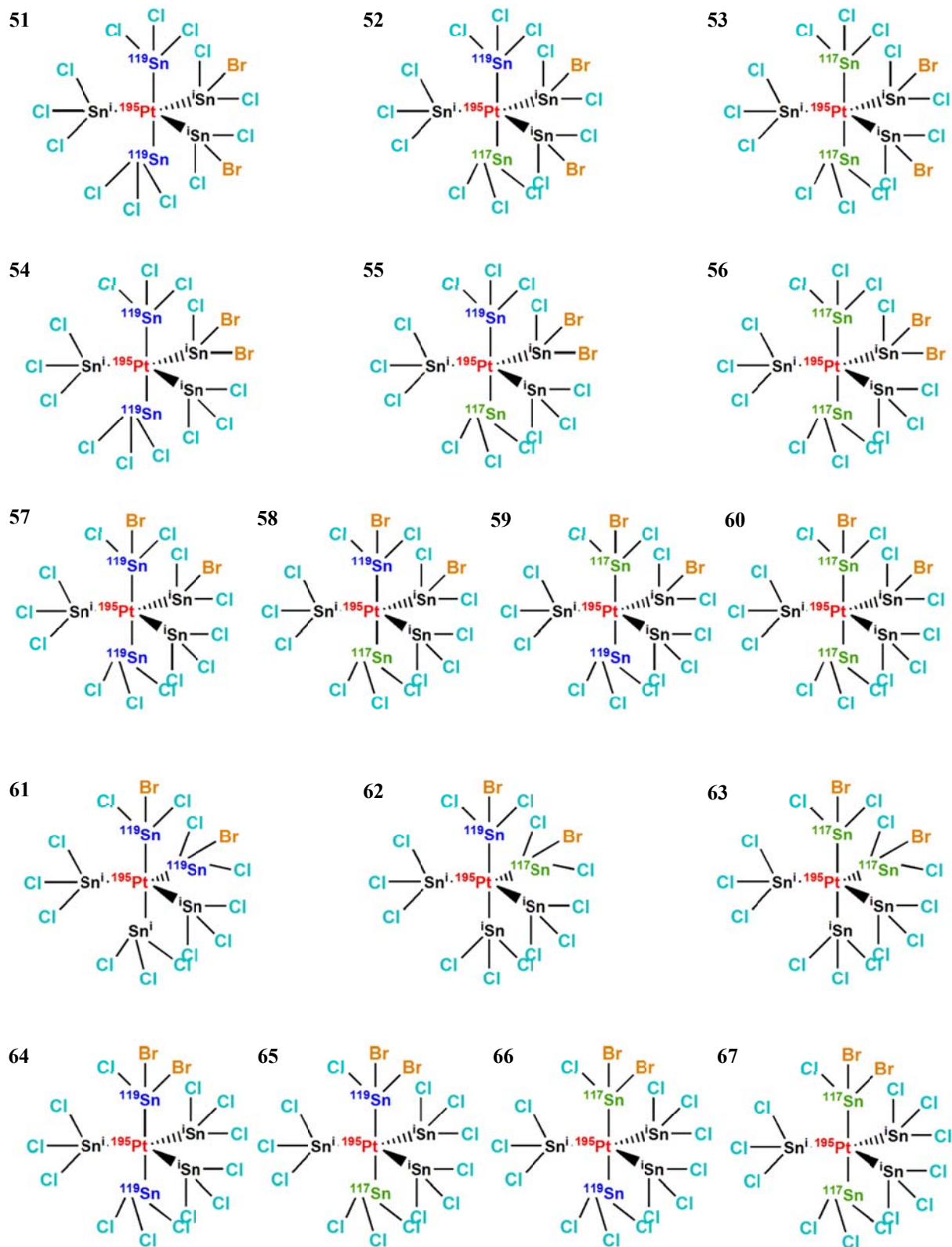
Scheme B3: Isotopologues of the $[\text{Pt}(\text{Sn}_5\text{Cl}_n\text{Br}_{15-n})]^{3-}$ ($n = 1 - 14$) complex anions responsible for the ^{195}Pt NMR signals numbered 2 - 15 in Figure 4.2. The 5 isotopologues discussed in more detail are encircled.



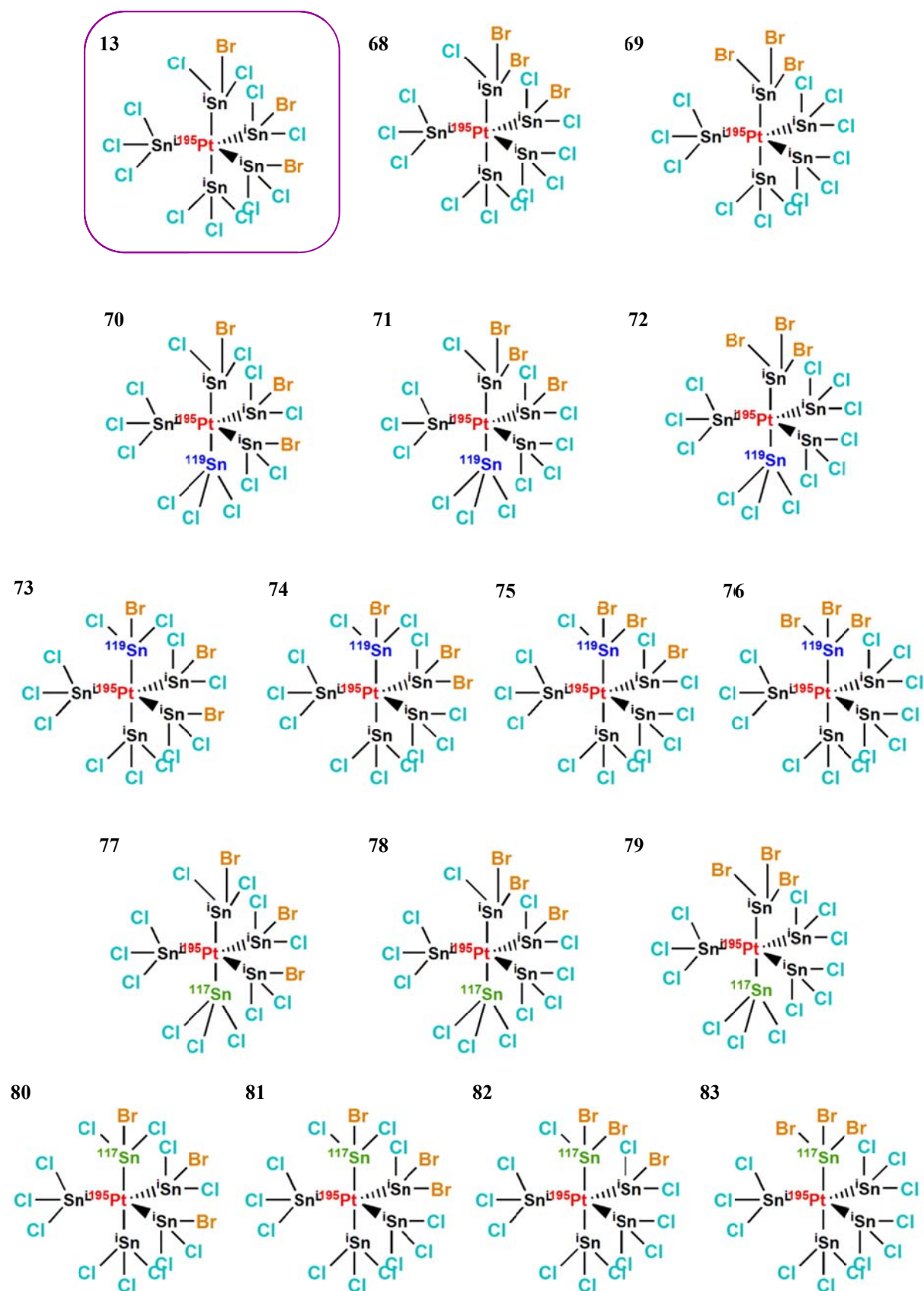
Scheme B4: Isotopologues and isotopomers of the $\text{Pt}(\text{Sn}_5\text{Cl}_{14}\text{Br})]^{3-}$ complex anion observed with ^{195}Pt NMR.



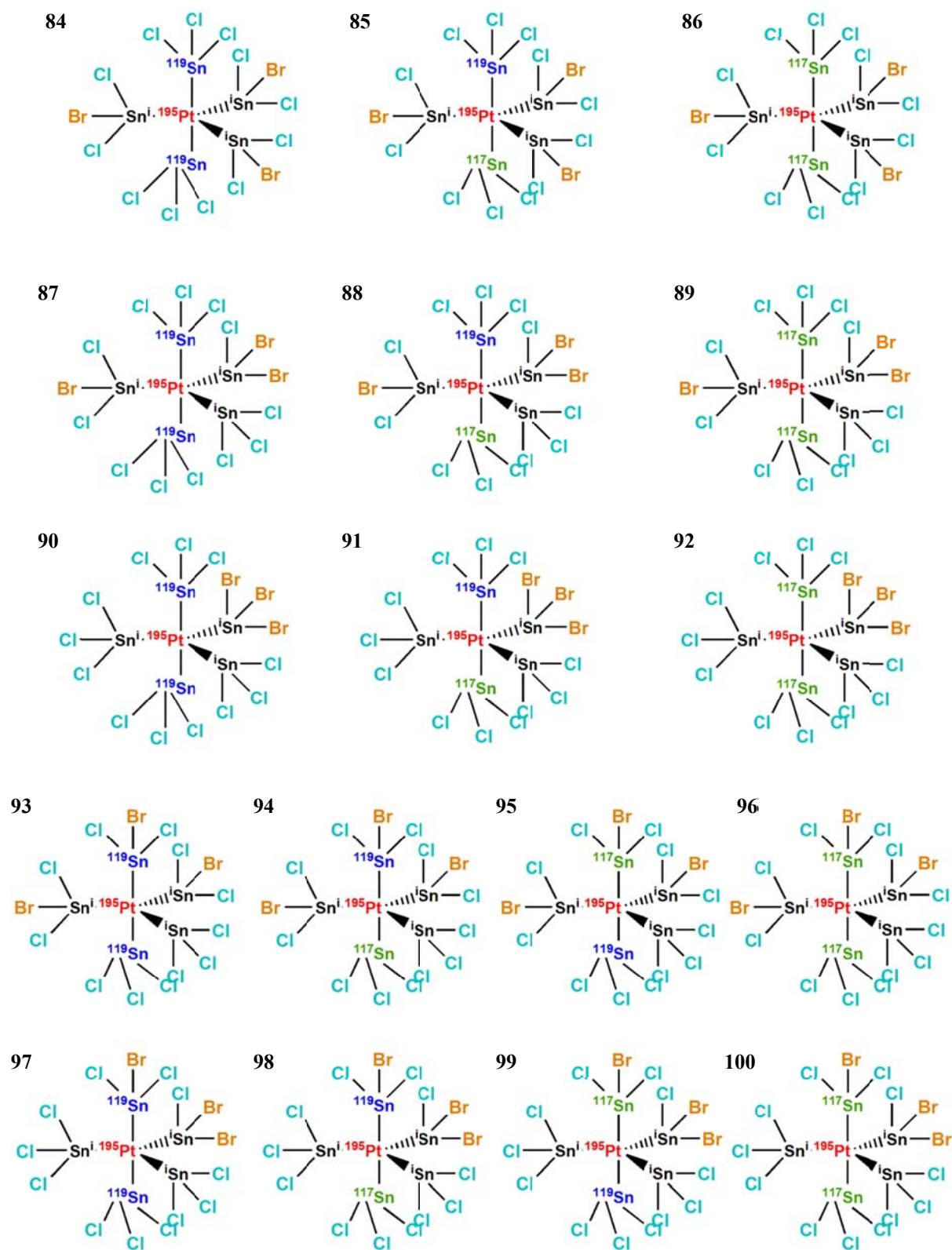
Scheme B5: Isotopologues and isotopomers of the $\text{Pt}(\text{Sn}_5\text{Cl}_{13}\text{Br}_2)]^{3-}$ complex anion observed with ^{195}Pt NMR.



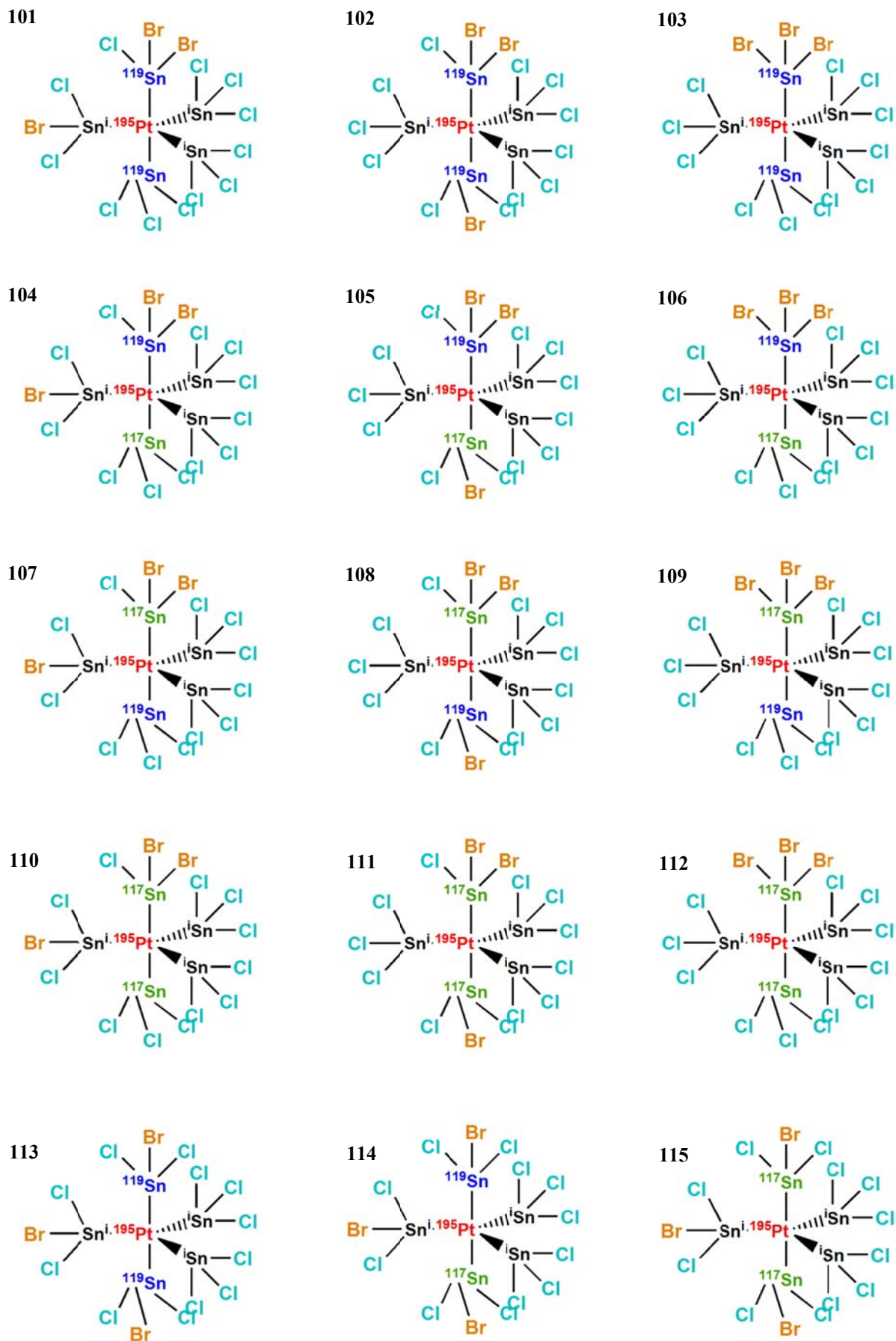
Scheme B6: Isotopologues and isotopomers of the $\text{Pt}(\text{Sn}_5\text{Cl}_{13}\text{Br}_2)]^{3-}$ complex anion observed with ^{195}Pt NMR.



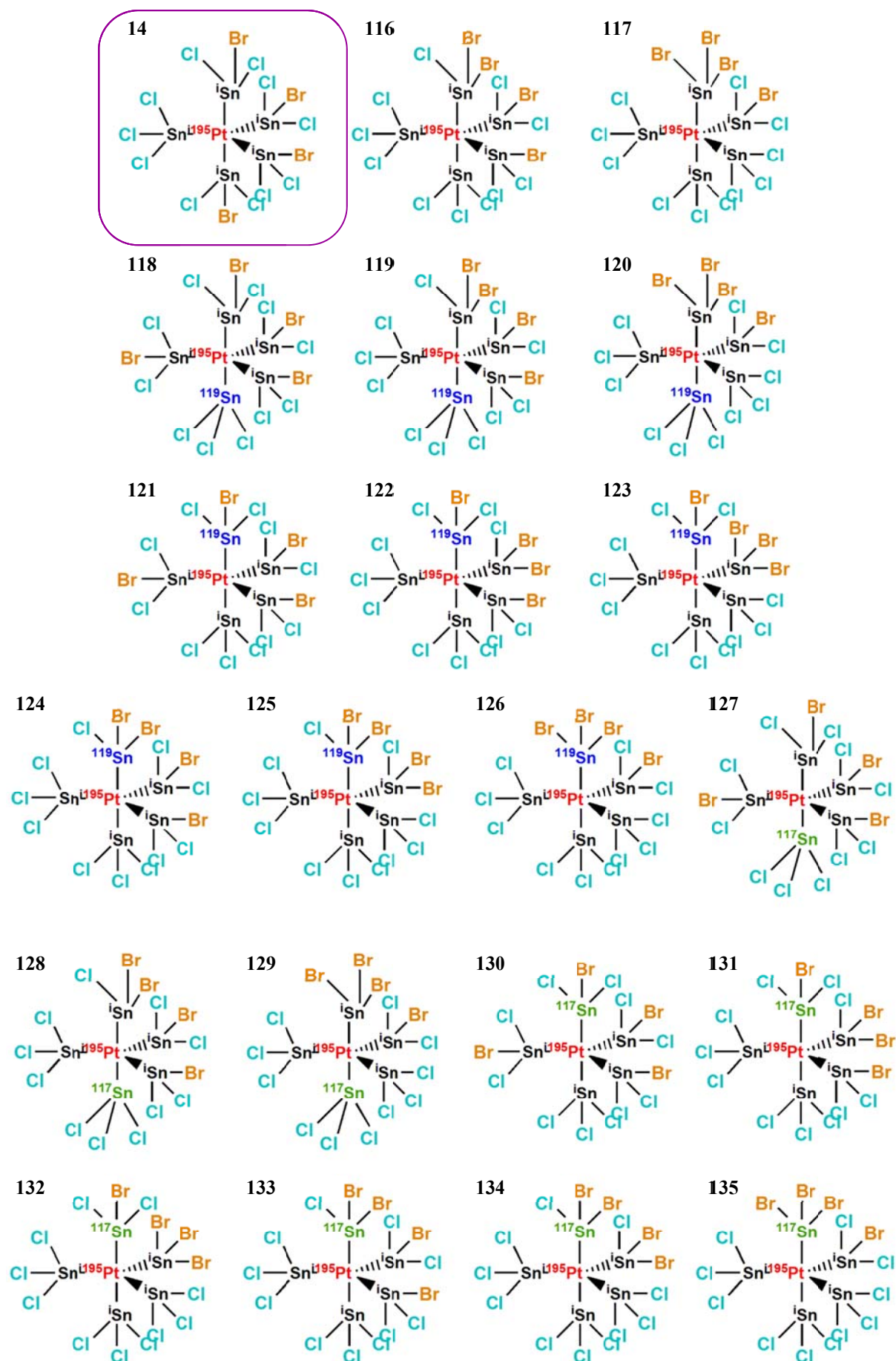
Scheme B7: Isotopologues and isotopomers of the $\text{Pt}(\text{Sn}_5\text{Cl}_{12}\text{Br}_3)]^{3-}$ complex anion observed with ^{195}Pt NMR.



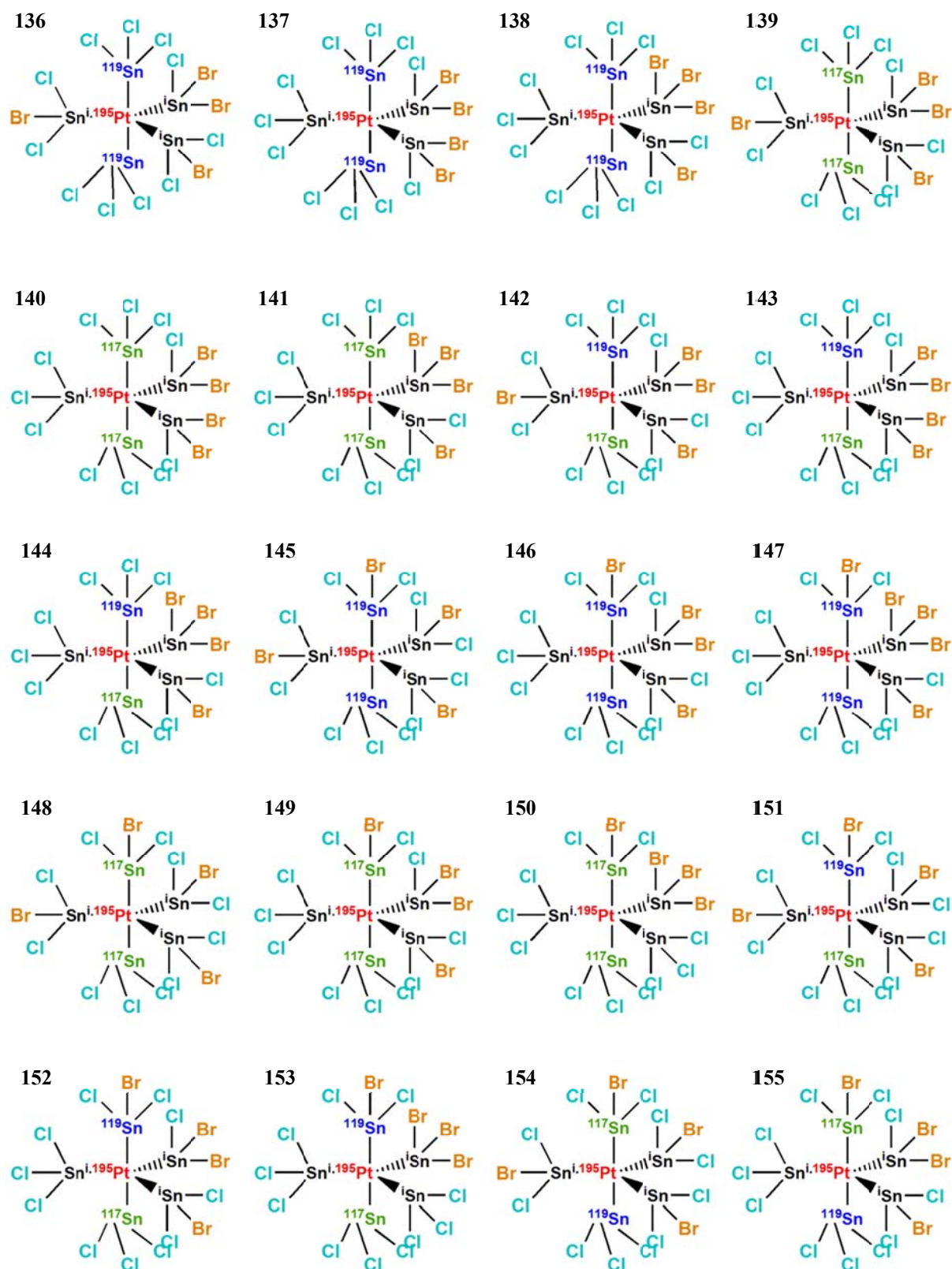
Scheme B8: Isotopologues and isotopomers of the $\text{Pt}(\text{Sn}_5\text{Cl}_{12}\text{Br}_3)]^{3-}$ complex anion observed with ^{195}Pt NMR.



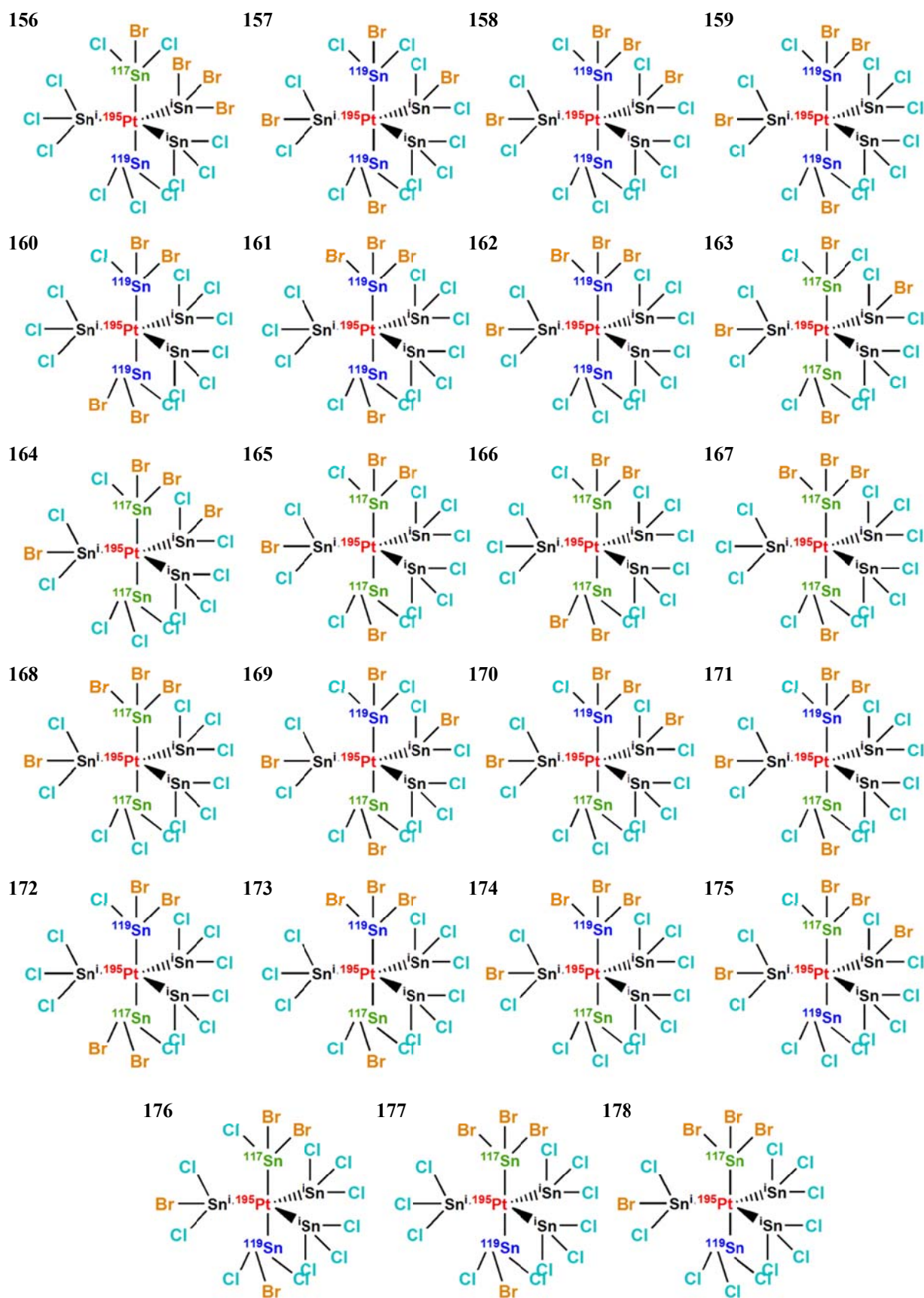
Scheme B9: Isotopologues and isotopomers of the $\text{Pt}(\text{Sn}_5\text{Cl}_{12}\text{Br}_3)]^{3-}$ complex anion observed with ^{195}Pt NMR.



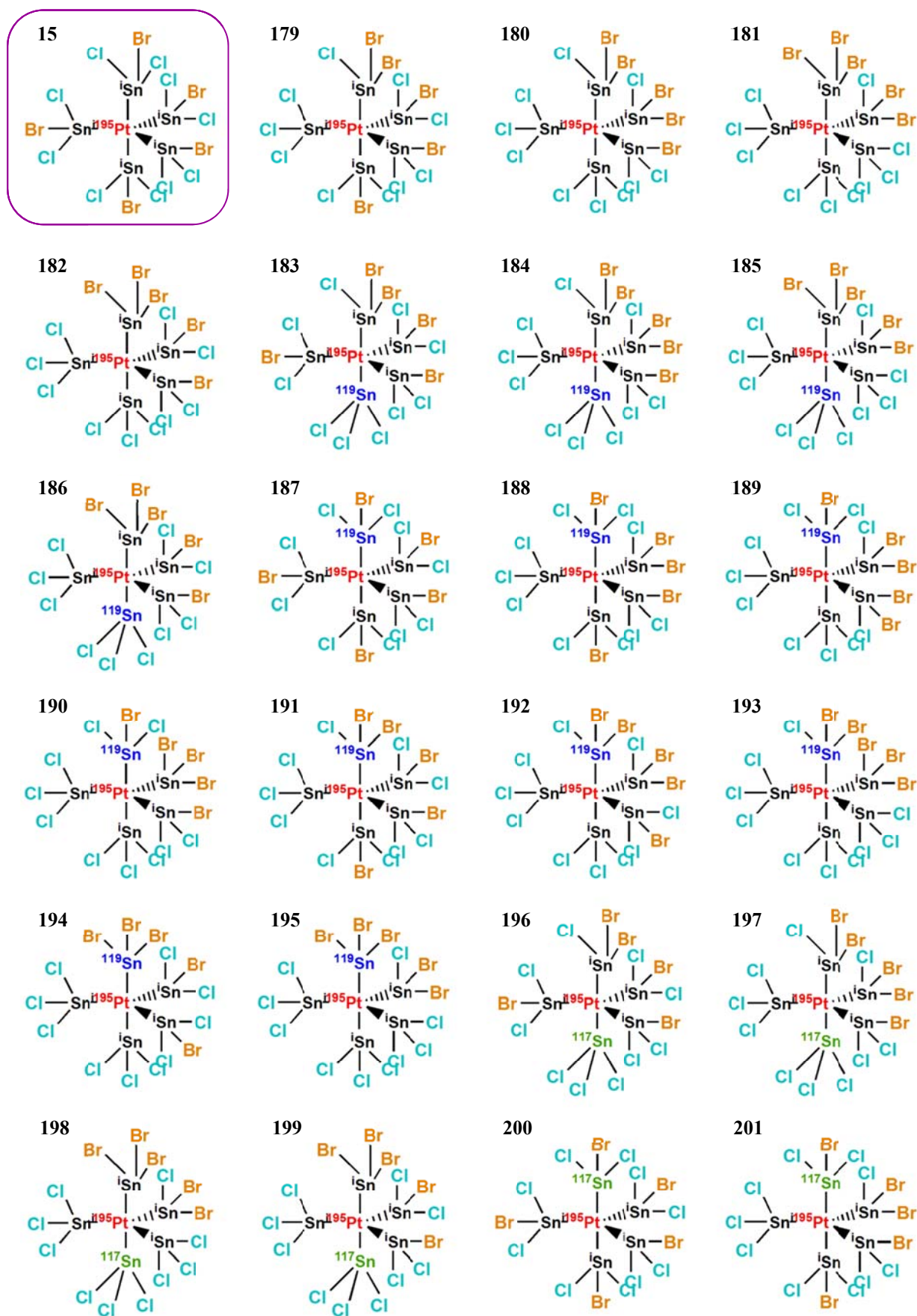
Scheme B10: Isotopologues and isotopomers of the $\text{Pt}(\text{Sn}_5\text{Cl}_{11}\text{Br}_4)]^{3-}$ complex anion observed with ^{195}Pt NMR.



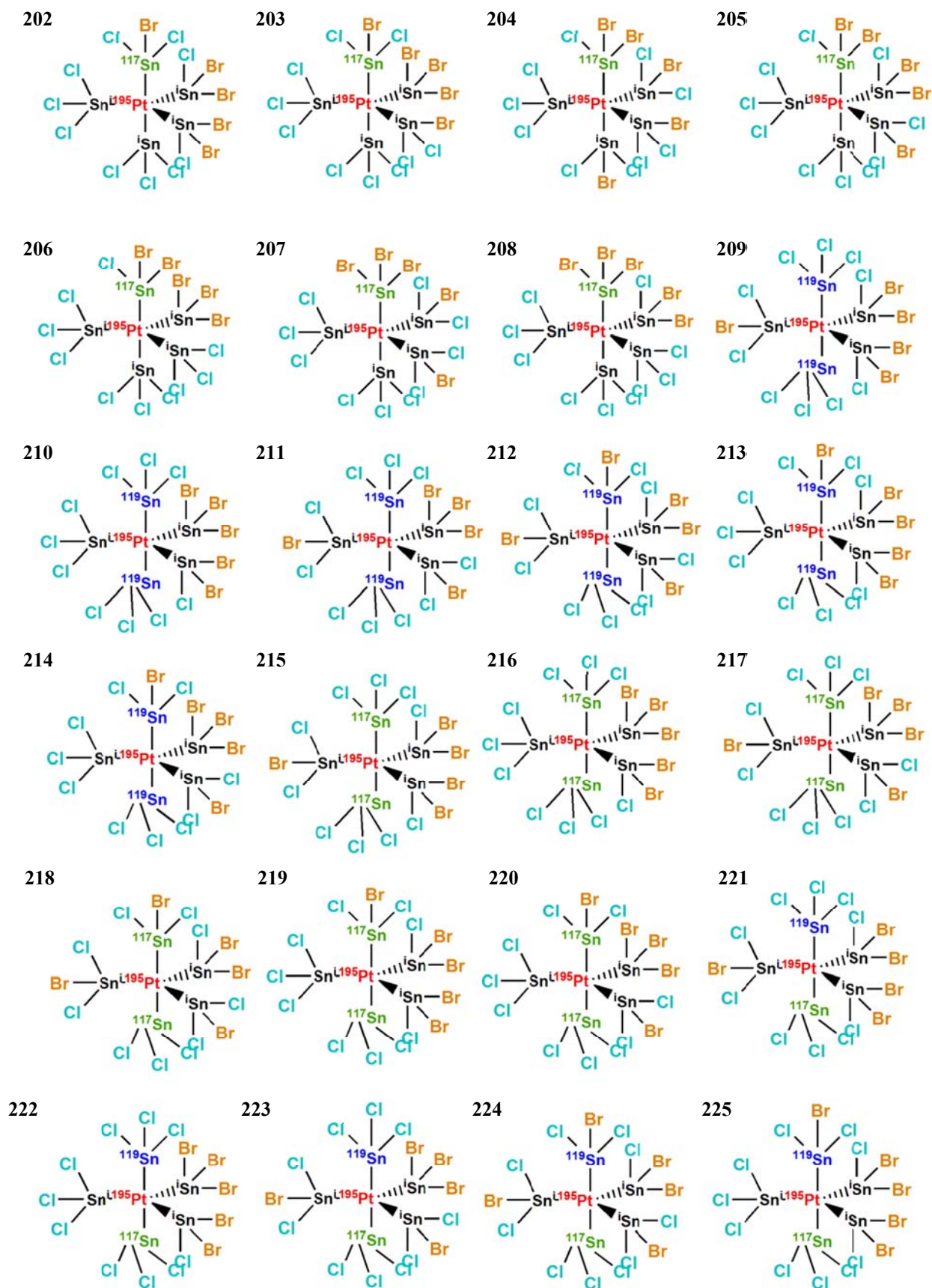
Scheme B11: Isotopologues and isotopomers of the $\text{Pt}(\text{Sn}_5\text{Cl}_{11}\text{Br}_4)]^{3-}$ complex anion observed with ^{195}Pt NMR.



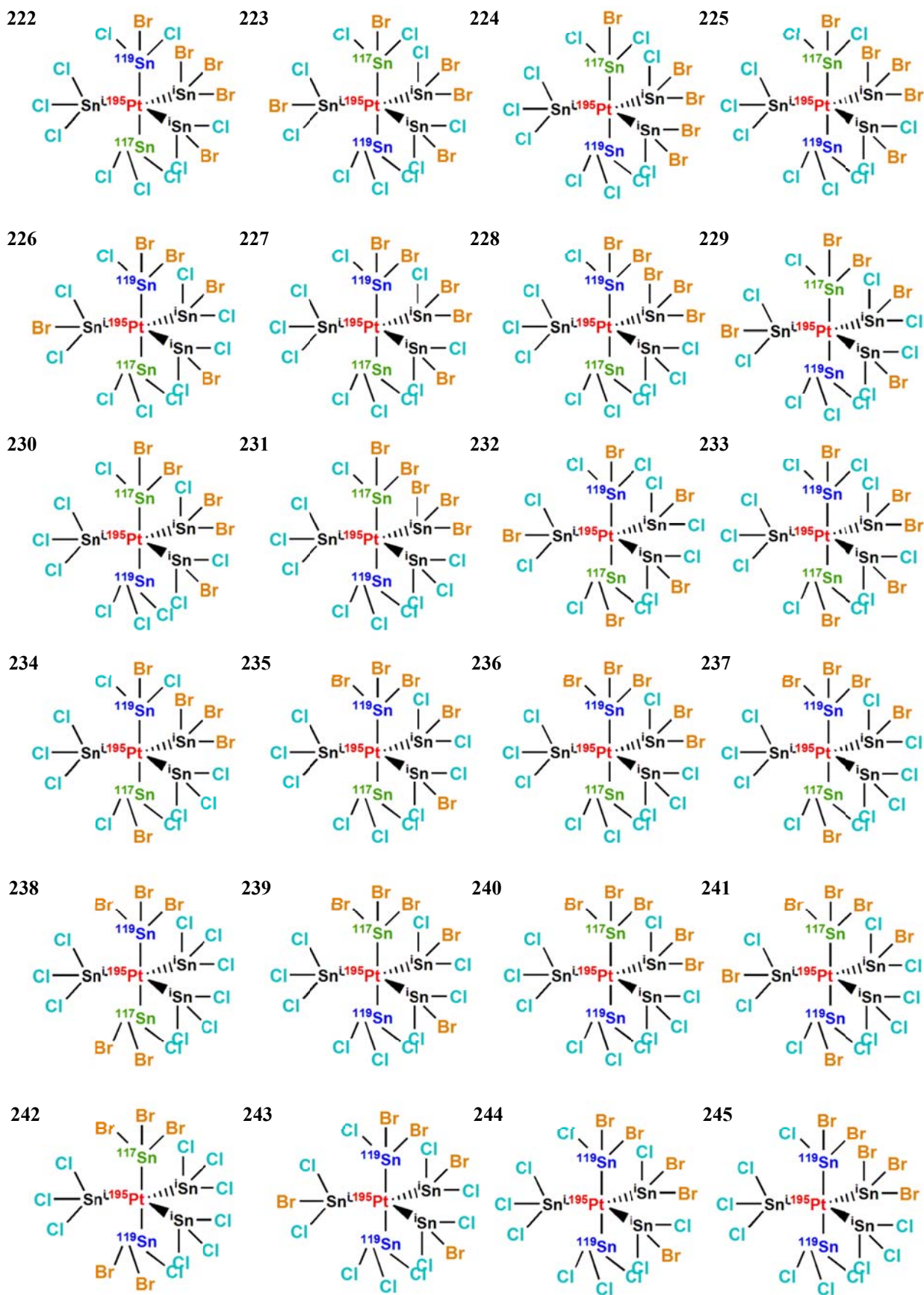
Scheme B12: Isotopologues and isotopomers of the $\text{Pt}(\text{Sn}_5\text{Cl}_{11}\text{Br}_4)]^{3-}$ complex anion observed with ^{195}Pt NMR.



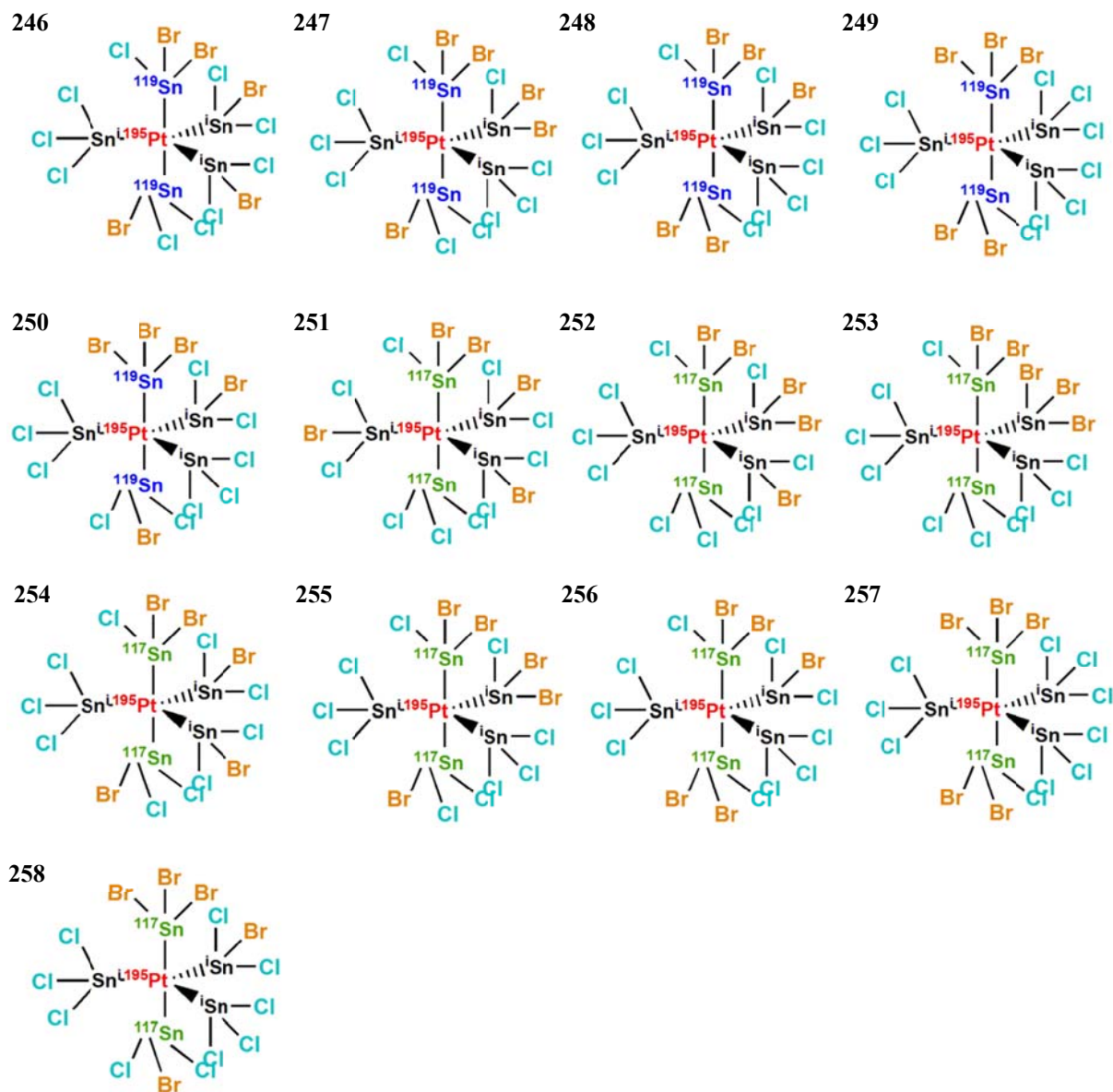
Scheme B13: Isotopologues and isotopomers of the $\text{Pt}(\text{Sn}_5\text{Cl}_{10}\text{Br}_3)^{3-}$ complex anion observed with ^{195}Pt NMR.



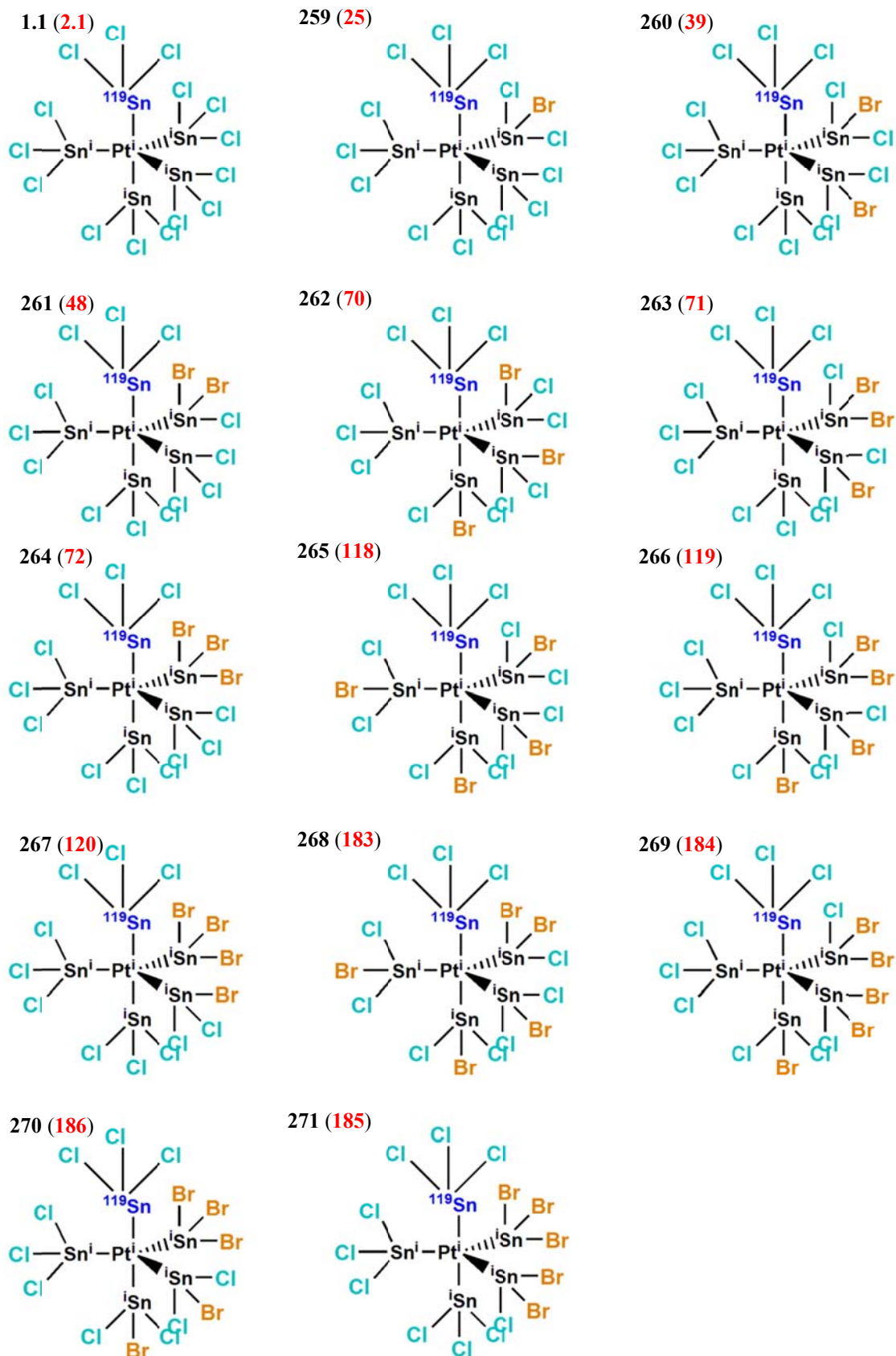
Scheme B14: Isotopologues and isotopomers of the $\text{Pt}(\text{Sn}_5\text{Cl}_{10}\text{Br}_5)]^{3-}$ complex anion observed with ^{195}Pt NMR.



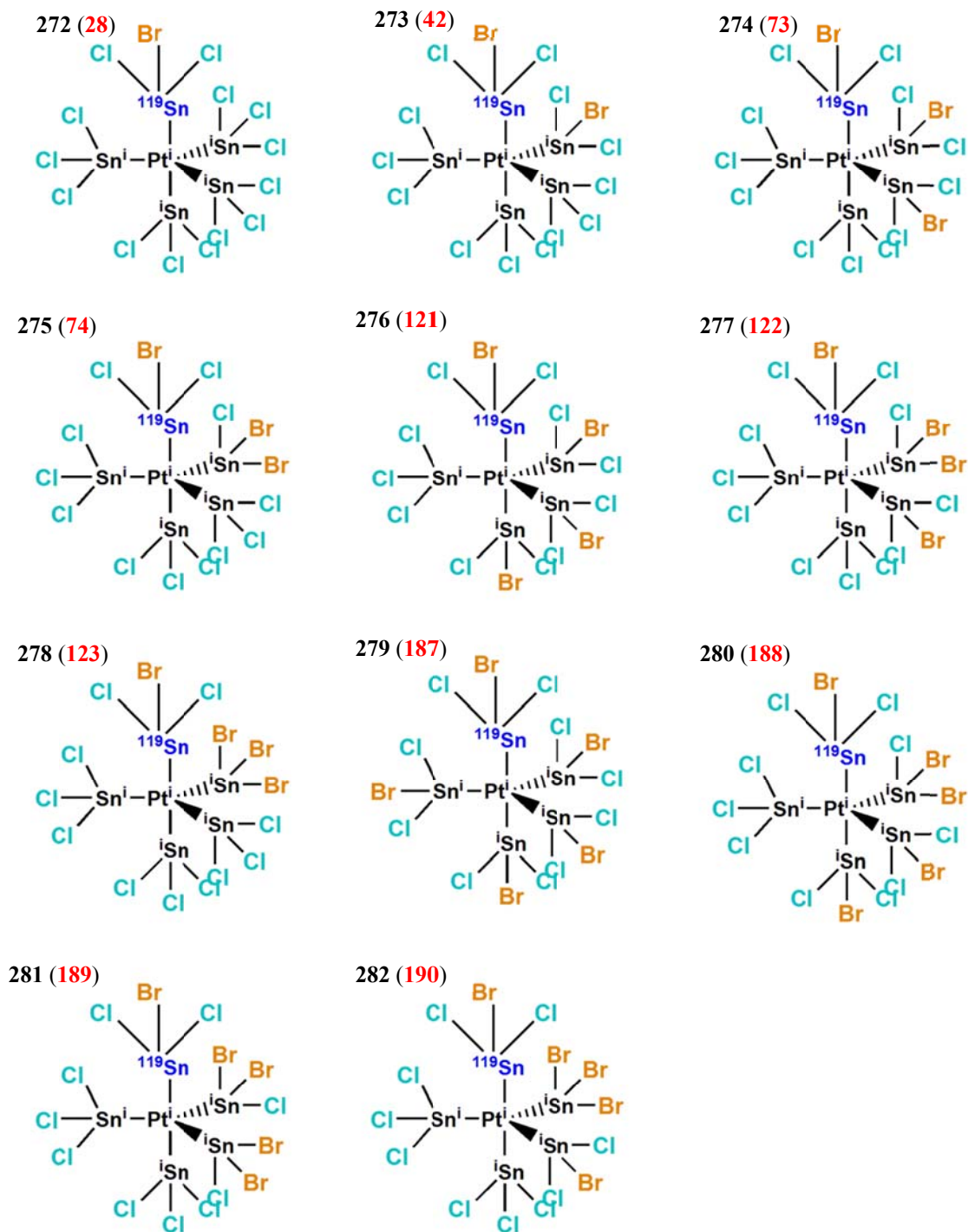
Scheme B15: Isotopologues and isotopomers of the $\text{Pt}(\text{Sn}_5\text{Cl}_{10}\text{Br}_3)]^{3-}$ complex anion observed with ^{195}Pt NMR.



Scheme B16: Isotopologues and isotopomers of the $\text{Pt}(\text{Sn}_5\text{Cl}_{10}\text{Br}_3)]^{3-}$ complex anion observed with ^{195}Pt NMR.

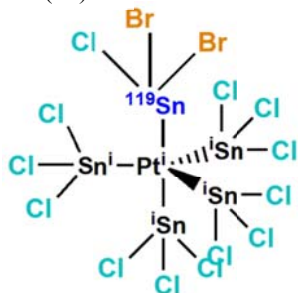


Scheme B17: Isotopologues and isotopomers of the $\text{Pt}(\text{Sn}_5\text{Cl}_n\text{Br}_{15-n})]^{3-}$ ($n = 10 - 15$) complex anion observed with ^{119}Sn NMR. In parenthesis are the numbers of the corresponding isotopologues that contains a ^{195}Pt nucleus.

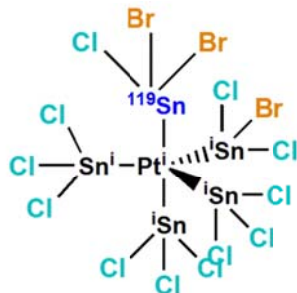


Scheme B18: Isotopologues and isotopomers of the $\text{Pt}(\text{Sn}_5\text{Cl}_n\text{Br}_{15-n})]^{3-}$ ($n = 10 - 15$) complex anion observed with ^{119}Sn NMR. In parenthesis are the numbers of the corresponding isotopologues that contains a ^{195}Pt nucleus.

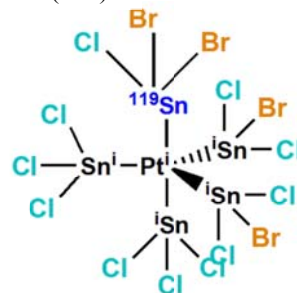
283 (45)



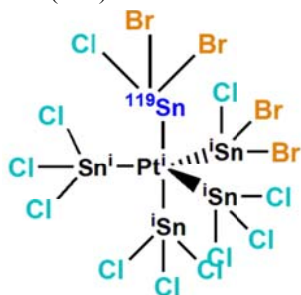
284 (75)



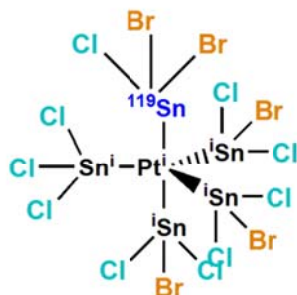
285 (124)



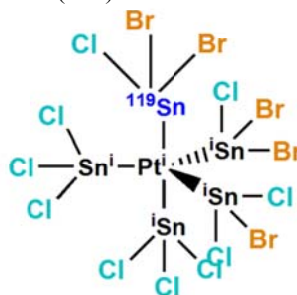
286 (125)



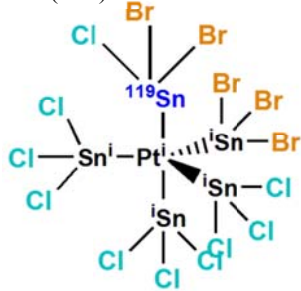
287 (191)



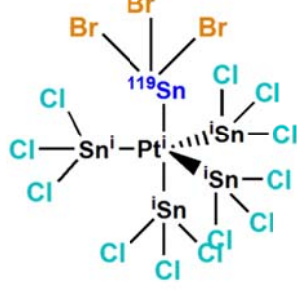
288 (192)



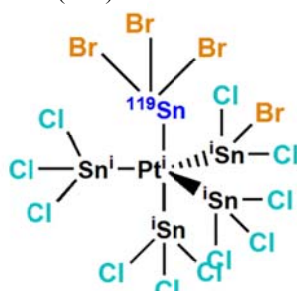
289 (193)



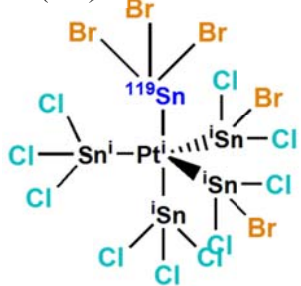
290 (76)



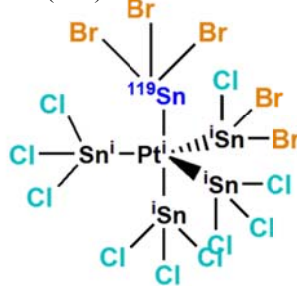
291 (126)



292 (194)



293 (195)



Scheme B19: Isotopologues and isotopomers of the $\text{Pt}(\text{Sn}_5\text{Cl}_n\text{Br}_{15-n})]^{3-}$ ($n = 10 - 15$) complex anion observed with ^{119}Sn NMR. In parenthesis are the numbers of the corresponding isotopologues that contains a ^{195}Pt nucleus.

Appendix C

^{195}Pt NMR spectra of the $[\text{Pt}(\text{SnCl}_n\text{Br}_{15-n})]^{3-}$ ($n = 0 - 15$) heteroleptic complex anions

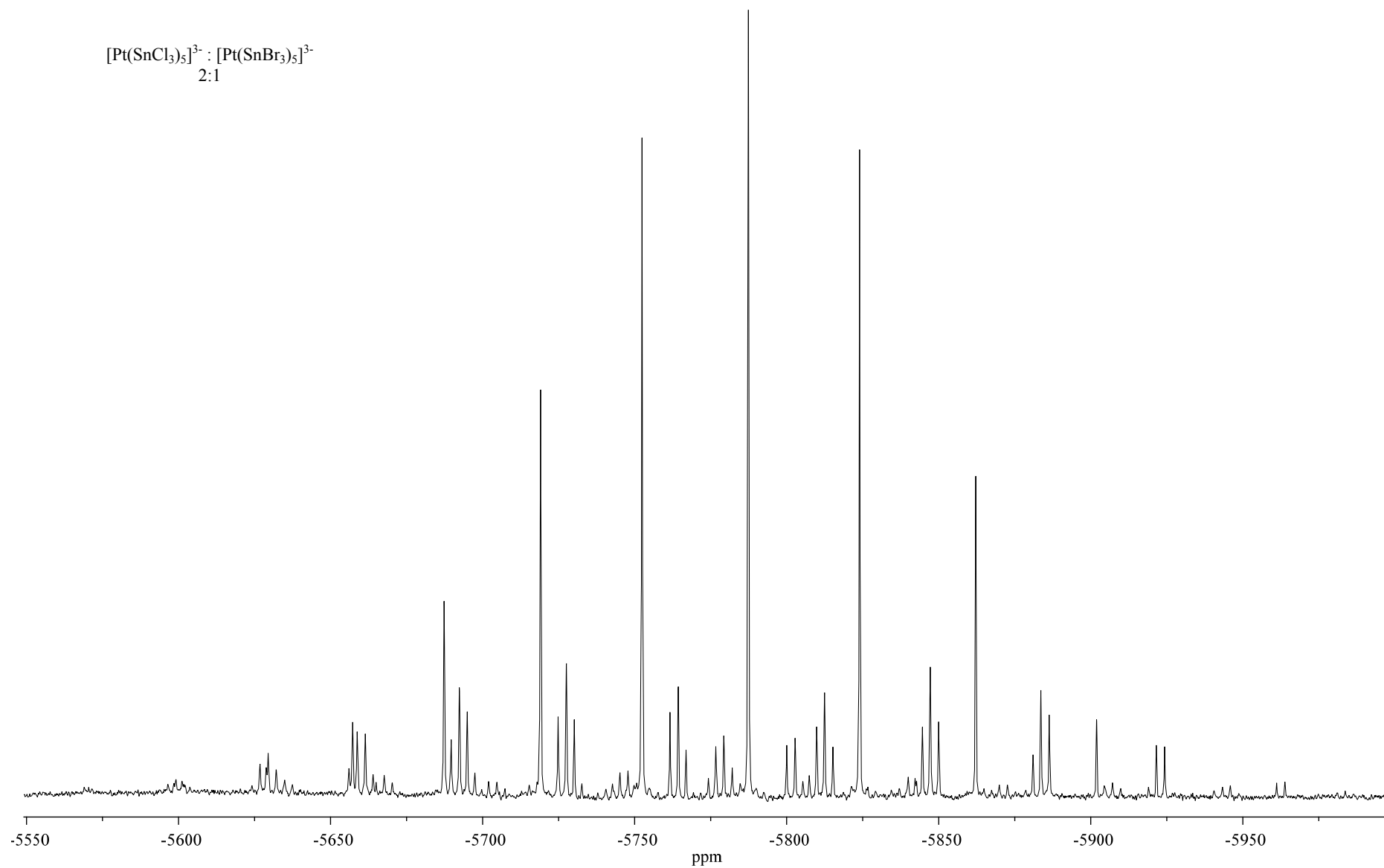


Figure C1: Expansion of the ^{195}Pt NMR spectrum shown in Figure 4.2B.

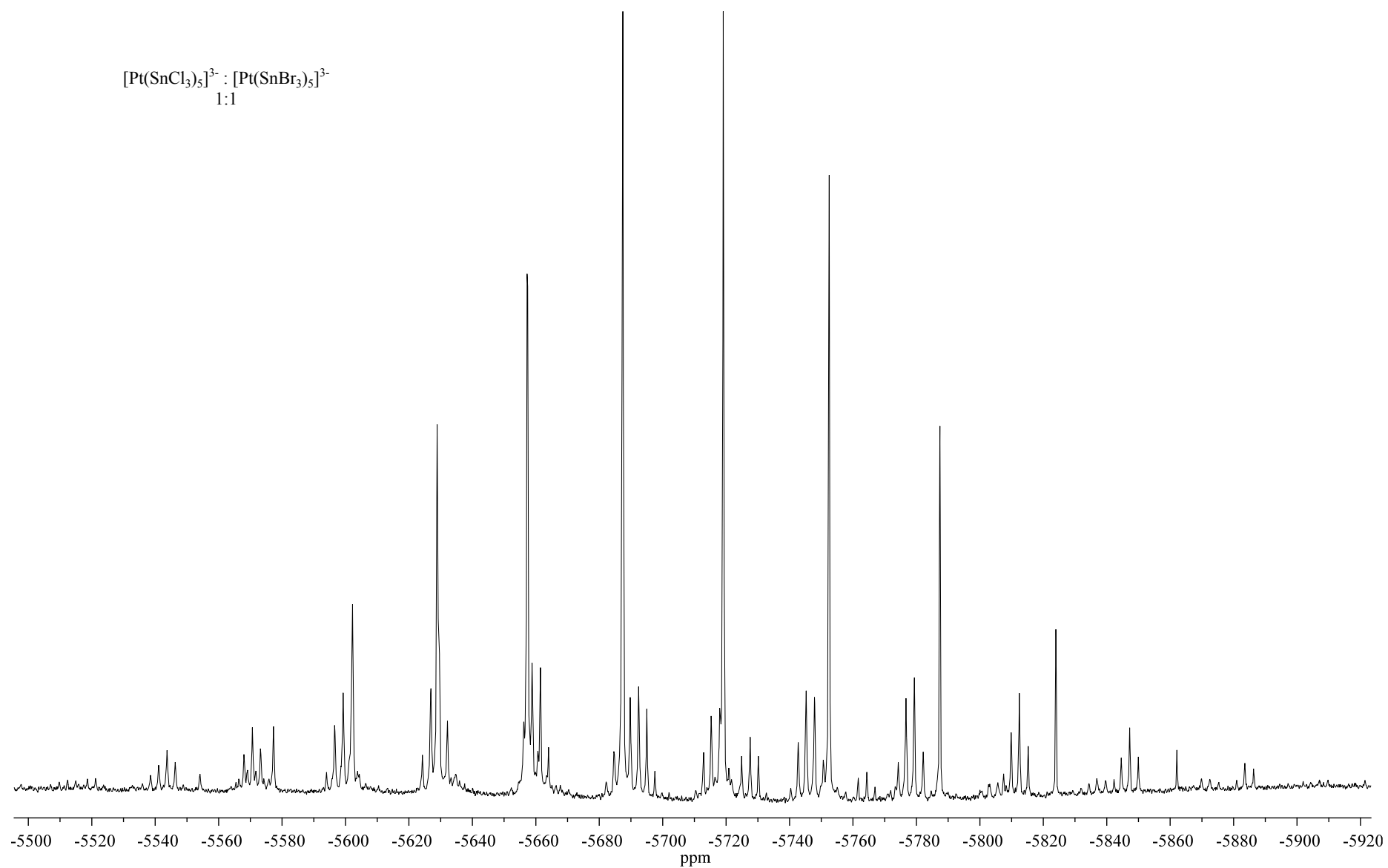


Figure C2: Expansion of the ^{195}Pt NMR spectrum shown in Figure 4.2C.

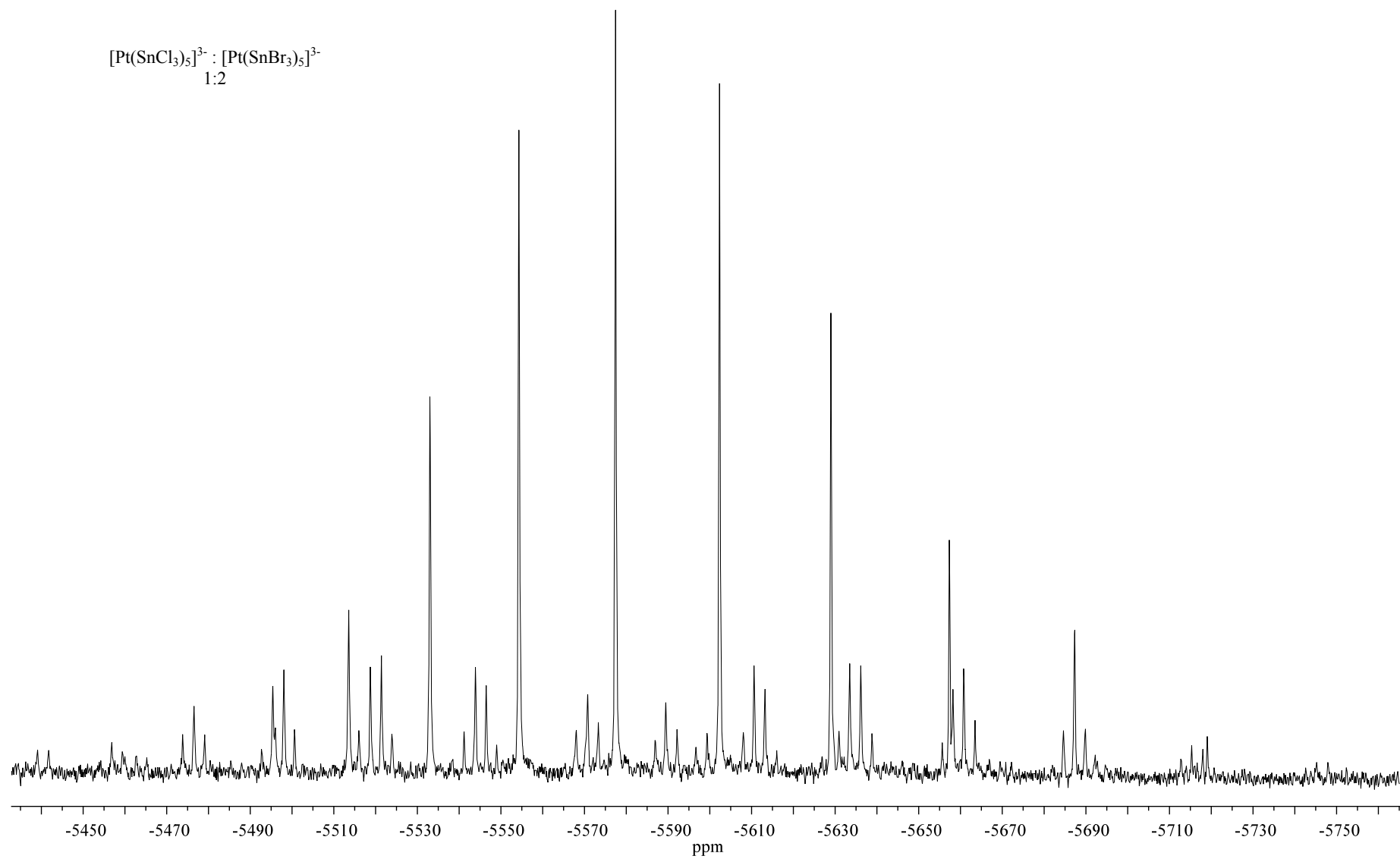


Figure C3: Expansion of the ^{195}Pt NMR spectrum shown in Figure 4.2D.

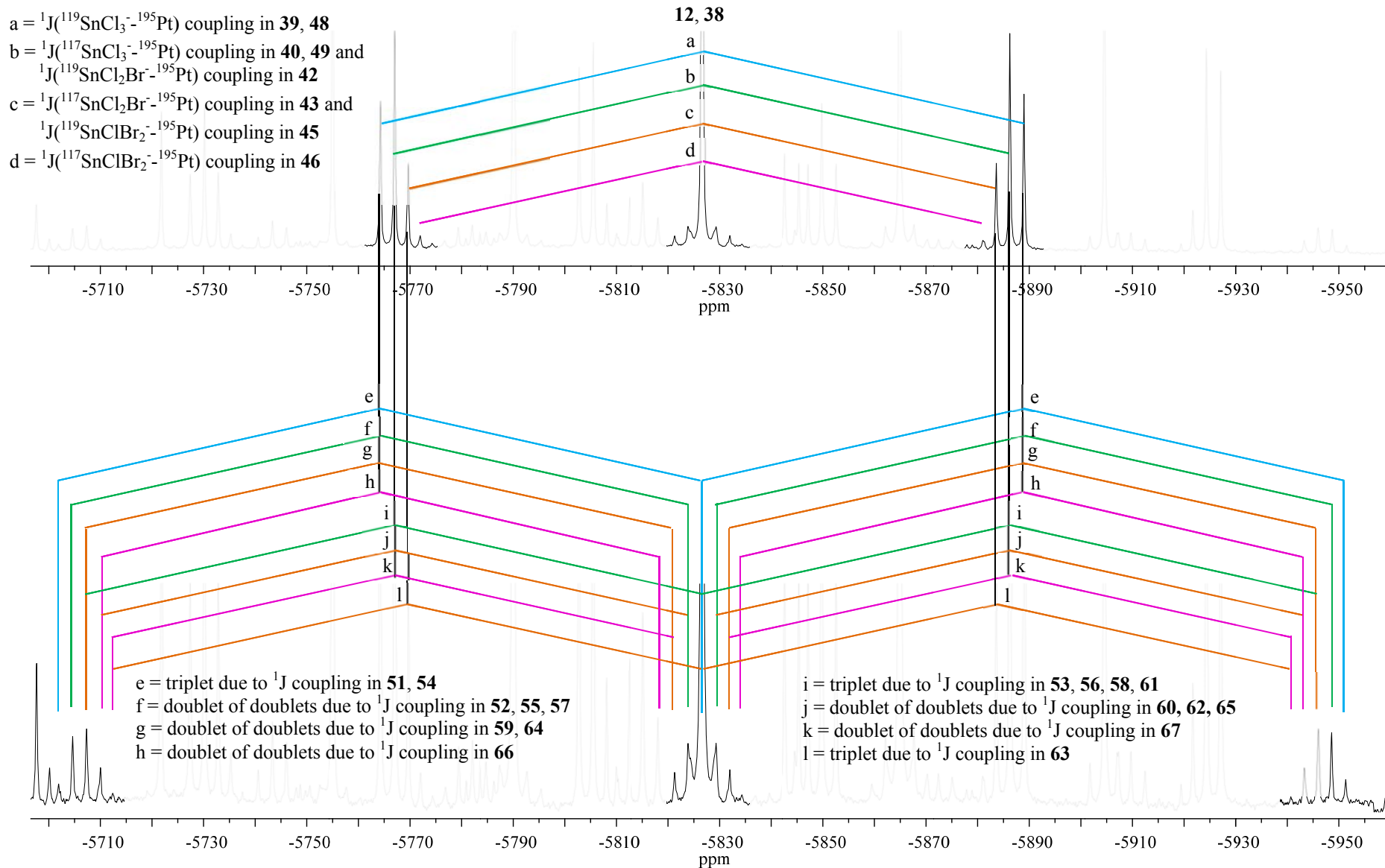


Figure C4: Partial part of ^{195}Pt NMR spectrum shown in Figure 4.2B that focuses on the ^{195}Pt NMR signal obtained for $[\text{Pt}(\text{Sn}_5\text{Cl}_{13}\text{Br}_2)]^{3-}$ and its respective ^1J satellites.

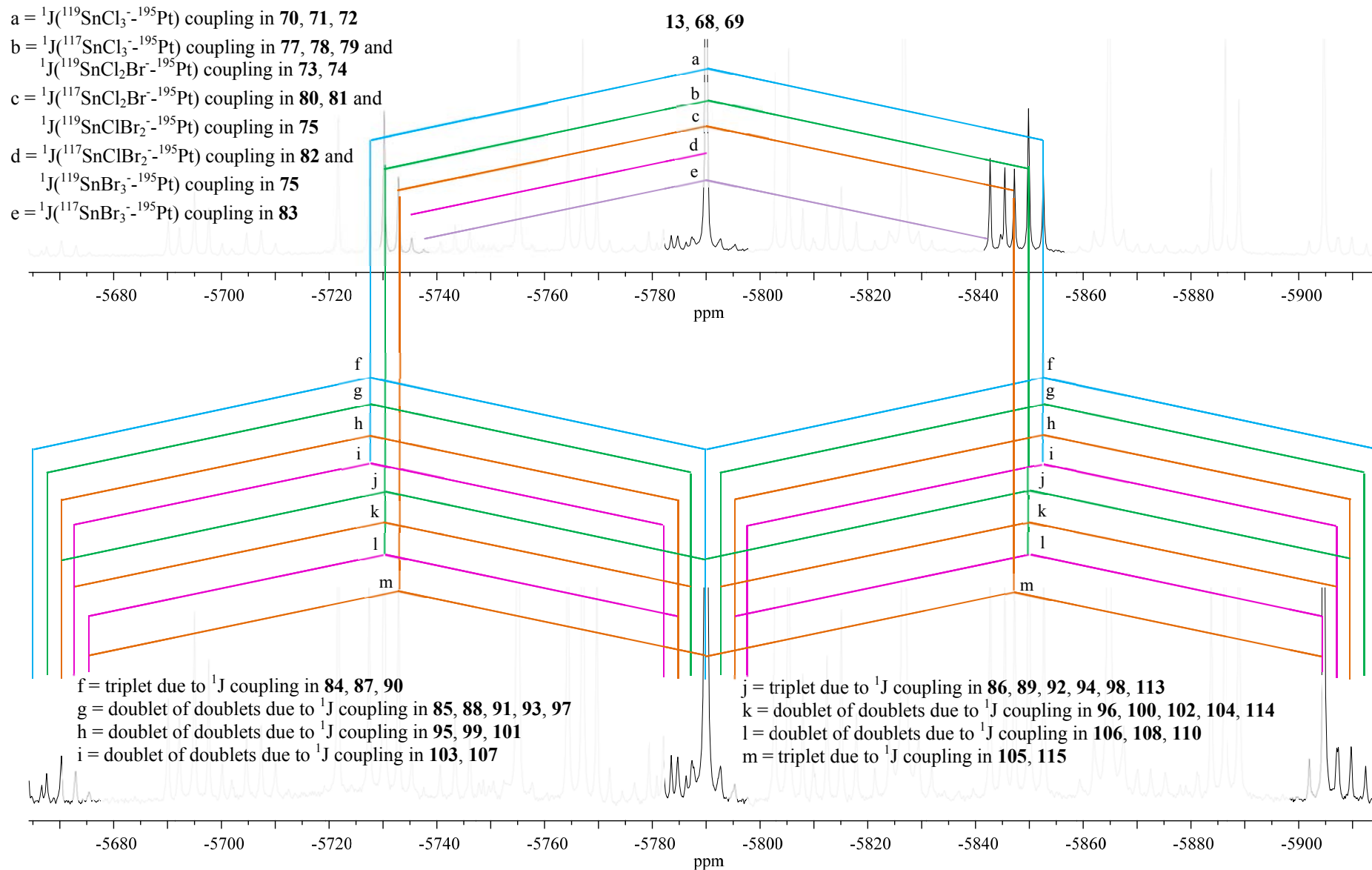


Figure C5: Partial part of ^{195}Pt NMR spectrum shown in Figure 4.2B that focuses on the ^{195}Pt NMR signal obtained for $[\text{Pt}(\text{Sn}_5\text{Cl}_{12}\text{Br}_3)]^{3-}$ and its respective ^1J satellites.

a = $^1\text{J}(^{119}\text{SnCl}_3\text{-}^{195}\text{Pt})$ coupling in **118, 119, 120**

b = $^1\text{J}(^{117}\text{SnCl}_3\text{-}^{195}\text{Pt})$ coupling in **127, 128, 129** and
 $^1\text{J}(^{119}\text{SnCl}_2\text{Br}\text{-}^{195}\text{Pt})$ coupling in **121, 122, 123**

c = $^1\text{J}(^{117}\text{SnCl}_2\text{Br}\text{-}^{195}\text{Pt})$ coupling in **130, 131, 132** and
 $^1\text{J}(^{119}\text{SnClBr}_2\text{-}^{195}\text{Pt})$ coupling in **124, 125**

d = $^1\text{J}(^{117}\text{SnClBr}_2\text{-}^{195}\text{Pt})$ coupling in **133, 134**
 and $^1\text{J}(^{119}\text{SnBr}_3\text{-}^{195}\text{Pt})$ coupling in **126**

e = $^1\text{J}(^{117}\text{SnBr}_3\text{-}^{195}\text{Pt})$ coupling in **135**

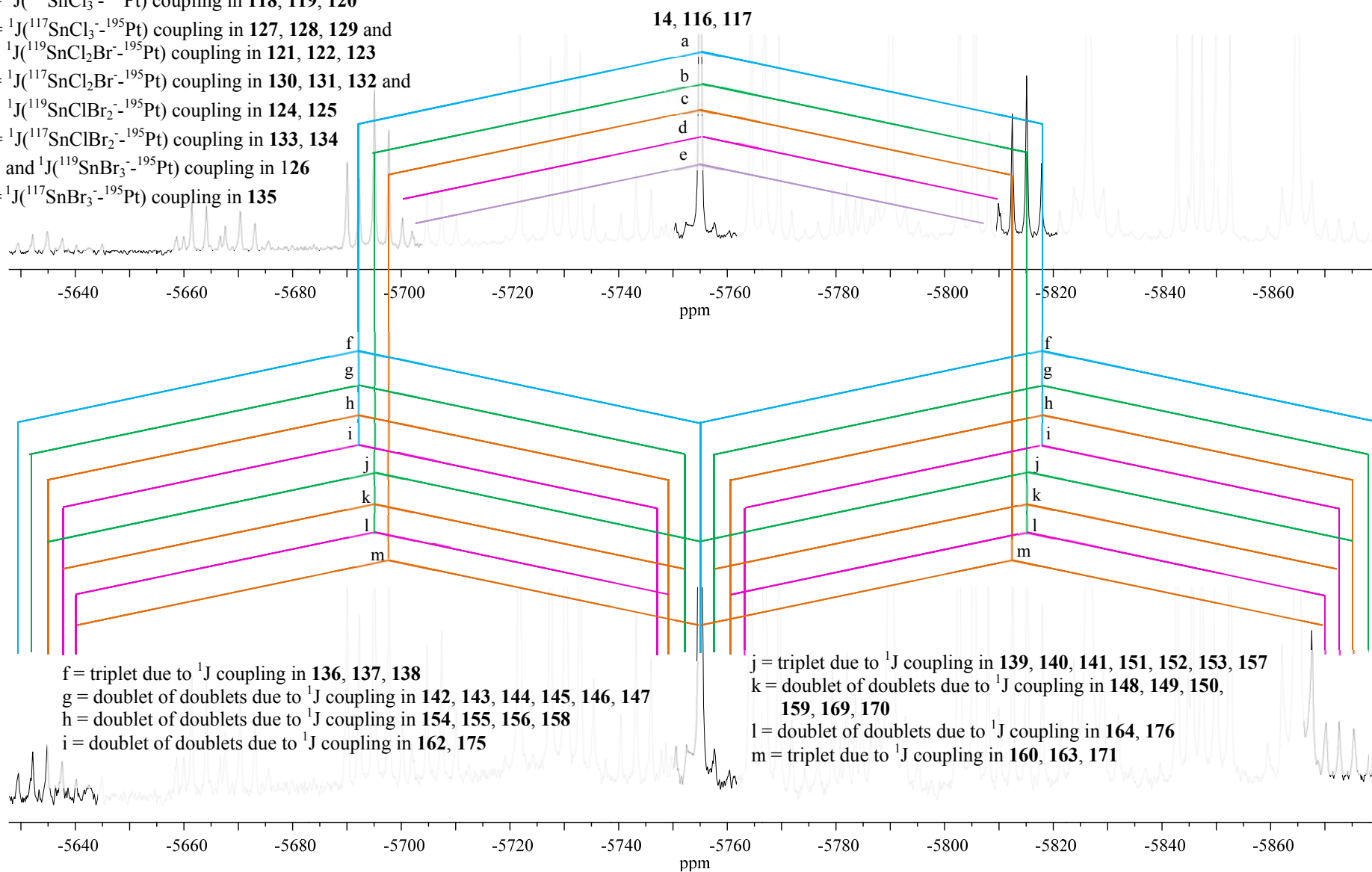


Figure C6: Partial part of ^{195}Pt NMR spectrum shown in Figure 4.2B that focuses on the ^{195}Pt NMR signal obtained for $[\text{Pt}(\text{Sn}_5\text{Cl}_{11}\text{Br}_4)]^{3-}$ and its respective ^1J satellites.